Assessing the impact of wrong-way risk on valuation adjustments of a portfolio of interest rate swaps

W. N. Jonkman

In cooperation with
Rabobank

Delft University of Technology
Faculty Electrical Engineering, Mathematics and Computer Science
January 13, 2020

TU Delft

Assessing the impact of wrong-way risk on valuation adjustments of a portfolio of interest rate swaps

by

W. N. Jonkman

to obtain the degree of Master of Science

at the Delft University of Technology,

to be defended publicly on Wednesday January 13, 2021 at 03:00 PM.

Student number:	4289765	
Project duration:	December 16, 2019 – January 13, 2021	
Thesis committee:	Prof. dr. ir. C. W. Oosterlee,	TU Delft, professor
	Dr. ir. L. A. Grzelak,	TU Delft, daily supervisor
	Dr. C. Kraaikamp	TU Delft
	Ir. T. van der Zwaard,	Rabobank
	Ir. J. van der Linden,	Rabobank

An electronic version of this thesis is available at http://repository.tudelft.nl/.

Cover image is from iex.nl, made by IEX in Actie on 31 maart 2020 15:45.

TU Delft

Assessing the impact of wrong-way risk on valuation adjustments of a portfolio of interest rate rwaps

W. N. Jonkman

Abstract

We study the impact of wrong-way risk (WWR) on the credit valuation adjustment (CVA) of a portfolio of interest rate swaps (IRSs), using an intensity-based reduced form model. To model WWR in IRSs we create a dependence between the underlying market risk factor of the IRS and the survival probability of the counterparty. The focus lies on modeling the credit part of the CVA, choosing the most suitable default model. Using a Monte Carlo (MC) framework, we correlate the Brownian increments of the stochastic processes that describe the interest rate and the hazard rate. Assuming the correlation parameter is chosen based on historical data, we solve the problem of leaking correlation. Two stochastic processes for the credit part are chosen, the CIR++ and the JCIR++, such that the influence of the model choice can be separated from the impact of WWR. With a case study, we vary the correlation parameter to quantify the impact of WWR on CVA of the portfolio. We show that the introduced dependence has a significant impact on the CVA, that depends on the calibration, the portfolio and the chosen correlation. Solving the leaking correlation problem can increase the impact of WWR on the CVA, especially using JCIR++ dynamics.

Preface

This thesis has been submitted for the degree of Master of Science in Applied Mathematics at Delft University of Technology, with a specialisation in Financial Engineering. The research has been done under the academic supervision of Dr. Ir. L.A. Grzelak and Prof. dr. ir. C. W. Oosterlee. From the Pricing Model Validation team at Rabobank, supervision was provided by Ir. T. van der Zwaard, Ir. J. van der Linden and partly by Dr. Ir. A. van der Stoep.

After an interesting final project of the T.U. Delft course Special Topics in Finance, I got enthusiastic about the topic of CVA. I asked Lech Grzelak, who was the lecturer of the course, for a similar project, enabling me to dive deeper in the subject. He not only helped me to get a three month internship, he also led me to this thesis project, both at the Pricing model validation team of Rabobank. The research combines the abstract world of mathematics to the practical financial industry. Since both interest me, I am thankful I was able to conduct this research.

I could not have completed this thesis without the help of many others. I would like to express my gratitude to my daily supervisors from Rabobank, Thomas van der Zwaard, Jan van der Linden and Anton van der Stoep, for their superb supervision and their valuable feedback. I have learned so much from them. I would like to thank my daily supervisor from the T.U. Delft, Lech Grzelak, not only for leading me to this project at Rabobank, but also for asking critical questions, giving useful insights and keeping me sharp on the topic. I would also like to thank my committee members Kees Oosterlee and Cor Kraaikamp for their time and feedback.

Furthermore I want to express my appreciation to Rabobank and to Erik van Raaij, for giving me the opportunity to work at a bank on actual applied mathematics and for providing a fun and supportive work environment, where I could learn about the financial industry. Finally, I'm grateful to my friends and family, who have supported me the last couple of months.

W. N. Jonkman
Delft, January 2021

Contents

Acronyms vii

1 Introduction 1

2 The concept of wrong-way risk 3
2.1 Wrong-way risk in CVA . . . 3
2.2 Survival probabilities . . . 4
2.3 Exposure profile . . . 4

3 literature overview for wrong-way risk modeling 7
3.1 Interest rate model . . . 7
3.2 Choice of default model . . . 9
3.2.1 Structural models . . . 9
3.2.2 Reduced form models . . . 11
3.2.3 Further models . . . 13
3.2.4 Conclusion default model choice . . . 13
3.2.5 Approaches for pricing counterparty credit risk including wrong-way risk . . . 14
3.3 Default model . . . 17
3.3.1 Default intensity modeling of the reduced form default model . . . 17
3.3.2 Implementation . . . 20
3.3.3 Introducing dependency . . . 22
3.3.4 Method of assessing WWR on the CVA of an IRS . . . 32
3.3.5 Calibration of the default model . . . 33

4 Results 39
4.1 Data . . . 39
4.1.1 Interest date data . . . 39
4.1.2 Credit data . . . 40
4.1.3 Other model parameters . . . 41
4.2 Generating survival probabilities . . . 41
4.3 Leaking correlation . . . 43
4.4 Volatility calibration . . . 51
4.5 Exposures . . . 52
4.6 CVA . . . 53
4.6.1 Longer IRS tenor . . . 55
4.6.2 Calibration per ρ-value . . . 56
4.6.3 JCIR++: more jumps, less instantaneous volatility . . . 56

5 Conclusion, discussion and future research 61
5.1 Summary . . . 61
5.2 Conclusion . . . 61
5.3 Limitations . . . 62
5.4 Future research . . . 63

A Hull-White experiments 65
A.1 Implementation of the HW1F model . . . 65

Acronyms

CDS Credit Default Swap

CDSO Credit Default Option

CIR Cox-Ingersoll-Ross

CVA Credit Valuation Adjustment

EAD Exposure at default

IRS Interest Rate Swap

JCIR Jump-Cox-Ingersoll-Ross

LGD Loss-given-default

PD Probability of default

RWR Right-way risk

SP Survival probability

OTC Over-the-Counter

WWR Wrong-way risk

1 Introduction

The interest rate derivative market has without doubt the largest part of all over-the-counter (OTC) derivatives, with a global notional amount outstanding of $495, compared to $607 trillion of the global notional amounts of all OTC derivatives combined [28]. Due to these obvious high amounts and the previous consequences of the Great Financial Crisis 2007 – 2009, financial institutions must calculate and reduce their credit risks regarding derivatives such as IRSs as much as possible. Banks and other financial institutions are required to apply and report valuation adjustments (xVA's) for OTC derivatives by their governments, and they must perform risk-management of the risks that arise from trading in OTCs.

One of those risks that has showed to be significant is the risk that the counterparty can default before fulfilling its payment obligations. That is called counterparty credit risk and the associated valuation adjustment is the Credit Valuation Adjustment. This is a positive adjustment to the default-free value of a portfolio traded with a counterparty and is by definition the difference between the risk-free and the risky portfolio.

The calculations of the CVA's in institutions' xVA engines often assume independence between the expected exposure to the counterparty and the default probabilities of that counterparty. As the interest rate decreased during the financial crises and more companies defaulted, there may be a dependency between the market risk factors and the counterparty's credit quality. This adverse relationship between the exposure to and the creditworthiness of that counterparty, is called wrong-way risk (WWR). A favourable relationship is called right-way risk (WWR), but often when speaking of WWR, both directions are meant to be included. This dependency may impact the CVA and therefore to accurate price and hedge CVA, WWR needs to be taken into account. Also the primary global standard setter for capital, the Basel Committee on Banking Supervision, state that banks are required to identify cases high exposures to WWR.

Given the large amounts dealt in the interest derivative OTC market and the fact that WWR becomes important when credit risks need to be hedged, this research focuses on IRSs. Despite the large amounts of money, research on WWR started only a couple of years ago and there is still no consensus on how to deal with the calculations of WWR in IRSs. Researching and quantifying the impact of WWR can help improving the pricing and hedging of counterparty credit risk. Therefore, this thesis aims to asses the impact of WWR on CVA of IRSs.

This gives rise to the question how this co-dependence relation between the creditworthiness of the counterparty and the value of the exposure to that counterparty should be modelled. Over the years, multiple models have been developed for quantifying WWR and measuring the impact on CVA pricing. Multiple approaches for modeling WWR for interest rate products can be found in literature. Within the MC framework, there is the simulation approach, which uses stochastic differential equations (SDEs) to model the interest rate and the intensity for the probability of default and which introduces dependence by correlating the Brownian increments of the SDEs [39, 9, 16], Also, introducing a functional relationship between the interest rate and hazard rate has been researched [33, 38]. Another widely researched approach is the use of copula functions, where a copula is used to couple the distribution of survival probability of the counterparty to the distribution of the interest rate [31, 32]. This research uses the SDE approach, where the interest rate is modeled with Hull-White one factor dynamics and for the credit part an intensity-based reduced form model is used. Both

the CIR++ and JCIR++ dynamics are used to model the intensity (hazard rate) of the credit part. After correlating the dynamics, WWR is quantified by varying the correlation coefficient. The two credit models, CIR++ and JCIR++, are calibrated to each other, to put the impact of WWR in perspective and to separate the impact of the model choice from the impact of WWR.

This thesis is organized as follows. In Chapter 2 we elaborate on the concept of WWR, together with related concepts. In Chapter 3 we give an overview of existing credit models. We discuss the default models that are most used in practice and we discuss multiple possibilities for modeling the intensity of the chosen credit model. Also, we discuss the way of introducing dependency, together with the problem of solving leaking correlation that is involved. In the last part of Chapter 3 we describe the used methods for calibrating certain parameters. In Chapter 4 we discuss the results from using the built CVA model. Finally, we conclude our work in Chapter 5, together with a list of possibilities for future research.

2

The concept of wrong-way risk

2.1. Wrong-way risk in CVA

When trading over-the-counter (OTC) interest rate (IR) products, the trader has to take into account the fact that there is the possibility that the counterparty will not fulfill its payment obligations due to a default. This risk is called counterparty credit risk or simply credit risk. Only when a company is exposed to a counterparty, credit risk is present. The price of credit risk is expressed in the Credit Value Adjustment. This is a (positive) adjustment to the default-free value of a portfolio traded with one counterparty in order to account for the possibility that the counterparty defaults.

The CVA depends on both the default-free value, current and expected future value, of the transactions with the counterparty and on the default probability of the counterparty. If the value of these transactions is positive for the investor, this value is called the positive exposure. In other words, the positive exposure is the total amount owed by the defaulting party to the investor. In formula form:

$$E(t) = \max(V(t), 0)\,. \tag{2.1.1}$$

$V(t)$ stands for the value of the portfolio traded with the counterparty. When there is an adverse, unfavourable relation between the exposure to a counterparty and the probability of default of that counterparty, this is called wrong-way risk (WWR). When the relation is favourable this is called right-way risk. Unless otherwise specified, when we speak of wrong-way risk in this thesis, we mean both wrong-way and right-way risk.

In this thesis we only consider the unilateral CVA, which means we only consider the possibility that the counterparty defaults, we take the position of a safe investor and assume to be default-free. The (unilateral) value CVA at time t,can be written as follows: unilateral CVA:

$$\mathrm{CVA}(t,T) = \mathbb{E}^{\mathbb{Q}}\left[\frac{B(t)}{B(\tau)}\,\mathrm{L_{GD}}\cdot\max(V(\tau),0)1_{\tau\leq T}\middle|\mathscr{F}(t)\right], \tag{2.1.2}$$

where $B(t)$ stands for the value of the bank-account at time t, $\mathrm{L_{GD}}$ is the loss-given-default, τ is the time of default, T is the maturity time of the portfolio and $\mathscr{F}(t)$ is the natural filtration containing all the market information up to and including t. The loss-given-default is a factor that determines the remaining value of the contract at time of default.

To calculate an accurate price for the CVA, WWR should be taken into account. Any other relationship than an independent relationship between the exposure and the credibility of the counterparty is called WWR. Therefore, not involving WWR greatly simplifies the CVA computation and as a result, the CVA charge can be approximated by [6]

$$\mathrm{CVA} \approx \mathrm{L_{GD}} \times \mathrm{PD} \times \mathrm{EPE},$$

where EPE is the expected positive exposure. Including WWR, the computation of the CVA can become difficult. Although WWR could be broader interpret, we only consider WWR as the dependence between the probability of default and the exposure at default. In some researches WWR is interpreted as the dependence between the $\mathrm{L_{GD}}$ and the probability of default, but that interpretation falls outside the scope of this research.

Assuming the L_{GD} to be constant simplifies the computation and the difficult modelling part consists of the exposure at default and the probability of default. However, using the Key Lemma, a result from stochastic calculus, the CVA can be written in a form which is not dependent on the time of default anymore [12]:

$$\text{CVA}(t,T) = -L_{GD}\mathbf{E}^{\mathbb{Q}}\left[\int_{t_0}^{T}\frac{B(t_0)}{B(u)}\max(V^{\text{IRS}}(u),0)\mathrm{d}\,\mathbb{Q}(\tau > u \mid \mathscr{F}(t)\right], \tag{2.1.3}$$

where we used the risk-neutral measure $\mathbb{Q}$. This equation is more efficient to work with in the MC framework, since we do not want to simulate the default time. The probabilities of default in each time-interval are very low. The probability of default is usually very small and therefore the actual default does not happen much. It would require a tremendous amount of simulations to achieve the desired amount of defaults for the computation of the expectation, which is computationally very intensive. We use $\mathbb{Q}(\tau > t)$, which is the survival probability under the risk-neutral measure. It is equal to one minus the probability of default and it means the probability that the default happens after time t.

Hence, we have reduced the problem of computing the CVA to finding the survival probabilities of the counterparty and finding the Expected Positive Exposures of the portfolio. We discuss the former in the following section and the latter in Section 2.3.

2.2. Survival probabilities

The survival probability $\text{SP}(t,T)$ is the probability that the default does not happen before time T, conditioned on not defaulting before time t. Using a reduced form model with intensity $\lambda(t)$, the survival probability can be computed as follows:

$$\text{SP}(t,T) = \mathbb{Q}(\tau > T \mid \mathscr{F}(t)) = \mathbb{E}^{\mathbb{Q}}\left[\exp\left(-\int_t^T \lambda(u)\mathrm{d}u\right)\middle|\mathscr{F}(t)\right]. \tag{2.2.1}$$

The probability of default is then defined as $\text{PD}(t,T) = 1 - \text{SP}(t,T)$. Market implied survival probabilities can be extracted from the credit curve. This a curve analogue of the yield curve and consists of the survival probabilities $\text{SP}(t_0,t)$, for which t_0 is today's date.

To find the survival probabilities needed for the computation of the CVA, we simulate the intensity $\lambda(t)$ and then use Equation (2.2.1). We use MC paths to find the expectation. We can calibrate the credit part of the CVA model to this credit curve, using Credit Default Swaps (CDSs) from the market. We explain more about the credit model, choice of the intensity dynamics, the simulating of the hazard rate, the computation of the survival probabilities and the calibration of the credit part in Chapter 3.2.

2.3. Exposure profile

Considering Equation (2.1.3), we need not only the value of the portfolio today, but also in the future. We need the expected value of the exposure profiles $E(t)$: the Expected Positive Exposures ($EPE(t)$). The portfolio consists of IRSs and an IRS is defined as follows:

$$V^{IRS}(t,\mathscr{T},\alpha,N,K) = N\sum_{k=i+1}^{m}\alpha_k P(t,T_k)(l(t;T_{k-1},T_k)-K), \tag{2.3.1}$$

with $\mathscr{T} = \{T_i, T_{i+1}, T_{i+2}, ..., T_m\}$ is the tenor with payment dates, $\alpha_k = T_k - T_{k-1}$ is the payment frequency, N is the notional, $P(t,T_k)$ is the discount factor from T_k to t and $l(t;T_{k-1},T_k)$ is the forward interest rate from T_{k-1} to T_k, valued at time t. This forward rate is defined as:

$$l(t_0;T_a,T_b) = \frac{1}{T_b - T_a}\left(\frac{P(t_0,T_a)}{P(t_0,T_b)} - 1\right).$$

For $t = t_0$, the value of the swap is deterministic and determined by zero-coupon bonds or discount factors $P(t_0,T_k)$ from the yield curve. These zero-coupon bonds are analogue to the survival probabilities and have the following value:

$$P(t,T) = \mathbb{E}^{\mathbb{Q}}\left[\exp\left(-\int_t^T r(u)\mathrm{d}u\right)\middle|\mathscr{F}(t)\right]. \tag{2.3.2}$$

Just as previous section, the values $P(t_0,T)$ can be extracted from the yield curve. However, for any time in the future t, we need Equation (2.3.2) and the interest rate $r(t)$ to compute the value of the discount factor.

Hence, to compute the value of the IRS, we use a stochastic process that simulates the interest rate. With the simulated MC paths we find the expectation in Equation (2.3.2) and compute the discount factors and forward interest rate, needed to compute the future IRS values.

Given those exposure profiles from Equation (2.1.1), we can compute the expected positive exposure at time at time t, valued at time t_0, as follows:

$$EPE(t_0, t) = \mathbb{E}^{\mathbb{Q}}\left[\frac{B(t_0)}{B(t)}E(t)\middle|\mathscr{F}(t_0)\right], \tag{2.3.3}$$

where $B(t)$ is the bank account. Dynamics of the bank account are given by Equation (3.1.2). We elaborate on the interest rate part of the CVA model in Section 3.1, where we discuss the simulation of the the interest rate, the computation of the discount factors and the calibration of the interest rate model to the yield curve.

Together with the survival probabilities from the previous section and a value for the L_{GD}, we have everything we need to compute the CVA for the portfolio from Equation (2.1.3). To incorporate WWR in Equation (2.1.3), we need a dependency between the survival probabilities and the expected positive exposure. We use the driving factors behind the survival probabilities and the exposures to introduce dependency. Within the MC framework we correlate the Brownian increments of the dynamics with a correlation coefficient. Dependent on that correlation coefficient, we can quantify WWR by comparing the CVA with and without correlation. In what follows, Chapter 3, we elaborate on the choices we make that result in the CVA model.

3

literature overview for wrong-way risk modeling

3.1. Interest rate model

The CVA model consists of two parts: the interest rate part for the exposure to the counterparty and the default probability part for the creditworthiness of the counterparty. The main objective is to create an understandable model that can be used to asses the impact of the dependence structure between the exposure to and the creditworthiness of the counterparty. In this chapter we describe the modeling choices we make for the interest rate model, needed for the simulation of the future exposures for the portfolio.

For the decision of the interest rate model, we take the following three characteristics of the model in consideration: modeling requirements, accuracy and computational costs. We want to use a model that gives us the modeling requirements without making the total CVA model unnecessarily complex, such that the model is still understandable. The Hull-White One Factor model is the desired choice. In what follows we explain why.

Complex multi-factor models give advantages that we do not need and bring challenges that lie beyond the scope of this research. Firstly, the importance of accuracy. As the CVA model consists of two parts, we do not need one of the parts to be more accurate than the other, since the error of the less accurate part would have a large impact. As input for the credit model, we use the credit curve, based on the term structure of Credit Default Swaps (CDSs) and an interpolation method. We will explain this in Section 3.3.5. Since the credit curve is already an approximation, we do not need a very sophisticated interest rate model that brings a high accuracy, because this accuracy will be lost due to the credit curve error.

Another reason for not using complex multi-factor models is the fact that their calibration is more complex, and the dependence structure with the default model will that be as well. This is due to the large covariance structure. With more factors the interest rate model requires a co-dependence structure between the different factors and the default model. This makes it more difficult to understand [24].

The computational performance could also play a role: complex multi-factor models are computationally more extensive and therefore they require more computation time than simpler models. Hence, the MC simulation will take more time. So, we have to decide whether we want a more complex and more accurate CVA model or a faster and more understandable model. We chose the latter, since we do not need more complexity to asses the impact of the dependence structure between the interest rate (the exposure) and the hazard rate (the creditworthiness) [35].

The use of a Hull-White One Factor model (HW1F) has some benefits. It is easy to understand and is an analytically tractable model. The bond price formula is one of the most used formulas and since it is analytically tractable, the bond price formula is explicit and in closed form. This means that we can compare analytically calculated zero coupon bond prices with Monte Carlo simulations and this also means that the bond prices can be calculated quickly. Furthermore the HW1F simple to calibrate. It is easy to calibrate to yield curve, which we show, and it is also easy to calibrate to European swaptions or IR caplet/floorlet prices.

Because of its simplicity, the HW1F does have some shortcomings. The volatility skew does not match market behaviour. Also, the model does not generate a rich set of yield curve shapes [24]. It is not a multi-curve model. These shortcomings make the HW1F a less realistic model, but as mentioned before, we do not need the complexity of a richer model to asses the impact of the dependence structure between the exposure and the creditworthiness to a company.

The Hull-White model One Factor is a model where the short-term interest rate is modeled as an extended Ornstein-Uhlenbeck mean reverting process:

$$\mathrm{d}r(t) = k(\theta(t) - r(t))\mathrm{d}t + \eta \mathrm{d}W^{\mathbb{Q}}(t), \tag{3.1.1}$$

where $\theta(t)$ is a time-dependent drift term, k represents the speed of mean reversion and η is the volatility of the interest rate. This means that a large value of k causes $r(t)$ to rapidly dampen its movements and to quickly go to the long-term mean $\theta(t)$. This reduces the long-term volatility. In practice, η is usually chosen to have a parametric form: $\eta = \eta(t)$, such as piecewise constant, to fit the Hull-White model to the term-structure of Interest Rate Swaptions. However, the calibration of the model lies beyond the scope of this research and for now a constant η will suffice.

The drift-parameter $\theta(t)$ is used to fit the yield curve generated by the model to the yield curve observed in the market. The Hull-White one factor model fits in the Heath-Jarrow-Morton (HJM) framework. This is a framework for interest rate (IR) models, in which the dynamics of the instantaneous forward rates can be modeled directly. This framework gives a direct relation between instantaneous forward rates, the zero-coupon bond price (and thus the yield curve) and the drift parameter $\theta(t)$ of the Hull-White dynamics. We use this relation to find $\theta(t)$ and calibrate the Hull-White model to the term structure of interest rates from the market [6].

We define $B(t)$ to be the value of a bank account at time $t \geq 0$. Assuming $B(0) = 1$ and interest rate $r(t)$, the bank account evolves according to the following differential equation:

$$\mathrm{d}B(t) = r(t)B(t)\mathrm{d}t, \quad B(0) = 1. \tag{3.1.2}$$

As a consequence, the variable $B(t)$ has the following value:

$$B(t) = \exp\left(\int_0^t r(s)\mathrm{d}s\right) \cdot B(0) = \exp\left(\int_0^t f^r(s,s)\mathrm{d}s\right) \cdot B(0).$$

In this definition $r(t)$ is the instantaneous spot interest rate at time t, which is a stochastic quantity. We define the zero-coupon bond (ZCB) $P(t,T)$ with maturity T, also referred to as the discount factor from t to T, to be the expectation of the value of the bank account w.r.t. the market filtration $\mathscr{F}(t)$ under the risk neutral measure:

$$P(t,T) = \mathbb{E}^{\mathbb{Q}}\left[\frac{B(t)}{B(T)}\middle|\mathscr{F}(t)\right] = \mathbb{E}^{\mathbb{Q}}\left[\mathrm{e}^{-\int_t^T r(s)\mathrm{d}s}\middle|\mathscr{F}(t)\right]. \tag{3.1.3}$$

We define $P_{\mathrm{MC}}(0,T)$ as the yield curve generated by the Monte Carlo (MC) paths from the model by taking expectation of the exponential of -1 times the simulated integrated short-rate:

$$P_{\mathrm{MC}}(0,T) = \mathbb{E}^{\mathbb{Q}}\left[\mathrm{e}^{-\int_0^T r_{\mathrm{MC}}(s)\mathrm{d}s}\middle|\mathscr{F}(t)\right].$$

We call the yield curve observed in the market $P_{\mathrm{mkt}}(0,T)$. The Hull-White process is arbitrage-free if and only if $\theta(t)$ is given by the following equation[6]:

$$\theta(t) := \frac{1}{k}\frac{\partial}{\partial t}f^r(0,t) + f^r(0,t) + \frac{\eta^2}{2k^2}(1 - \mathrm{e}^{-2kt}). \tag{3.1.4}$$

In this equation the instantaneous forward rate is defined as:

$$f^r(0,t) = -\frac{\partial}{\partial t}\log P_{\mathrm{mkt}}(0,t). \tag{3.1.5}$$

Therefore, the value of a ZCB with value $P_{\mathrm{MC}}(0,T)$ from the model with start date today ($t = 0$) is due to this construction equal to the value of a ZCB $P_{\mathrm{mkt}}(0,T)$ with the same start date and maturity from the market i.e.,

$$P_{\mathrm{MC}}(0,T) = \mathbb{E}^{\mathbb{Q}}\left[\mathrm{e}^{-\int_0^T r_{\mathrm{MC}}(s)\mathrm{d}s}\middle|\mathscr{F}(0)\right] \approx P_{\mathrm{mkt}}(0,T).$$

Considering the dynamics of the short-rate in Equation (3.1.1), we can use Itô's lemma and an integration factor to obtain the solution of this interest rate process. The solution is given by:

$$r(t) = \mathrm{e}^{-kt} r(0) + k \int_0^t \theta(z) \mathrm{e}^{-k(t-z)} \mathrm{d}z + \eta \int_0^t \mathrm{e}^{-k(t-z)} \mathrm{d}W_r(z). \tag{3.1.6}$$

In this solution we notice two deterministic terms and a stochastic term. The stochastic term is an Itô integral, which has a normal distribution with expectation of 0 and a variance of $\int_0^t |\eta \mathrm{e}^{-k(t-z)}|^2 \mathrm{d}z = \frac{\eta^2}{2k}(1-\mathrm{e}^{-2kt})$. This means that the interest rate $r(t)$ is normally distributed with mean:

$$\mathbb{E}\left[r(t)|\mathscr{F}(t_0)\right] = \mathrm{e}^{-kt} r(t_0) + k \int_0^t \theta(z) \mathrm{e}^{-k(t-z)} \mathrm{d}z, \tag{3.1.7}$$

for $t_0 = 0$ and with variance:

$$\mathbb{V}ar\left[r(t)|\mathscr{F}(t_0)\right] = \frac{\eta^2}{2k}\left(1-\mathrm{e}^{-2kt}\right). \tag{3.1.8}$$

With the described interest rate model we can simulate the interest rate and compute the zero-coupon bonds $P_{\mathrm{MC}}(t,T)$, the forward rates, the IRS values and therefore the expected positive exposures, needed for the CVA computation. More experiments with the Hull-White model, for example a robustness analysis, can be found in Appendix A.

3.2. Choice of default model

As explained in Chapter 2, one of the key aspects to compute the CVA of the portfolio, is the survival probabilities of the counterparty. In this chapter we explain what possibilities we have to model that survival probability function. We discuss different default models, also called credit risk models. For each model, we discuss its key aspects, its benefits and drawbacks and we also explain the model choice for the CVA calculations.

For the possible ways to model the default of an entity, the focus lies on models available for modeling the credit curve for one company. When considering a portfolio of credit products and therefore a portfolio of companies, dependency between the default of companies is introduced. Including this dependency gives another variety of models. There are many more models available considering a portfolio of companies, but we focus on the models considering one company. Even for one company, we do not cover all possible default models. We focus on the most commonly used models and the ones that have been researched the most. So, not all available models are discussed, but this chapter does give a good indication what kind of alternatives exist for modeling the credit-curve and the survival probabilities of an entity.

We categorize the type of credit risk models we found in the literature in the following four types: structural models, reduced form models, financial statement models and further models. While structural and reduced form models fit in the arbitrage-free framework and have amathematical foundation, financial statement models are based on formal records of the financial activities and position of an entity. Therefore, financial statement models lie beyond the scope of this research and are not covered in this report. In Section 3.2.1 we discuss the key aspects of structural models and in Section 3.2.2 we explain the basic concepts of reduced form models. Other models are discussed in Section 3.2.3. In Section 3.2.4 we explain why we use a reduced form model as default model.

3.2.1. Structural models

In a structural model, the default event is determined by looking at the evolution of the firm's structural values (assets, debt etc.). Structural models are also called firm value models. A default occurs if a random variable X, the latent variable, has a lower value than some threshold D. Often X is interpreted as asset value at time T - usually the maturity date of the debt or liability - and D is often interpreted as the liabilities or debt of the reference entity. An advantage of structural models is that the default time is dependent on the firm's structural values, which represent the firm's economic and financial conditions. Thus, there is a link between the creditworthiness of the company and its financial status. This means that the structural models model defaults endogenously (within the model). This is a difference with reduced form models, where defaults are modelled exogenously. We discuss reduced form models in Section 3.2.2.

Merton developed the first structural model [34]. Other structural models are based on his model. In this section we explain the key aspects of the following structural models: Merton's model, first passage models,

liquidation process models and state dependent models. The latter three are extensions of the Merton model and they can all be used within a risk neutral pricing setting.

In Merton's model we consider the firm's asset value $V(t)$ at time t, consisting of equity with value $E(t)$ and debt with value $D(t)$. The company's asset value $V(t) = E(t) + D(t)$. The value of the debt is represented by the value of a zero-coupon bond with face value $D(T)$ and maturity time T. For example, the company could finance its equity with a zero-coupon bond with maturity time T. The firm can only default at time T, if $V(T) < 0$.So, if at maturity T the firm's asset's are large enough to pay back the dept (which is the face value at T), there is no default. Otherwise the firm defaults [34].

In the Merton model the firm's asset value follow risk-neutral dynamics of the form:

$$\mathrm{d}V(t) = rV(t)\mathrm{d}t + \sigma_V V(t)\mathrm{d}W(t), \tag{3.2.1}$$

where r is the risk free interest rate, σ_V is the asset volatility and $W(t)$ is a Brownian motion. By corresponding the default to the event $V(T) < D(T)$, we see that the equity at time T has value $E(T) = \max(V(T) - D, 0)$ and that the Black-Scholes pricing formula can be used to determine the value of the equity at time t. The probability of default at time T is given by $P(V(T) < D(T)) = \Phi(-d_2)$, where $\Phi(\cdot)$ is the distribution function of the standard normal random variable and with

$$d_2 = \frac{\ln\left(\frac{\exp(r(T-t))V(t)}{D(T)}\right) + \frac{1}{2}\sigma_V^2(T-t)}{\sigma_V\sqrt{T-t}}.$$

So, this model has the restriction that the reference entity is only being able to default at T, independent of the value of the debt before maturity. This characteristic is not realistic, since there are restrictions for the value of debt for a company that can cause default for a company at any time and in reality firms can have bonds with different maturity dates. More important, to compute the CVA of a portfolio, we need the probability of default of the reference entity for every future date from now until the maturity date of the portfolio. Hence, Merton's model is not usable for our purpose.

An extension of Merton's model is the group of models that are called first passage models (FPMs) and are introduced by Black and Cox [22]. Instead of having the restriction of only being able to default at T, these type of models are built such that the firm can default at any time. The main idea of FPMs is that we no longer only look at the firm's asset value $V(T)$ at maturity time T of the debt, but we also observe if and when the asset value falls below a certain threshold. If this happens, a default occurs.

The process of the firm's asset value $V(t)$ has the same form as in Merton's model, see Equation (3.2.1). However, we also have to observe the default threshold $v(t)$. This can be a constant, but also a time dependent or even a random threshold. It can be exogenously fixed and can be interpreted as a safety rule to protect bondholders: they are allowed to take over when the threshold is hit. It can also be endogenously fixed, it can be made dependent on $V(t)$ and then it can be interpreted as way of maximizing the firm's value by the choice of the threshold.

The default time is defined as $\tau := \inf\{t \in \mathbb{R}_+ : V(t) \leq v(t)\}$. From this default time we can compute the default probability $\mathbb{Q}(\tau \leq t | \tau > s)$ for any $s < t < T$, which has an inverse Gaussian probability distribution under the risk-neutral measure $\mathbb{Q}$ [41].

FPMs have the following drawback: the credit spreads (difference in yield between undefaultable bonds and defaultable bonds of the reference entity) are underpredicted by this model. This means that within this model, the pricing of bonds and also the survival probabilities are both inaccurate. This disadvantage could be countered by making the model less predictable, by for example incorporating jumps in the asset value process [19, 42].

Besides incorporating jumps, FPMs can also be made more realistic by taking into account stochastic interest rates, safety covenants, paying dividends, restrictions on the sale of assets, bankruptcy costs, taxes, debt subordination or strategic, etc. [21, 41]. One of the extensions of the FPM is called a liquidation process. An example of such a model is explained in [17].

Liquidation process models (LPMs) are very similar to first passage models, but in LPMs there is a distinction between a default event and a liquidation. A liquidation of a firm is when it stops with its activity and when the remainder of the company gets divided among the claim holders. When the asset value goes below the

threshold the default event still takes place, but there is no immediate liquidation. Instead a liquidation process begins. After it has completed, this process will determine whether the firm will liquidate or survives. For example, the (weighted) time below the threshold could be measured. If this time is shorter than a predefined time, the company survives. Otherwise, it liquidates.

The last extension of Merton's model we discuss is the extension of incorporating state dependent variables. These models are called state dependent models. A state can represent a recession or an expansion of the economy, the state can represent the firm's external rating or simply the season of the year. Features that might be state dependent include cash-flows, bankruptcy costs and funding costs.

There are various ways to implement state dependent variables into the structural models. For example, cash-flows can follow a geometric Brownian motion which is scaled by the business cycle factor or bankruptcy costs can be scaled by such a state factor as well. An exogenous component will influence the probability of switching between states. Also the threshold can be chosen state-dependent. State-dependency can also be incorporated by using ratings from rating agencies. For example, bond coupons could be represented as a function of ratings and the threshold can be dependent on the ratings. In that case a different rating implies a different state of the model [18, 20].

An advantage of state-dependent models is their ability to reduce the predictability of default. In this model parameters are influenced by exogenous processes, which in their turn influence the default probabilities. The default probabilities are influenced by components from outside the model and are therefore harder to predict. However, just as liquidation process models, these models have not been empirically tested, so we cannot say how well these models perform and how they predict credit spreads [19].

Besides the previously mentioned drawbacks, the main reason for not using structural models is that knowledge about the firms assets and capital structure is needed to calibrate the model correctly. This information cannot always be found in the market and it cannot always be easily obtained. Acquiring accurate information about the value of a company's asset can be difficult or expensive. Usually this information is updated every three to six months, so an up-to-date capital structure of a company can be difficult between update-moments [35]. Therefore, in the next section, we discuss the other important default default model: the reduced form model.

3.2.2. Reduced form models

In the structural approach, the creditworthiness of a company and its survival probabilities are linked to its asset values, whereas in the reduced form approach an exogenous component is used to determine the default of the company. In this section we discuss the main concepts and present an overview of the different kinds of reduced form default models.

There is a big difference between reduced form models and the previously discussed structural models. With structural models we assume full knowledge about the firm. With reduced form models, we assume to have incomplete knowledge of the entity, we assume to have the same information as the market. So, instead of linking the default of a firm to its value, the default time is modelled through an exogenous jump process. The default is the first jump of a Poisson process. The Poisson process can have a deterministic or a stochastic parameter, the latter is also called a Cox process. This parameter can be calibrated to market data, such that the survival probabilities can be computed. The parameter of the Poisson process is called the intensity and therefore these models are also called intensity-based models. The intensity is also known as the hazard rate.

In a reduced form model, we consider a non-negative random variable τ on the probability space $(\Omega, \mathcal{G}, \mathbb{Q})$, satisfying $\mathbb{Q}(\tau = 0) = 0$ and $\mathbb{Q}(\tau > t) > 0$ for any $t \in \mathbb{R}_+$. The random variable τ represents the default time of the reference entity and is the first jump of a Poisson process with intensity $\lambda(t)$. $\mathbb{Q}$ is the risk-neutral probability measure and $\mathcal{G}$ is called the filtration with default monitoring: the filtration with information about the time of default. Mathematically, we can write:

$$\mathcal{G}(t) = \mathcal{F}(t) \vee \sigma(\{\tau < u\}, u \leq t),$$

with $\mathcal{F}(t)$ being the default free market filtration and $\sigma(\{\tau < u\}, u \leq t)$ is the sigma algebra generated by all the sets $\{\tau < u\}$, for which the default time τ is smaller than u and where $u < t$. We use theory about the Poisson process to compute the survival probability after time t conditioned on the survival until time t_0 - the probability that the default happens after time t - of the reference entity. This survival probability is

described by

$$\mathbb{Q}(\tau > t | \mathscr{F}(t_0)) = \mathbb{E}^{\mathbb{Q}}\left[\exp\left(-\int_{t_0}^{t} \lambda(u)\mathrm{d}u\right)\middle| \mathscr{F}(t_0)\right],$$

where we take the risk-neutral expectation, where τ is the time of default and $\lambda(t)$ is the intensity. The intensity itself can be constant, deterministic and time-dependent or even stochastic with some form of dynamics. How the intensity is modelled, influences how the credit curve is constructed. What kind of intensity is chosen, depends on the desired properties of the model.

An advantage of using a reduced form model, is that we can calibrate the intensity and therefore the model to market data, such that we have market-implied survival probabilities, which we can use to build the credit curve. How this credit curve is built, depends on the method we use and the properties of the intensity. In [35] some desired properties of the credit curve building method are stated. Firstly, we want an exact fit to the CDS market quotes provided. Secondly, the interpolation should be sensible. Thirdly, the construction method should be local. Then a change in CDS rate of one maturity year will only change the curve locally. Satisfying this requirement makes it easier to understand model-implied hedges. Fourthly, the curve building algorithm should be fast. However, for this research and for understanding the impact of WWR on the CVA, a fast algorithm is not essential. Furthermore, the curve needs to be smooth. However, there is a conflict between localness and smoothness since smoothness necessarily links together different parts of the curve via their derivatives. We prefer localness to smoothness. Finally, most importantly, with the choice of the intensity we should be able to simulate WWR and asses the impact of it on the CVA of the portfolio. In the next two paragraphs we first give key properties of using deterministic intensity and after that of using stochastic intensity.

Deterministic intensity

There are many deterministic intensity possibilities available, such as: constant, piecewise constant, piecewise linear, cubic splines or based on a different model (with various parameters). An advantage of a varying intensity is that it is possible to calibrate the intensity to the market and take the term structure of credit spreads into account. An implication of a deterministic intensity is that many pricing formula's simplify. Deterministic intensities are appropriate for products that have a low dependency on the volatility of the intensity [35].

Constant hazard rates are the simplest form and therefore easiest to implement. However, constant hazard rates cannot take into account the term structure of credit rates. Therefore, although the method is fast and smooth, it is not sensible and not local at all.

The model that most companies in the CDS market use, is the piecewise constant hazard rate model. This is used the most because of the following two reasons. Firstly, piecewise constant intensities behave better than alternatives such as piecewise linear intensities and they are numerically stable. This means that they do not magnify approximation errors. Secondly, there is no information on the intensities between CDS maturities. Piecewise constant intensities are the simplest assumption that take the term structure of credit rates into account. So, a piecewise constant method is sensible, gives an exact fit, is local and could deliver fast calibration. It is not smooth, but in a conflict between smoothness and localness, localness is preferred. According O'Kane and Gregory, this model is the most suitable to use, considering the available information on the reference entity and considering the described desired properties [24, 35, 25].

Piecewise linear intensities have the advantage of a continuous function. The calibration for piecewise linear intensities would be the same as for piecewise constant intensities. So, it does take into account the term structure of credit rates, the algorithm could be fast and piecewise linear intensities give an exact fit to the CDS market quotes provided. However, piecewise linear intensities are numerically unstable and where the implied intensity and probability becomes negative, this method can lead to arbitrage opportunities [24, 35].

Other alternatives also provide more disadvantages than advantages. Cubic splines, for example, have the advantage of being continuous and smooth. However, cubic splines are less local. A CDS with a far away maturity will impact the entire curve, which seems counter-intuitive. According to Green, another reason for not using more advanced methods, is the fact that CDS traders are not really exposed to the intensities between CDS maturities. Therefore a simpler method is already sufficient [24].

Deterministic hazard rates do not take into account the volatility of the credit spreads. For this stochastic intensities can be used. Also, with the goal of creating a dependency between creditworthiness of a company

and the exposure to this company in mind, a stochastic intensity offers more possibilities.

Stochastic intensity

With a stochastic intensity Poisson process, the intensity and therefore the probability of default itself is random. Since it is both stochastic in the jump variable and in the intensity, this is also called a doubly stochastic Poisson process or a Cox process. Although modeling the survival probabilities can be more complex than with a deterministic intensity, with a stochastic intensity the credit spread volatility can be taken into account [11].

The stochastic intensity can be modelled in a diffusion setting as explained in [11]. An advantage of such a setting is that we can correlate the stochastic interest rate and the intensity easily by correlating the Brownian motions of their diffusion processes. This is a practical advantage for modeling wrong-way risk.

There are various options to model the stochastic intensity, but the fact that the intensity cannot become negative, limits the number of options. A negative intensity on some interval gives negative survival probabilities. Therefore the main choices found in recent literature to model the intensity are log-normal processes or a form of the CIR process. In Section 3.2.5 we first discuss how we use this intensity to take WWR into account, after which we discuss the choice of the form of the intensity in Section 3.3.1.

3.2.3. Further models

In this section we mention other models that are used in practice or that can be found in the literature, but that are not widely used, have not been studied much or lie beyond the scope of this research. We have described key aspects of both structural and reduced form models in previous sections. There are also other models that have properties of both models and are therefore called hybrid models. We did not find much literature on those models. Another type of models are market models. In these models, the survival probabilities are directly modeled through markets payoffs. These models are calibrated to market payoffs and prices, instead of producing them. It is a model that does not really value CDSs, but it calibrates to CDSs. So, with a market model for survival probabilities, we can use the CDS pricing formula to bootstrap survival probabilities from market quotes, such that the generated survival probabilities make these CDSs fair. Then the survival probabilities can be used to price more complicated derivatives [11].

Finally, also credit rating models or financial statement models are used in practice. These models use information from the company, such as their financial status, to determine the likelihood of default for that company. Sometimes also macro-variables like unemployment or level of interest rates are used.

3.2.4. Conclusion default model choice

We discussed different kinds of models for generating the probability of default. The two main approaches for modeling single-name credit curves are the structural approach and the reduced form approach. Structural models are suitable models to create a credit curve and model survival probabilities, since they link the creditworthiness of the company with its financial status. Also recovery rates can be determined endogenously and the models can be used to price equity and bonds. However, these models need much information of the corresponding firm. This is the main difference between structural models and reduced form models: in structural models full knowledge about the firm is assumed. When this is not the case and only market information can be observed, reduced form models offer a solution. These models can be calibrated to market data to take into account the term structure of credit rates and the volatility of credit spreads. We concluded to best use reduced form models are the most suitable for constructing credit curves and price credit derivatives, when only market info is available [35].

Therefore, we use a reduced form model with a stochastic intensity. With this choice of as model, we can compute the credit curve and find the survival probabilities of the counterparty. Due to these survival probabilities of the counterparty and the exposure to that counterparty, we can compute the CVA of the portfolio including WWR. When using a reduced form model, there are multiple ways to incorporate WWR into the CVA calculations. In Section 3.2.5 we discuss the possible approaches of taking WWR into account and we give the reasoning for using correlated stochastic differential equations. Then, in Section 3.3.1 we argue which stochastic differential equations we use to model the intensity of the reduced form default model.

3.2.5. Approaches for pricing counterparty credit risk including wrong-way risk

As stated in Section 2.1, wrong-way risk (WWR) is the adverse relationship between the creditworthiness of the counterparty and the exposure to that counterparty. In terms of the CVA, this means that we want to incorporate the dependency between the creditworthiness of the counterparty and the exposure to the counterparty. For modeling this specific kind of dependence structure, we need an approach that fits within the reduced form model. We choose one of the three main approaches that we found in literature: the SDE approach with correlated dynamics. Why we focus on this approach is explained in this section.

For pricing counterparty credit risk we have found three main categories of approaches that take into account WWR. We explain all three of the approaches in the following subsections and we explain the reasoning for focusing on the SDE approach.

The first approach is proposed by Hull and White [33]. In this approach a reduced form model is used to describe the default probabilities and functional forms are used to establish the relation between the hazard rate of the intensity model (and thus the default probability) and the market risk factors.

The second approach uses copula techniques or similar frameworks to generate the joint distribution of the exposure and the time of default. One of the first papers that describes this approach is [7], but also others use this technique [31, 32, 7, 12].

In the section that follows we discuss the third method, which uses stochastic differential equations (SDEs) to model the hazard rate of the reduced form model. Also the market risk factors (e.g., the interest rate) that drive the price of the financial instruments in the portfolio are modeled this way. Then a dependency is created by correlating the Brownian motions of the SDEs of these variables. Examples of studies of this approach can be found in [39] and [8].

Functional relationship

In this approach a functional relationship is imposed between the survival probability of the counterparty and the value of variables which are related to the exposure to the counterparty, such as the portfolio value or the interest rate level. This could be done via the hazard rate $\lambda(t)$ of a reduced form model, such as in [33], or directly via the probability of default, such as in [27].

In the approach of [33], a reduced form model with hazard rate $\lambda(t)$ is used to model the default probabilities. The hazard rate is coupled via a function $g(t)$ to a market variable $x(t)$: $\lambda(t) = g(x(t))$. Variable x is related to the exposure and can be generated as part of the Monte Carlo simulation used to calculate the CVA. The impact of WWR on the CVA can be assessed by comparing the CVA computed with and without the functional relationship between $x(t)$ and the hazard rate. An example of a function that is tested in [33] is the following:

$$\lambda(t) = \exp[a(t) + b(t)x(t) + \sigma\epsilon], \tag{3.2.2}$$

where $b(t)$ represents the amount of WWR, $x(t)$ is the portfolio value and $a(t)$ is a function of time, with the purpose that the hazard rate can be calibrated to the market credit rates (such that the CDSs in the market still price back to par). $\sigma > 0$ is a constant and it represents the noise in the relation between the hazard rate and the portfolio value, while ϵ is a standard normal random variable. In practice the $\sigma\epsilon$ term is set to zero, since it has a low impact on the results.

Another example of the functional relationship approach is discussed in [27]. In this article the authors impose a direct relationship between the default probability and the market variable $x(t)$, with the following equation:

$$PD = f(x(t)) + \sigma\epsilon,$$

where function $f : \mathbb{R} \to \mathbb{R}$ gives the dependence structure and just as in Equation (3.2.2), σ is a constant that represents the noise in the relation and ϵ is a standard normal random variable. The authors test four forms for the relation function f, to see which function gives the best fit to market data and has the smallest noise. A power, exponential, logarithmic and linear function for f are tested:

$$\begin{aligned} f_1(x(t)) &= A_1 x(t)^{B_1}, \\ f_2(x(t)) &= A_2 e^{x(t)B_2}, \\ f_3(x(t)) &= A_3 + B_3 \ln(x(t)), \\ f_4(x(t)) &= A_4 + B_4 x(t). \end{aligned}$$

The authors conclude that the power function performs best, not the exponential function as used in [33]. Other functional forms are researched in [2].

In [27] the authors describe some great advantages of using a functional relationship as dependence structure. The approach is simplistic from a mathematical point of view and the approach involves a relatively small adjustment to the method used to calculate CVA when the usual assumption of independence between exposure and probability of default is made [33]. Furthermore, it can be back-tested easily: past hazard rates can be estimated from historical data on credit spreads, combined with historical data on x to test whether the assumed relationship between $\lambda(t)$ and $x(t)$ held in the past [33]. It uses a dependence that can be found in the market, so that there is no need for extra variables that cannot be observed in the market [27]. Moreover, the calibration to empirical data is robust [27]. Also, it can be used to incorporate credit triggers. An approximate relationship between the counterparty's credit spreads (and thus hazard rate) and its credit rating can be estimated. Then adjustments to the CVA model can be made, to reflect the counterparty's credit rating. On top of that, models involving a functional relationship between hazard rates and other observable variables are simpler and computationally faster than more complex models found in literature [33].

A drawback of using this method is that it cannot be easily extended for multiple counterparties, multiple trades and different products or multiple interest rates. Additionally, a number of different observable variables can be chosen. Further research is needed to determine variables which work best and to determine the appropriate functional form for the relationship. And for some parameters, historical data is used. That means it is assumed is that historical data are a good prediction for future.

Copula function

This method is also known as a re-sampling technique and is very popular among practitioners as it simplifies the way CVA can be evaluated under WWR. The technique with copula functions creates a multivariate distribution from univariate ones (remember that wrong-way risk means joining the exposure distribution with the distribution for the probability of default in a way other than assuming that the two are independent of each other).

We can generate the marginal distribution for default probability relatively easily, with a reduced form model for example. We do not have an analytic form for the exposure distribution. Using a Monte Carlo method, a discrete set of exposures at a discrete set of times can be obtained. Empirical (discrete) distribution of portfolio values can be obtained using an interval for exposure values and ranking the portfolio values such that one is smaller than the other.

With the two CDFs of the distributions and using a copula function, we can describe the CDF of the joint distribution. This can be used to determine the expectation of the portfolio conditioned on the time of default (or the survival probability) [24]. Both in [7] and in [31, 32] the authors use copula functions to generate a general formula for the CVA of a portfolio of interest rate swaps, including WWR. The authors use known values of CDSs and IRSs and combine these values to form a formula for the CVA value. The impact of WWR on the CVA of their IRS can be assessed by comparing the CVA value computed with the new CVA function from the joint distribution with the CVA computed with two marginal distributions and assuming independence between the variables.

Using a copula function for the dependence structure has some benefits. Copula functions come in all shapes and sizes and they can create many different kinds of dependence structures. For example, different kinds of upper and lower tail dependencies can be introduced. Also, with this approach it is easy to compare the CVA calculation with and without taking WWR into account, since first the exposure and the credit distributions can be considered separately and after that a copula function can be used to introduce dependence. Furthermore, we can use semi-analytical functions to calculate the CVA, which significantly simplifies the whole computational process and semi-analytical functions give better approximations than numerical and can be calculated faster as well [31, 32]. Finally, we can re-use Monte Carlo paths that do not incorporate counterparty credit risk, and impose copula function on top of this. This allows for easy comparison.

However, using copula functions also come with drawbacks. The distribution of the exposure is only known empirically on a set of discrete time points and for a set of Monte Carlo paths. Since the distribution of the exposure can only be obtained empirically, the marginal distribution of the exposure is dependent on the Monte Carlo simulation, choice of grid, number of paths and the method of translating the values of the paths into a distribution. This could result in an inaccurate joint distribution, used for the CVA calculation. Furthermore,

this approach cannot easily be extended for multiple counterparties, multiple trades, different products or multiple interest rates as well. New copula functions and dependencies are needed for an extension. Fitting to market data can be difficult and inaccurate and using the copula function can result in arbitrage situations. Also, it has no mathematical justification [12]. For this reason, we do not choose the copula approach in this thesis.

Stochastic differential equations and correlated dynamics

In this approach a reduced form model with a stochastic hazard rate is used for the default probability and another model with a stochastic process is used to describe the interest rate dynamics. Joint stochasticity is needed to introduce correlation. The dynamics of the hazard rate is correlated with the dynamics of the interest-rate level or with the dynamics of the volatility of the interest rate, by correlating the Brownian motions of the processes.

There are multiple processes available to describe the dynamics of the hazard rate and the interest rate. For the hazard rate often a form of a CIR process is chosen to maintain non-negativity of the hazard rate [29]. For the interest rate there are many possibilities. We discuss the interest rate model in Section 3.1.

The interest rate and the hazard rate processes can be calibrated to market data, to produce accurate exposures to and survival probabilities of the counterparty. Then one or multiple correlation parameters are used to form the dependence structure. For the correlation parameter, often historical data is used, since there are no products in the market to calibrate the correlation parameter to. The impact of WWR can be assessed by varying the correlation parameter(s) and producing the CVA value of both zero and nonzero values of the correlation. Articles that use this approach are for example [39, 9, 16].

For example in the recent article [39], a CCG model is chosen for the interest rate (see [30]). This model provides a stochastic interest rate level, a stochastic interest volatility and a stochastic long-run mean, driven by a two-dimensional Brownian motion. The interest rate level and interest rate volatility are correlated. For the hazard rate a CIR process is chosen. A Cholesky decomposition is used to correlate the Brownian motion of the hazard rate with both the interest rate level and volatility. Then, by varying the correlation parameter for the interest rate level $\rho_{r\lambda}$ and by varying the correlation parameter $\rho_{V\lambda}$ for the interest rate volatility, they asses the impact of WWR on the CVA of interest rate swaps and swaptions. The authors conclude that there is a large effect on the CVA of an IRS for a nonzero value of $\rho_{r\lambda}$ and a small effect on the CVA of IRSs and interest rate swaptions for a nonzero value of $\rho_{V\lambda}$.

This approach has some drawbacks. Because of its simplicity, we can only create one type of dependence structure. We can create a dependence between multiple variables in the SDEs, but we cannot create different tail dependencies for example. Also, it can be difficult to estimate the correlation parameter, since there is no liquid market data to calibrate to available. Estimating can be done by using historical data, but then it is assumed that historical data gives a good prediction of the future. Furthermore, using Monte Carlo processes can be time consuming and computationally intensive and using complex dynamics for the stochastic processes can make the calibration complex. Finally, to calibrate the stochastic hazard rate, liquid CDS option prices are needed. This could be a problem, since CDS options are illiquid financial instruments in many markets.

However, there are also multiple benefits to using this approach. First, the correlated dynamics approach is a natural extension of the yield-curve framework to the credit process. Also, its simplicity is a benefit. This approach involves a relatively small adjustment to the method used to calculate CVA when the usual assumption of independence between exposure and probability of default is made. Furthermore, it can easily be extended for multiple counterparties, multiple trades, different products or multiple interest rates, by adding extra processes, without changing the whole model significantly. Additionally, there are many numerical tools available to model these stochastic processes. On top of that, it is an arbitrage-free setup.

To conclude, although using SDEs as arbitrage-free models to incorporate WWR can be complex, time consuming and computationally intensive, this approach is a natural extension of the yield-curve framework to the credit process. In contrary to the use of copula functions, it is an arbitrage-free method. It involves a relatively small adjustment to the method used to calculate the CVA when the usual assumption of independence between exposure and probability of default is made and it can easily be extended for multiple counterparties, multiple trades and different products or multiple interest rates. These advantages do not hold for the other two approaches and these are the main reasons for choosing this approach above the other approaches.

What kind of SDEs we use to incorporate WWR into the CVA, in particular which process we use to model the the hazard rate, is discussed in Section 3.3. Which we use to model the interest rate has been discussed in Section 3.1.

3.3. Default model

As described in Section 3.2, we use a reduced form model to model the default of the counterparty. We use SDEs to describe both the interest rate and the hazard rate over time. To include WWR into the CVA of the portfolio, we use the approach of correlating the Brownian motions of the SDEs, described in Section 3.2.5. We have done a literature study to find the most suitable SDE's to describe the hazard rate and to asses the impact of WWR.

First we consider log-normal processes as possibilities for the hazard rate, but, ruling them out, we discuss CIR processes. We argue why CIR processes are a reasonable choice for modelling the intensity process. Thereafter we explain why adding jumps to the CIR process might even be more suitable.

After we choose the dynamics for modelling the intensity, we discuss the implementation of the intensity-based reduced form model in Section 3.3.2. Then, in Section 3.3.3, we elaborate on how we introduce a desired dependence between the hazard rate and the interest rate and we explain which problems we have to tackle to get that dependence. Furthermore, in Section 3.3.5 we explain how we choose the model parameters and how we calibrate to artificial market data. We show how the credit curve can be constructed with a reduced form model in Section 3.3.5. How the hazard rate can be calibrated to the credit curve is showed in Section 3.3.5. In Section 3.3.5, we show how we calibrate the hazard rate volatility to artificial Credit Default Swaptions and how we choose the other parameters of the model. Finally, in Section 3.3.4 we have all the ingredients to explain how we use the model to asses the impact of WWR on the CVA of a portfolio of IRSs.

3.3.1. Default intensity modeling of the reduced form default model

As mentioned before, a necessary property of the hazard rate process is that it should not be able to become negative. This would give negative survival properties. This is the only necessary property of the hazard rate, but this already eliminates all the Gaussian models for the hazard rate. This leaves us with the option for log-normal and for CIR processes.

What is left is to find the process with the most desirable properties. According to [23], the hazard rate should be a mean reverting process. Hence, one of the desired properties is that the hazard rate should be mean reverting. Also, an affine diffusion process is desired, since affine dynamics are convenient for efficient computation. Furthermore, some studies show that the variance of the credit spreads grows if the credit spreads grow. This is a desired property as well. Finally, analytically tractable processes are desired as well, since we can easily validate their implementation. In the sections that follow, we discuss three log-normal dynamics used in practice. After we explain why a log-normal process is not a suited option, we elaborate on the CIR and JCIR dynamics and conclude that they have the most desirable properties for modelling the hazard rate.

Lognormal

We searched in literature to find a log-normal process which has the desired properties mentioned before. We have found three dynamics that are used in practice: Dothan, Exponential Vasicek and Black-Karasinksi processes. Unfortunately, the log-normal processes do not have the desired properties.

Dothan process

Dothan dynamics are as folows:

$$d\lambda(t) = a\lambda(t)dt + \sigma\lambda(t)dW(t),$$

with a is a real constant. With this process, conditionally on $\mathcal{F}(s)$, $\lambda(t)$ is log-normally distributed and is therefore always positive. It does have analytical formulas for survival probabilities. Also, the Dothan model could be extended to a shifted log normal distribution. Then it could fit the credit curve and it still has an analytical formula for survival probabilities. However, this formula is very complex: it needs numerical integrations of functions consisting of hyperbolic sines and cosines. Another drawback is that the process is mean reverting if and only if $a < 0$ and then it reverts to zero. Another disadvantage of the Dothan model is that is is not affine.

Exponential Vasicek process

In this model the logarithm of the default intensity follows an Ornstein-Uhlenbeck process under risk neutral

measure. The Exponential Vasicek (EV) process has the following dynamics:

$$\lambda(t) = e^{y(t)},$$
$$dy(t) = \big(\theta - a y(t)\big)\,dt + \sigma W(t), \quad \theta, a, \sigma > 0.$$

Equivalently:

$$d\lambda(t)^{\alpha} = \lambda(t)^{\alpha}\left[\theta + \frac{\sigma^2}{2} - a\ln y(t)^{\alpha}\right]dt + \sigma y(t)^{\alpha} dW(t),$$

where $y_0^{\alpha} > 0$ and $\alpha = \{\theta, a, \sigma\}$. This process is mean reverting. However, it does not have explicit formulas for the ZCB or other financial instruments. The model is sometimes used in practice because it could be extended such that the model exactly fits the current term structure of credit rates. Again, this model is not affine.

Black-Karasinksi process
If the Black and Karasinski model is used to model the default intensity, then the intensity is the exponential of an Ornstein-Uhlenbeck process with time dependent coefficients. Therefore this model cannot give negative values to the default intensity. This model is frequently used by financial engineers and pracitioners for interest rate modelling because it can be calibrated to market data quite well and also to the swaption volatiltity surface [11]. However, the Black-Karasinski model is just as the Exponential Vasicek model not analytically tractable and therefore there are no analytical formulas for survival probabilities.

So, even the lognormal processes that are used in practice, are not as suited to model the hazard rate. Therefore, in the next sections we discuss the other options: CIR processes.

CIR

The most common dynamics to describe the intensity is the Cox-Ingersoll-Ross (CIR) model, which is a square-root diffusion process. Because the CIR process cannot become negative, it is the most common model used for modeling the default intensity. In this section we describe more desirable properties of the CIR process and reasons for choosing the CIR process to model the default intensity. We also discuss the extended CIR process, which is the CIR process with an additional deterministic function to have a good fit of the initial term structure.

The CIR dynamics of intensity λ are the following:

$$d\lambda(t) = \kappa(\mu - \lambda(t))dt + \nu\sqrt{\lambda(t)}dW_{\lambda}(t), \tag{3.3.1}$$

with $W(t)$ a standard Brownian motion under the risk-neutral measure, the parameter κ corresponds to the speed of adjustment to long-term mean μ and ν corresponds to the volatility. The drift factor $\kappa(\mu - \lambda(t))$ ensures mean reversion of the intensity, towards μ. The square root of the intensity in the diffusion term makes sure that negative values of the intensity are impossible. When the intensity becomes very small, the standard deviation factor $\nu\sqrt{\lambda(t)}$ becomes also very small. If the intensity goes to zero, then random shock of intensity also goes to zero. Then the drift factor surely dominates the process and pushes the intensity upwards again. Hence, the intensity cannot become negative. When the Feller condition is satisfied, that is when

$$2\kappa\mu \geq \nu^2,$$

then the CIR process cannot reach the origin at all. A side note has to be made that this is only true in the analytical case. When a CIR process is simulated, a time-discretized scheme is used, where, some schemes can still give negative values for the CIR process. Therefore we have to be cautious when simulating the CIR process. We discuss the implementation of the hazard rate in Section 3.3.2.

In papers of [39, 1, 23, 12] the authors all use the CIR process for modelling the intensity. The authors describe the following advantages of using the CIR process:

1. The CIR process guarantees that the intensity cannot become negative.
2. CIR is used to describe the interest-rate process. Intensity models allow us to apply the results for interest rate modeling in the default model setting, since survival probabilities are interpreted as zero coupon bonds and intensities as instantaneous credit spreads [11].

3. As described above, the CIR process is mean-reverting. Also, when the Feller condition is satisfied and the constant parameters are positive, then there exits an unique solution $\lambda(t)$, adapted to the filtration $\mathcal{F}(t)$ satisfying the SDE (3.3.1) [23].

4. There is a closed form for the survival probability, using a reduced form model with the intensity modelled as a CIR process.

5. Studies show that the variance of the credit spreads grow if the credit spread itself increases (instead of being constant). This is modeled in the CIR process.

6. The CIR process and the extension we will describe, belong to the Affine Jump Diffusion class. Affine dynamics are convenient for efficient computation.

The extended CIR process

Although the CIR process is a good starting point to model the intensity, much research has been done on improving the model [11, 14, 15, 8, 26, 12]. The authors use an extension of the CIR process, which is called the CIR++ process. This process has an extra deterministic time-dependent term, that shifts the CIR process such that the hazard rate is calibrated to market data. The CIR++ model has the following form:

$$\begin{aligned} \lambda(t) &= y(t) + \psi(t), \quad t \geq 0, \\ \mathrm{d}y(t) &= \kappa(\mu - y(t))\mathrm{d}t + \nu\sqrt{y(t)}\mathrm{d}W(t), \end{aligned} \tag{3.3.2}$$

where $\psi(t)$ is a deterministic function, and also depends on κ, μ, ν, y_0, with κ, μ, ν, y_0 positive deterministic constants with the same meaning as in the normal CIR model. So, $\psi(t) = \psi(t; \kappa, \mu, \nu, y_0)$, however, we omit the last four parameters for notational convenience. ψ should be integrable on closed intervals. We take $y(t)$ to be a CIR process [29]. As usual, $W(t)$ is a standard Brownian motion process under the risk neutral measure. Again, the CIR++ cannot become zero, as long as the Feller condition is satisfied. The initial condition parameter is $y(t_0)$. Therefore at time $t_0 = 0$, we have $\lambda(t_0) = y(t_0) + \psi(t_0)$. This means we have another initial condition:

$$\psi(t_0) = \lambda(t_0) - y(t_0).$$

The ++ in the CIR++ model stands for a shifted CIR process: the extra deterministic function that is added to the process, such that the process can be calibrated to the term structure of credit rates. The extra deterministic term of the CIR++ model makes sure that the generated (implied) survival probability curve (credit curve) from the model agrees with a given credit curve and this allows for an automatic calibration of the term structure of credit rates [8, 12].

Like CIR, CIR++ ensures strictly positive and mean-reverting paths with the additional advantage of fully calibrating to market data via the function ψ, for t $\geq$ 0. Moreover, there are closed-form solutions for zero-coupon bonds if we model the interest rate with a zero-coupon bond. Since survival probabilities are analogue to zero-coupon bonds, the CIR++ also gives closed-form solutions for survival probabilities, just as in the CIR model [26, 8]. Also, the CIR++ model extension is more analytically tractable and avoids problems concerning the use of numerical solutions (compared to the CIR model)[10].

Although it might seem that the CIR++ is the obvious choice to model the hazard rate, the CIR++ has some drawbacks. The volatilities of CDSs implied by the CIR++ model are usually lower than the CDS volatilities quoted in the market with CDS options [9]. With the CIR++ process as intensity, the intensity cannot attain large levels (such as 50%) of implied volatility for CDS rates, they never exceed levels higher than 30% [11, 14, 13]. However, it is shown that market implied volatilities easily exceed 50% [4, 11]. Although the CDS volatilities quoted in the market are not liquid and therefore there should not be paid too much attention to this drawback, the authors still introduce more volatility by adding jumps [9].

The reason that the CIR++ cannot attain high levels of volatility is twofold. The shift parameter $\psi(t)$ needs to stay positive and this limits the configurations of parameters, since for some values of parameters $\psi(t)$ becomes negative. With these limited possibilities for the parameters, it is hard to find values that give high values of implied volatility. The second problem is more fundamental and is related to the structure of the square root diffusion dynamics. For the explanation we consider the homogeneous CIR dynamics described in Equation (3.3.1), since the following holds for both the CIR and the CIR++ dynamics. These dynamics generate a high implied volatility for option prices if the volatility parameter ν is high. However, the value of ν is restricted by the Feller condition. Since we still want the intensity to remain positive, we restrict the

parameters of the dynamics with the condition of $2\kappa\mu \geq \nu^2$. This restriction tells us that if volatility parameter ν is large, then we must have a large κ and/or μ as well. Both of these cases are undesirable and work against a high volatility.

For high values of κ, the speed of the mean-reverting process increases. This means that the process goes towards the long-term mean faster and hence the randomness reduces more quickly in time. So, for the same value of ν, the process has less stochasticity. Therefore, high values of κ counter the high value of ν and the implied volatility decreases [13].

High values of μ correspond to a high value of the long-term mean. This is undesirable since this means that the intensity will possibly attain very high values [13].

In [4] the authors show that in practice implied volatilities can easily reach volatilities of 50% or higher. This is the reason that there are situations where no realistic values of the parameters can be found. Therefore, in [26, 9, 14, 15, 38] the authors present the following solution: including jumps into the CIR++ model. What follows, is the JCIR++ model.

JCIR

The JCIR process is the CIR process with added jumps. With the same analogy as in Section 3.3.1, the JCIR++ is the JCIR process with an added time-dependent deterministic function. The dynamics of intensity in the JCIR++ model are almost the same as for the CIR++ process, but now include a jump term:

$$\begin{aligned} \lambda_J(t) &= y_J(t) + \psi(t), \quad t \geq 0, \\ \mathrm{d}y_J(t) &= \kappa(\mu - y_J(t))\mathrm{d}t + \nu\sqrt{y_J(t)}\mathrm{d}W(t) + J(t)\mathrm{d}X_P(t), \\ J(t) &= \sum_{i=1}^{X_P(t)} J_k, \end{aligned} \tag{3.3.3}$$

with all the parameters are the same as in Section 3.3.1) and where $X_P(t)$ is a Poisson process with jumps arrival rate (intensity) $\xi > 0$ and jump sizes equal to one. $J(t)$ is an exponential random variable, such that the jump size distribution is on $\mathbb{R}^+$. This is assumed such that the jumps can only have positive values and therefore there are only upward jumps. This makes sure that the JCIR(++) process cannot become negative by a jump. The mean of the exponential distribution is $\gamma > 0$. Hence, the larger ξ, the more frequent the jumps. The larger γ, the larger the sizes of the occurring jumps.

According to Ameur, Brigo and Errais [26] and Brigo and El-Bachir [14], the JCIR++ model can be calibrated to the CDS term structure and a few default swaptions, to price and hedge other credit derivatives consistently. The authors show that the model implies plausible volatility smiles and they state that the valuation of more exotic instruments like Bermudan default swaptions requires the use of a model that accurately incorporates both the term structure of default swap rates, and the dynamical movements and changes of this term structure [26, 14]. A side note must be made that the single-name default swap markets are not very liquid, especially default swaptions are not liquid. Hence, calibration of the model with many parameters on swaptions from the market would become inaccurate. Therefore, we use synthetic CDS and Default Swaption data for the calibration. We discuss the calibration to Default Swaptions in Section 3.3.5.

Conclusion modelling the hazard rate process

To conclude, we have not found a better process to model the default intensity than the CIR process or an extension of the CIR process. In the most recent literature, the most common model to simulate the stochastic intensity is the CIR model or some extension of the CIR model. The reasons for this choice can be found in Sections 3.3.1 and 3.3.1, but the most relevant reasons are the following: the intensity remains non-negative and with restrictions of the parameters it stays positive. Although log-normal processes are positive as well, CIR processes have more desirable properties. The (J)CIR(++) process can have an exact fit of any observed term structure of credit rates. Furthermore, the CIR process is analytically tractable, it gives analytical formulas for bond prices, CDS prices and credit default swaptions. Other positive processes are not analytically tractable, affine or mean-reverting. Therefore, we only use the CIR process and extensions of the CIR process in the default model. In the section that follows, we discuss the implementation of the default model.

3.3.2. Implementation

We use the mean reverting square-root CIR++ process for the hazard rate of the default model. Defined under the risk-neutral $\mathbb{Q}$-measure, the process is described in Equation (3.3.2). Before we go into the implementa-

tion of the CIR++ model, we first discuss more properties of the CIR process. We discuss the distribution of the CIR process, after which we discuss the challenges with standard discretization schemes and explain the reason for using the reflecting Euler scheme to implement the CIR process. The reflecting Euler scheme is as follows:

$$\begin{aligned}\hat{y}_{i+1} &= y_i + \kappa(\mu - y_i)\Delta t + \nu\sqrt{y_i \Delta t}Z,\\ y_{i+1} &= |\hat{y}_{i+1}, 0|.\end{aligned}$$

The $y(t)$ is modeled with a CIR process and therefore it follows the non-central chi-squared distribution. Conditional on state $y(s), s < t$, the distribution at time t is given by [6],

$$y(t)|y(s) \sim \bar{c}(t,s)\chi^2\left(\bar{d}, \bar{k}(t,s)\right), \quad t > 0, \tag{3.3.4}$$

with

$$\bar{c}(t,s) = \frac{\nu^2}{4\kappa}\left(1 - e^{-\kappa(t-s)}\right), \quad \bar{d} = \frac{4\kappa\mu}{\nu^2}, \quad \bar{k}(t,s) = \frac{4\kappa e^{-\kappa(t-s)}}{\nu^2\left(1 - e^{-\kappa(t-s)}\right)} y(s). \tag{3.3.5}$$

For $\kappa = 0.2$, $\mu = 0.001$ $\nu = 0.02$, $t_0 = 0$, $T = 3$, we have plotted two densities for the intensity $\lambda(T)$ in Figure 3.1.

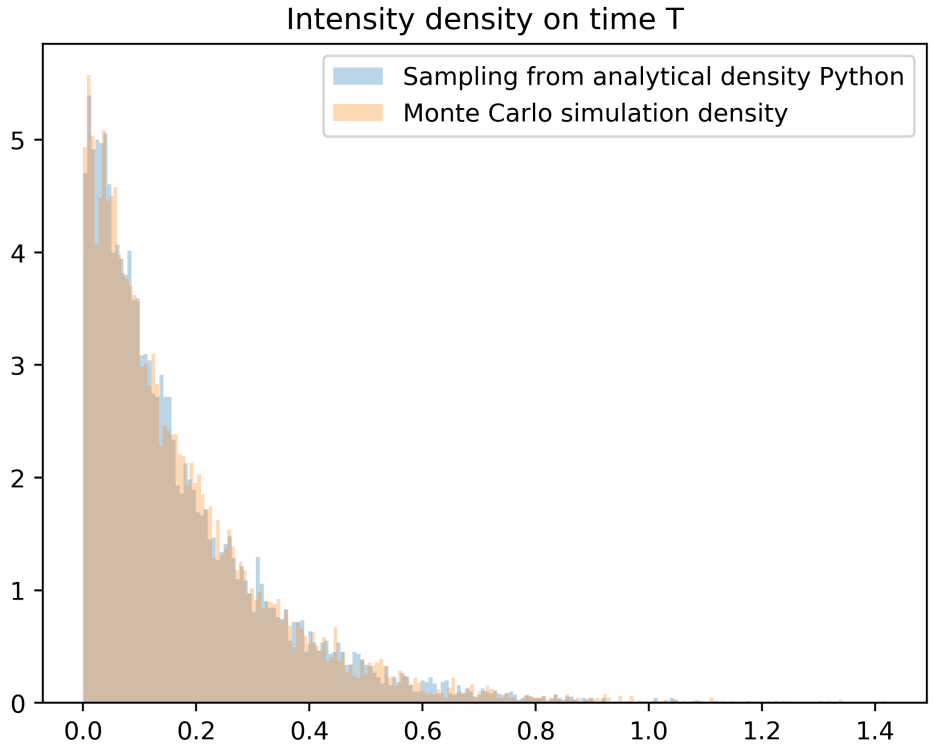

Figure 3.1: Intensity λ densities, calculated at $T = 3$, with parameter values: $\kappa = 0.5$, $\mu = 0.05$, $\nu = 0.15$, 10^5 paths and 400 Steps per year.

Using knowledge of the noncentral chi-squared distribution, this gives the following mean and variance of the $y(t) \mid y(s)$ process:

$$\begin{aligned}\mathbb{E}\left[y(t)|\mathscr{F}(s)\right] &= y(s)e^{-\kappa(t-s)} + \mu\left(1 - e^{-\kappa(t-s)}\right),\\ \mathbb{V}ar\left[y(t)|\mathscr{F}(s)\right] &= y(s)\frac{\nu^2}{\kappa}\left(e^{-\kappa(t-s)} - e^{-2\kappa(t-s)}\right) + \mu\frac{\nu^2}{2\kappa}\left(1 - e^{-\kappa(t-s)}\right)^2.\end{aligned} \tag{3.3.6}$$

Since we know the distribution at time t, conditional on the state $y(s)$ at time $s < t$, an exact simulation scheme sounds like a sensible choice to simulate the paths of the CIR process $y(t)$. With this method, an

instant $y(t_{i+1})$ can be found, conditional on $y(t_i)$, by computing $\bar{c}(t_{i+1},t_i)$ and $\bar{k}(t_{i+1},t_i)$ and then sample from noncentral chi-squared distribution as follows:

$$y(t_{i+1}) \sim \bar{c}(t_{i+1},t_i)\chi^2\left(\bar{d},\bar{k}(t_{i+1},t_{i+1})\right), \tag{3.3.7}$$

with some initial value $y(t_0)=y_0$. However, as we correlate the interest rate with the hazard rate in the wrong-way risk model, the distribution of the hazard rate changes. Therefore, it would be difficult to use the exact simulation scheme. Instead, we use a different discetization scheme. Standard discretization schemes such as the Euler and the Milstein schemes, are based on sampling from the normal distribution. Because the samples from a normal distribution can become arbitrarily negative, the CIR process with a Euler or Milstein scheme can become negative as well. The continuous CIR process is not able to become negative, but without the right discetization scheme, the discretization can become negative.

A solution to this problem is using a truncated Euler scheme. However, this solution can give inaccurate Monte Carlo paths. Because of the truncation, the paths become numerically different than if you would follow the original paths. The accuracy is parameter-dependent and the truncated paths can be highly inaccurate, especially when the Feller condition is not satisfied [6]. Another drawback of using this scheme is the possibility to have paths with multiple consecutive steps equal to zero. This should not be possible, because for the CIR process the origin is accessible, but it is not an absorbing boundary [6].

A better solution is to use the reflecting Euler scheme. With this scheme, the Monte Carlo paths stay positive and they instantly move away from zero. The reflecting Euler scheme is given by the original Euler scheme and an extra computation:

$$\hat{y}_{i+1} = y_i + \kappa(\mu-\lambda_i)\Delta t + \nu\sqrt{y_i\Delta t}Z, \tag{3.3.8}$$

$$y_{i+1} = |\hat{y}_{i+1}| \tag{3.3.9}$$

There are other schemes possible that preserve positivity, however, we choose to use this simple scheme and do not focus on the impact of the simulation scheme. To check whether the simulation is done correctly, we compare the density simulated with the reflecting Euler scheme with the density simulated by an exact simulation scheme.

3.3.3. Introducing dependency

In this section we explain how we introduce dependency between the hazard rate and the interest rate. We explain the used Cholesky decomposition and we discuss the problem that arises when correlating the Brownian motions of the hazard rate and the interest rate process: the leaking correlation problem.

Introducing correlation

To introduce dependence between the hazard rate and the interest rate, we correlate the Brownian increments of the stochastic processes with correlation parameter ρ. We have correlated Brownian increments, which reads $\mathrm{d}W_y(t)\cdot\mathrm{d}W_r(t)=\rho\mathrm{d}t$ and $\mathbb{E}\left[W_y(t)\cdot W_r(t)\right]=\rho t$.

The Cholesky decomposition of a matrix, is the decomposition of the form $\mathbf{C}=\mathbf{L}\mathbf{L}^*$, where $\mathbf{L}$ is a lower triangular matrix with positive real diagonal entries and $\mathbf{L}^*$ is the (conjugate) transpose of $\mathbb{L}$. For the hazard rate together with the interest rate, we have a two dimensional Brownian motion (independent of each other) that we wish to correlate with a correlation of ρ: $\mathbf{Z}(t)=[Z_1(t),Z_2(t)]^T$. Then for the (2×2)-correlation matrix $\mathbf{C}$, we have the following decomposition:

$$\mathbf{C} \overset{\text{def}}{=} \begin{bmatrix} 1 & \rho \\ \rho & 1 \end{bmatrix} = \begin{bmatrix} 1 & 0 \\ \rho & \sqrt{1-\rho^2} \end{bmatrix}\begin{bmatrix} 1 & \rho \\ 0 & \sqrt{1-\rho^2} \end{bmatrix}.$$

Our matrix $\mathbf{C}$ is symmetric and the signs of the pivots are positive, so it is positive definite, so we can use the Cholesky decomposition. Then, we can compute the correlated two-dimensional Brownian motion with $\mathbf{L}\cdot\mathbf{W}(t)$, which reads:

$$\begin{bmatrix} W_r(t) \\ W_y(t) \end{bmatrix} = \begin{bmatrix} 1 & 0 \\ \rho & \sqrt{1-\rho^2} \end{bmatrix}\begin{bmatrix} Z_1(t) \\ Z_2(t) \end{bmatrix} = \begin{bmatrix} Z_1(t) \\ \rho Z_1(t)+\sqrt{1-\rho^2}Z_2(t) \end{bmatrix}.$$

Using these Brownian motions, will give the desired correlation between the Brownian motions. However, we have noticed a problem when simulating the interest rate and the hazard rate. Over time, the correlation between the interest rate and the hazard rate does not stay the same. We notice that the correlation goes to 0 as time goes to infinity. We call this phenomenon 'leaking correlation' and is discussed in the next section.

Leaking correlation problem

In this section we explain how we overcome the leaking correlation problem when using the Hull-White dynamics for the interest rate and the CIR++ dynamics for the hazard rate under the risk-neutral measure:

$$\begin{aligned}\lambda(t) &= y(t) + \psi(t), \quad t \geq 0,\\ \mathrm{d}y(t) &= \kappa(\mu - y(t))\mathrm{d}t + \nu\sqrt{y(t)}\mathrm{d}W_y(t),\\ \mathrm{d}r(t) &= k(\theta(t) - r(t))\mathrm{d}t + \eta\mathrm{d}W_r(t),\end{aligned} \tag{3.3.10}$$

where $W_r(t)$ and $W_y(t)$ are correlated Brownian motions, such that $\mathrm{d}W_y(t)\cdot\mathrm{d}W_r(t) = \rho\mathrm{d}t$, for correlation parameter ρ. To understand the problem of leaking correlation, we have to know the difference between instantaneous correlation and terminal correlation. Instantaneous correlation is the correlation ρ_{inst} that we use to correlate the Brownian increments. The terminal correlation is the actual correlation between the interest rate and the hazard rate as generated by the model. The terminal correlation is calculated using the following:

$$\begin{aligned}\rho_{\text{term}}(t) &= \text{corr}(\lambda(t), r(t))\\ &= \frac{\text{COV}(\lambda(t), r(t) \mid \mathscr{F}(0))}{\sqrt{\mathbb{V}ar[\lambda(t) \mid \mathscr{F}(0)]\,\mathbb{V}ar[r(t) \mid \mathscr{F}(0)]}}\\ &= \frac{\mathbb{E}\left[(\lambda(t) - \mathbb{E}\left[\lambda(t)|\mathscr{F}(0)\right])(r(t) - \mathbb{E}\left[r(t) \mid \mathscr{F}(0)\right]) \mid \mathscr{F}(0)\right]}{\sqrt{\mathbb{V}ar[\lambda(t) \mid \mathscr{F}(0)]\,\mathbb{V}ar[r(t) \mid \mathscr{F}(0)]}}.\end{aligned} \tag{3.3.11}$$

Note that since function $\psi(t)$ is purely deterministic, the correlation between the hazard rate $\lambda(t)$ and the interest rate $r(t)$ when using CIR dynamics for the hazard rate is the same as when we use CIR++ dynamics. So, the shifted dynamics $\lambda(t)$ give the same correlation as the non-shifted dynamics $y(t)$:

$$\begin{aligned}\text{COV}[\lambda(t), r(t) \mid \mathscr{F}(0)] &= \mathbb{E}\left[(\lambda(t) - \mathbb{E}\left[\lambda(t) \mid \mathscr{F}(0)\right])(r(t) - \mathbb{E}\left[r(t) \mid \mathscr{F}(0)\right]) \mid \mathscr{F}(0)\right]\\ &= \mathbb{E}\left[(y(t) + \psi(t) - (\mathbb{E}\left[y(t) \mid \mathscr{F}(0)\right] + \psi(t)))(r(t) - \mathbb{E}\left[r(t) \mid \mathscr{F}(0)\right]) \mid \mathscr{F}(0)\right]\\ &= \mathbb{E}\left[(y(t) - \mathbb{E}\left[y(t) \mid \mathscr{F}(0)\right])(r(t) - \mathbb{E}\left[r(t) \mid \mathscr{F}(0)\right]) \mid \mathscr{F}(0)\right].\end{aligned}$$

In Figure 3.2 an example of leaking correlation is shown. In the figure we use an instantaneous correlation of 0.5 and we plot it against the correlation of the computed Monte Carlo paths of the hazard rate and interest rate. The latter is called the sample correlation. To solve this leaking correlation problem, we need to find out which instantaneous correlation ρ_{inst} gives the desired terminal correlation ρ_{term}. To find this instanteneous correlation, we look at the analytical formula of the terminal correlation and rewrite this, such that we have the instantaneous correlation expressed as the terminal correlation. To do so, we first find the covariance between the hazard rate $\lambda(t)$ and the interest rate $r(t)$, which is equal to the covariance between $r(t)$ and $y(t)$. We write both $r(t)$ and $y(t)$ as their integral form. For both we use an integrating factor such that we write the interest rate and the non-shifted hazard rate as a deterministic term and a stochastic term:

$$\begin{aligned}y(t) &= e^{-\kappa t}y(0) + \kappa\mu\int_0^t e^{-\kappa(t-u)}\mathrm{d}u + \nu\int_0^t e^{-\kappa(t-u)}\sqrt{y(u)}\mathrm{d}W_y(u),\\ r(t) &= \mathrm{e}^{-kt}r(0) + k\int_0^t \theta(u)\mathrm{e}^{-k(t-u)}\mathrm{d}u + \eta\int_0^t \mathrm{e}^{-k(t-u)}\mathrm{d}W_r(u).\end{aligned}$$

Then the covariance can be computed as follows:

$$\begin{aligned}\text{COV}[\lambda(t), r(t) \mid \mathscr{F}(0)] &= \text{COV}[y(t), r(t) \mid \mathscr{F}(0)]\\ &= \mathbb{E}\left[(\lambda(t) - \mathbb{E}\left[\lambda(t) \mid \mathscr{F}(0)\right])(r(t) - \mathbb{E}\left[r(t) \mid \mathscr{F}(0)\right]) \mid \mathscr{F}(0)\right]\\ &= \mathbb{E}\left[\left(\eta\int_0^t e^{-k(t-u)}\mathrm{d}W_r(u)\right)\left(\nu\int_0^t e^{-\kappa(t-u)}\sqrt{y(u)}\mathrm{d}W_y(u)\right)\middle|\mathscr{F}(0)\right]\\ &= \eta\nu\int_0^t e^{-(k+\kappa)(t-u)}\rho(u)\,\mathbb{E}\left[\sqrt{y(u)}\middle|\mathscr{F}(0)\right]\mathrm{d}u,\end{aligned} \tag{3.3.12}$$

where we used that $\mathbb{E}\left[\mathrm{d}W_r(u)\mathrm{d}W_y(u)\middle|\mathscr{F}(0)\right] = \rho(u)\mathrm{d}u$, we used a generalization of Ito-isometry and we used Fubini's theorem to switch the integral and the expectation. Hence, using Equation (3.3.11) and Equation

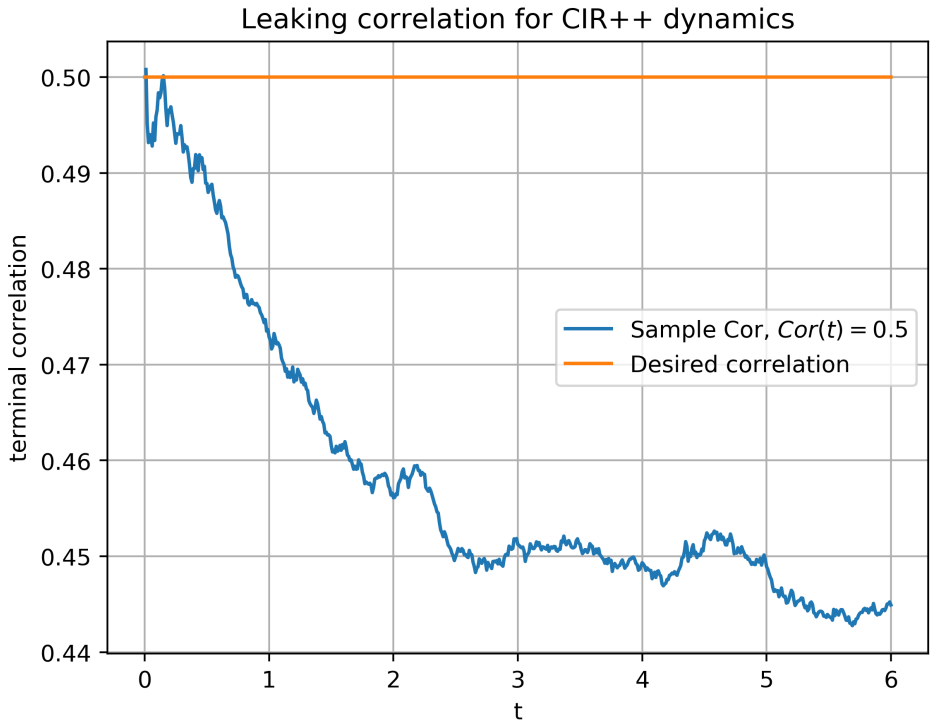

Figure 3.2: Correlation between the hazard rate and the interest rate with CIR++ and HW dynamics, $\rho(t) = 0.5$, $\kappa = 0.5$, $\mu = 0.05$, $\nu = 0.15$, $\lambda(0) = 0.04$, $r(0) = 0.05$, $k = 0.5$, $\eta = 0.1$ and $0 \leq t \leq 3$.

(3.3.12), we have:

$$\begin{aligned}\rho_{\text{term}}(t) &= \frac{\eta\nu\int_0^t e^{-(k+\kappa)(t-u)}\rho(u)\,\mathbb{E}\left[\sqrt{y(u)}\middle|\mathscr{F}(0)\right]\mathrm{d}u}{\sqrt{\mathbb{V}ar[\lambda(t)\,|\,\mathscr{F}(0)]\,\mathbb{V}ar[r(t)\,|\,\mathscr{F}(0)]}} \\ &=: \int_0^t \rho(u)f(u)\mathrm{d}u \cdot \frac{\eta\nu e^{-(k+\kappa)t}}{\sqrt{\mathbb{V}ar[\lambda(t)\,|\,\mathscr{F}(0)]\,\mathbb{V}ar[r(t)\,|\,\mathscr{F}(0)]}}, \\ f(u) &:= e^{(k+\kappa)u}\,\mathbb{E}\left[\sqrt{y(u)}\right],\end{aligned} \tag{3.3.13}$$

$$\Longrightarrow \rho^{\text{CIR}}(t) = \frac{1}{f(t)}\frac{\mathrm{d}}{\mathrm{d}t}\left(\rho_{\text{term}}(t)\frac{\sqrt{\mathbb{V}ar[\lambda(t)\,|\,\mathscr{F}(0)]\,\mathbb{V}ar[r(t)\,|\,\mathscr{F}(0)]}}{\eta\nu e^{-(k+\kappa)t}}\right), \tag{3.3.14}$$

where $\mathbb{V}ar\,[\,\lambda(t)|\mathscr{F}(0)]$ is given in Equation (3.3.6) and $\mathbb{V}ar\,[\,r(t)|\mathscr{F}(0)]$ is given in Equation (3.1.8). If we want for example a terminal correlation of 0.5 between the interest rate and the hazard rate, then we use Equation (3.3.14). In this equation, we set the terminal correlation $\rho_{\text{term}}(t)$ equal to 0.5. Then this equation will provide the instantaneous correlation that we need for a desired terminal correlation of 0.5: $\rho_{\text{inst}}(t) = \rho^{\text{CIR}}(t)$.

To use Equation (3.3.14), we need the expectation of the square-root CIR process. We could use the density of the CIR process and compute it as follows:

$$\mathbb{E}\left[\sqrt{y(u)}\right] = \int_0^\infty \sqrt{u} f_{y(t)}(u)\mathrm{d}u.$$

However, this function is computationally intensive and we have found that it gives numerical instability

around $t = 0$. According to [6], the expectation and variance of a square-root CIR process, are as follows:

$$\mathbb{E}\left[\sqrt{y(t)}\middle|\mathscr{F}(0)\right] = \sqrt{2\bar{c}(t,0)}e^{-\bar{k}(t,0)/2}\sum_{i=0}^{\infty}\frac{1}{i!}\left(\frac{\bar{k}(t,0)}{2}\right)^i\frac{\Gamma\left(\frac{1+\bar{d}}{2}+i\right)}{\Gamma\left(\frac{\bar{d}}{2}+i\right)},$$

$$\mathbb{V}ar\left[\sqrt{y(t)}\middle|\mathscr{F}(0)\right] = \bar{c}(t,0)(\bar{d}+\bar{k}(t,0)) - 2\bar{c}(t,0)e^{-\bar{k}(t,0)}\left(\sum_{i=0}^{\infty}\frac{1}{i!}\left(\frac{\bar{k}(t,0)}{2}\right)^i\frac{\Gamma\left(\frac{1+\bar{d}}{2}+i\right)}{\Gamma\left(\frac{\bar{d}}{2}+i\right)}\right)^2,$$

where $\bar{c}(t,0)$, $\bar{d}$ and $\bar{k}(t,0)$ are defined as in Equation (3.3.5) and with $\Gamma(i)$ the Gamma function. This analytic expression for the square-root expectation of the CIR process is also computationally intensive [6]. Therefore, we use an approximation for this expectation, given by [6]:

$$\mathbb{E}\left[\sqrt{y(t)}|\mathscr{F}(0)\right] \approx \sqrt{\bar{c}(t,0)(\bar{\lambda}(t,0)-1) + \bar{c}(t,0)\bar{d} + \frac{\bar{c}(t,0)\bar{d}}{2(\bar{d}+\bar{\lambda}(t,0))}} =: \varepsilon(t), \tag{3.3.15}$$

with $\bar{c}(t,0)$, $\bar{k}(t,0)$ and $\bar{d}$ given in Equation (3.3.5) and the parameters κ, μ, and ν are the parameters from the CIR++ dynamics given in Equation (3.3.10). A note to this formula, is that it is well-defined if the Feller condition is satisfied.

In Figure 3.3 it can be observed that using the approximation $\varepsilon(t)$ of Equation (3.3.15) for computing the analytical terminal correlation fits the sample correlation (the correlation from the simulated MC paths) quite well. In the figure the blue line is the sample correlation of the MC paths, when the instantaneous correlation $\rho(t)$ is equal to 0.5. In the figure, the green line is the analytical correlation, computed with Equation (3.3.12) and Equation (3.3.15). This means that we can use Equation (3.3.15) as approximation for $\mathbb{E}\left[\sqrt{y(t)\,|\,\mathscr{F}(0)}\right]$ in Equation (3.3.14). Hence, we have a time-dependent instantaneous correlation, that solves the leaking correlation problem. Simulating the hazard rate and the interest rate with a instantaneous correlation equal to Equation (3.3.14), gives a terminal correlation approximately equal to the desired terminal correlation. In Figure 3.3 two other lines can be observed as well. The desired terminal correlation can be observed as the orange line, which is equal to 0.5. Also, the red line can be observed, which is the terminal correlation of the simulated hazard rate and interest rate. This simulated terminal correlation is computed using the instantaneous correlation equal to Equation (3.3.14) and using Equation (3.3.15) for $\mathbb{E}\left[\sqrt{y(t)\,|\,\mathscr{F}(0)}\right]$. To check whether Equation (3.3.14) works well, we did a convergence analysis. We calculated the average absolute difference between the desired correlation and the sample correlation when we use Equation (3.3.14), for multiple number of paths. With a Monte Carlo simulation, this difference should converge to zero. In Table 3.1 these errors are shown. It can be seen that for an increasing number of paths, the error decreases. Since for every number of steps the number of paths increase with a factor 10, theoretically, the standard error of the MC simulation should decrease with a factor of $\sqrt{10}$. Hence, if (3.3.11) works well, the difference between the desired correlation and the terminal correlation should converge as well. If you divide entry (i,j) by entry (i,j+1) in Table 3.1, you get the decrease factors. Decrease factors higher than 1 indicate convergence. In Table 3.4 these decrease factors are shown.

Steps - Paths	10^2	10^3	10^4	10^5
50	$4.45722976\cdot10^{-2}$	$2.4885973\cdot10^{-2}$	$9.5174467\cdot10^{-3}$	$6.92248\cdot10^{-3}$
100	$5.3003384\cdot10^{-2}$	$1.67489424\cdot10^{-2}$	$8.78655964\cdot10^{-3}$	$4.9071107\cdot10^{-3}$
200	$1.18245224\cdot10^{-1}$	$3.2514144\cdot10^{-2}$	$9.8393681\cdot10^{-3}$	$2.7531267\cdot10^{-3}$
400	$1.03691794\cdot10^{-1}$	$1.963234\cdot10^{-2}$	$7.410646\cdot10^{-3}$	$4.52903745\cdot10^{-3}$

Table 3.1: Average absolute difference between desired correlation ρ and terminal correlation for $t \in [0,5]$.

Table 3.4 shows decrease factors with a value larger than 1. This means that the average absolute difference between the desired correlation ρ and the terminal correlation converges. Hence, we have found the solution for the leaking correlation problem when using CIR++ dynamics.

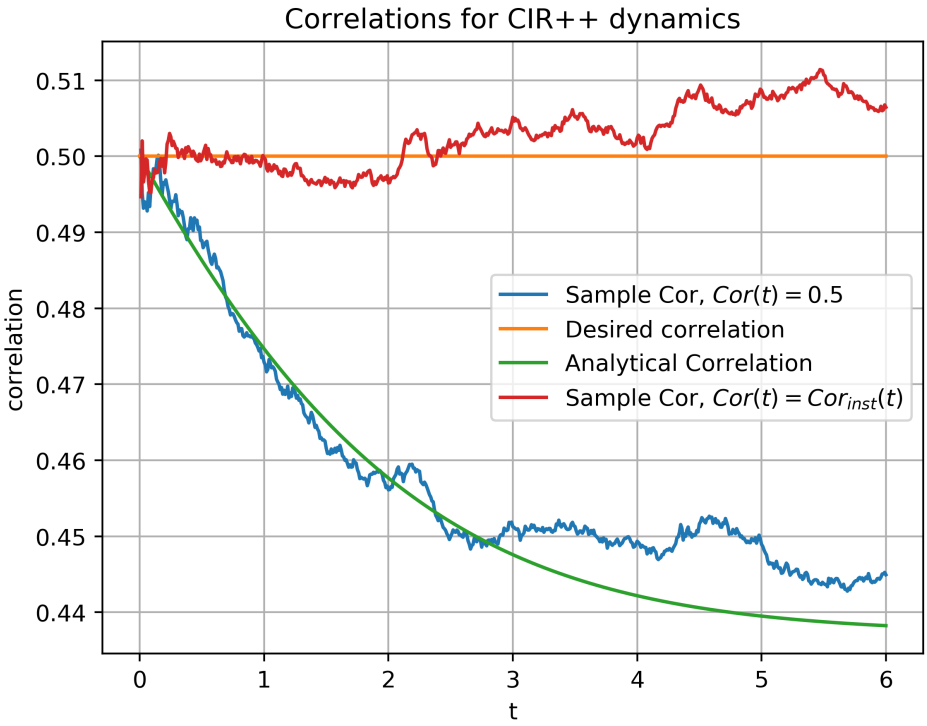

Figure 3.3: Correlation between the hazard rate and the interest rate using a CIR++ model, where we plotted the analytical and sample correlation using instantaneous correlation $\rho = 0.5$. Also, using Equation (3.3.14) the sample correlation is plotted together with the desired correlation of 0.5. Used parameters: $\rho = 0.5$, $\kappa = 0.5$, $\mu = 0.17$, $\nu = 0.4$, $\lambda(0) = 0.17$, $r(0) = 0.05$, $k = 0.5$, $\eta = 0.1$ and $0 \le t \le 5$.

Steps - error^i/error^{i+1}			
50	1.791	2.614	1.374
100	3.164	1.906	1.790
200	3.6379	3.304	3.573
400	5.281	2.649	1.636

Table 3.2: Error decrease of terminal correlation convergence.

Leaking correlation JCIR++

In this section we describe solving the leaking correlation problem when using the JCIR++ dynamics for the hazard rate, instead of CIR++ dynamics. The JCIR++ dynamics, as described in (3.3.16), are the following:

$$\begin{aligned} \lambda_J(t) &= y_J(t) + \psi(t), \quad t \ge 0, \\ \mathrm{d}y_J(t) &= \kappa(\mu - y_J(t))\mathrm{d}t + \nu\sqrt{y_J(t)}\mathrm{d}W(t) + J(t)\mathrm{d}X_P(t). \end{aligned} \tag{3.3.16}$$

Since the function $\psi(t)$ is purely deterministic, the correlation between the hazard rate $\lambda_J(t)$ and the interest rate $r(t)$ is the same when using JCIR dynamics as when using JCIR++ dynamics. Hence, in this section we only look at the non-shifted JCIR dynamics $y_J(t)$.

We solve the leaking correlation problem for the JCIR dynamics the same way we solved it for the CIR dynamics. First we find the analytical terminal correlation between the hazard rate with JCIR dynamics and the interest rate with Hull-White dynamics. Then we rewrite the formula and express the instantaneous correlation in terms of the terminal correlation.

First, for the terminal correlation, we need the covariance $\mathrm{COV}\left[y_J(t), r(t) \mid \mathcal{F}(0)\right]$ between $y_J(t)$ and the variances of $r(t)$ and $y_J(t)$, see Equation (3.3.11). To use this equation we first need the integral representation of both $y_J(t)$ and the interest rate.

Using Ito's lemma and an integrating factor, we have the following expression for $y_J(t)$, conditioned on $y_J(s)$:

$$\begin{aligned} y_J(t) \mid y_J(s) =& y_J(s)e^{-\kappa t} + \kappa\mu \int_s^t e^{-\kappa(t-u)}\mathrm{d}u \\ &+ \int_s^t e^{-\kappa(t-u)} J(u)\mathrm{d}X_P(u) + \nu \int_s^t \sqrt{y_J(u)}e^{-\kappa(t-u)}\mathrm{d}W(u). \end{aligned} \tag{3.3.17}$$

For the covariance we need the expectation of $y_J(t)$.

$$\mathbb{E}\left[y_J(t) \mid \mathscr{F}(0)\right] = y_J(0)e^{-\kappa t} + \kappa\mu \int_0^t e^{-\kappa(t-u)}\mathrm{d}u + \mathbb{E}\left[\int_0^t e^{-\kappa(t-u)} J(u)\mathrm{d}X_P(u)\middle|\mathscr{F}(0)\right], \tag{3.3.18}$$

where we used that the expectation of an Ito integral equals zero. We assume that $J(t)$ and $X_P(u)$ are both independent. We define $f(u) = e^{-\kappa(t-u)}$ and find the expectation of the jump-term in Equation (3.3.18) by using the so-called smoothing lemma from [3]. Since we have

$$\mathbb{E}\left[\int_0^t |f(u)|\mathrm{d}u\right] = \int_0^t e^{-\kappa(t-u)}\mathrm{d}u = \frac{1}{\kappa}\left(1-e^{-\kappa t}\right) < \infty,$$

the expectation is given by:

$$\begin{aligned} \mathbb{E}\left[\int_0^t f(u_-)J\mathrm{d}X_P(u)\right] &= \xi\,\mathbb{E}[J]\,\mathbb{E}\left[\int_0^t e^{-\kappa(t-u_-)}\mathrm{d}u\right] \\ &= \xi\gamma\frac{1}{\kappa}\left(1-e^{-\kappa t}\right). \end{aligned}$$

Hence, the expectation of $y_J(t)$ is given by:

$$\mathbb{E}\left[y_J(t) \mid \mathscr{F}(0)\right] = y_J(0)e^{-\kappa t} + \kappa\mu \int_0^t e^{-\kappa(t-u)}\mathrm{d}u + \gamma\xi \int_0^t e^{-\kappa(t-u)}\mathrm{d}u \tag{3.3.19}$$

$$= y_J(0)e^{-\kappa t} + \mu\left(1-e^{-\kappa t}\right) + \xi\gamma\frac{1}{\kappa}\left(1-e^{-\kappa t}\right). \tag{3.3.20}$$

In Equation (3.3.19) we used that $J(t)$ is an exponential random variable, with expectation $\mathbb{E}[J(t)] = \gamma$ and $\mathbb{E}[\mathrm{d}X_P(t)] = \xi\mathrm{d}t$. The latter is due to the properties of a Poisson process with intensity parameter ξ.

Then, using Equation (3.3.11) for the covariance, Equations (3.3.17) and (3.1.6) for the integral representation of $y_J(t)$ and $r(t)$ and Equations (3.3.19) and (3.1.7) for their expectations, the covariance of $y_J(t)$ and $r(t)$ becomes:

$$\begin{aligned} \mathrm{COV}\left[y_J(t), r(t) \mid \mathscr{F}(0)\right] = \mathbb{E}\Bigg[&\left(\int_0^t e^{-\kappa(t-z)} J(u)\mathrm{d}X_P(u) + \nu\int_0^t e^{-\kappa(t-u)}\sqrt{y_J(u)}\mathrm{d}W_y(u)\right. \\ &\left.-\gamma\xi\int_0^t e^{-\kappa(t-u)}\mathrm{d}u\right)\left(\eta\int_0^t e^{-\kappa(t-u)}\mathrm{d}W_r(u)\right)\Bigg|\mathscr{F}(0)\Bigg] \\ = \eta\nu\int_0^t e^{-(k+\kappa)(t-u)}\rho(u)\,\mathbb{E}\left[\sqrt{y_J(u)}\middle|\mathscr{F}(0)\right]\mathrm{d}u. \end{aligned} \tag{3.3.21}$$

In the equations above, $J(t)$ and $X_P(t)$ are independent. Some of the terms drop out due to Ito's table and together with Ito's isometry and Fubini's theorem this gives the result. Hence, the covariance for the JCIR process with the interest rate can be computed in the same way as when using the CIR process. So, we need to compute $\mathbb{E}\left[\sqrt{y_J(t)}\right]$.

We also need the variance of $y_J(t)$. Looking at Equation (3.3.17), we observe that the JCIR process consists of two parts: the jump term, equal to $\int_0^t e^{-\kappa(t-u)}J(u)\mathrm{d}X_P(u)$ and the CIR-part of the JCIR process, which is the rest of Equation (3.3.17). This CIR-part looks like a CIR-process, but because of the jumps, it is not exactly like the CIR process. Using Equation (3.3.17) and the properties of the variance, we can write the variance of $y_J(t)$

conditional on $y_J(s)$ as follows:

$$\begin{aligned}\mathbb{V}ar\left[\,y_J(t)\middle|\mathscr{F}(s)\right] =& \mathbb{V}ar\left[\,y_J(s)e^{-\kappa t}+\kappa\mu\int_s^t e^{-\kappa(t-u)}\mathrm{d}u+\nu\int_s^t\sqrt{y_J(u)}e^{-\kappa(t-u)}\mathrm{d}W(u)\middle|\mathscr{F}(s)\right]\\ &+\mathbb{V}ar\left[\int_s^t e^{-\kappa(t-u)}J(u)\mathrm{d}X_P(u)\middle|\mathscr{F}(0)\right]\\ &+2\mathrm{COV}\left[\,y_J(s)e^{-\kappa t}+\kappa\mu\int_s^t e^{-\kappa(t-u)}\mathrm{d}u+\nu\int_s^t\sqrt{y_J(u)}e^{-\kappa(t-u)}\mathrm{d}W(u),\right.\\ &\left.\int_s^t e^{-\kappa(t-u)}J(u)\mathrm{d}X_P(u)\middle|\mathscr{F}(0)\right].\end{aligned}\tag{3.3.22}$$

Since $\mathbb{E}[J(t)]=\gamma$ and $\mathbb{E}[X_P(t)]=\xi t$, the process $JX_P(t)-\xi t\gamma$, is a martingale, and is called a compensated Poisson Process. To find the variance of the jump term, we use kind Itô isometry, formulated in [37]. Since we have

$$\mathbb{E}\left[\int_s^t|f(u)|^2\mathrm{d}u\middle|\mathscr{F}(s)\right]=\mathbb{E}\left[\int_s^t e^{-2\kappa(t-u)}\mathrm{d}u\middle|\mathscr{F}(s)\right]=\frac{1}{2\kappa}\left(1-e^{-2\kappa(t-s)}\right)<\infty,$$

we can find the variance of the jump term as follows:

$$\begin{aligned}\mathbb{V}ar\left[\int_s^t e^{-\kappa(t-u)}J(u)\mathrm{d}X_P(u)\middle|\mathscr{F}(s)\right] &= \mathbb{E}\left[\left(\int_s^t e^{-\kappa(t-u)}J(u)\mathrm{d}X_P(u)-\gamma\mathbb{E}[J(t)]\int_s^t e^{-\kappa(t-u)}\mathrm{d}u\right)^2\middle|\mathscr{F}(s)\right]\\ &= \mathbb{E}\left[\left(\int_s^t e^{-\kappa(t-u)}\left(J(u)\mathrm{d}X_P(u)-\gamma\mathbb{E}[J(t)]\mathrm{d}u\right)\right)^2\middle|\mathscr{F}(s)\right]\\ &= \xi\,\mathbb{E}\left[J^2\right]\mathbb{E}\left[\int_s^t e^{-2\kappa(t-u_-)}\mathrm{d}u\right]\\ &= \xi\left(\mathbb{V}ar\left[J\right]+\mathbb{E}\left[J\right]^2\right)\frac{1}{2\kappa}\left(1-e^{-2\kappa(t-s)}\right)\\ &= \xi\gamma^2\frac{1}{\kappa}\left(1-e^{-2\kappa(t-s)}\right).\end{aligned}\tag{3.3.23}$$

We can remove the absolute operator, since both the exponential distribution and $f(u)$ only assume positive values. Furthermore, we need to find the first term of Equation (3.3.22). This can be computed as follows:

$$\begin{aligned}&\mathbb{V}ar\left[\,y_J(s)e^{-\kappa t}+\kappa\mu\int_s^t e^{-\kappa(t-u)}\mathrm{d}u+\nu\int_s^t\sqrt{y_J(u)}e^{-\kappa(t-u)}\mathrm{d}W(u)\middle|\mathscr{F}(s)\right]\\ =&\mathbb{E}\left[\left(\nu\int_s^t e^{-\kappa(t-u)}\sqrt{y_J(u)}\mathrm{d}W(u)\right)^2\middle|\mathscr{F}(s)\right]\\ =&\mathbb{E}\left[\,\nu^2\int_s^t e^{-2\kappa(t-u)}y_J(u)\mathrm{d}u\middle|\mathscr{F}(s)\right]\\ =&\nu^2\int_s^t e^{-2\kappa(t-u)}\mathbb{E}\left[\,y_J(u)\middle|\mathscr{F}(s)\right]\mathrm{d}u\\ =&\nu^2\int_s^t e^{-2\kappa(t-u)}\left(y_J(s)e^{-\kappa(t-s)}+\mu\left(1-e^{-\kappa(t-s)}\right)+\xi\gamma\frac{1}{\kappa}\left(1-e^{-\kappa(t-s)}\right)\right)\mathrm{d}u\\ =&y_J(s)\frac{\nu^2}{\kappa}\left(e^{-\kappa(t-s)}-e^{-2\kappa(t-s)}\right)+\mu\frac{\nu^2}{2\kappa}\left(1-e^{-\kappa(t-s)}\right)^2\\ &+\xi\gamma\frac{\nu^2}{2\kappa^2}\left(1-e^{-2\kappa(t-s)}\right)-\xi\gamma\frac{\nu^2}{\kappa^2}\left(e^{-\kappa(t-s)}-e^{-2\kappa(t-s)}\right)\\ =&\mathbb{V}ar\left[y(t)|y(s)=y_J(s),\mathscr{F}(s)\right]+\xi\gamma\frac{\nu^2}{2\kappa^2}\left(1-e^{-2\kappa(t-s)}\right)-\xi\gamma\frac{\nu^2}{\kappa^2}\left(e^{-\kappa(t-s)}-e^{-2\kappa(t-s)}\right).\end{aligned}\tag{3.3.24}$$

In the first equation we used Equation (3.3.17) and the definition of the variance, in the second equation we used Ito isometry and in the third equation we used the theorem of Fubini to switch the integral and the expectation. In the fourth equation we used the expectation of $y_J(u)$ from Equation (3.3.19). It can be observed that Equation (3.3.24) can be written as the variance of the CIR process plus a jump term part, if the initial value $y(s)$ equals the initial value of the JCIR process $y_J(s)$. The covariance between the jump term and

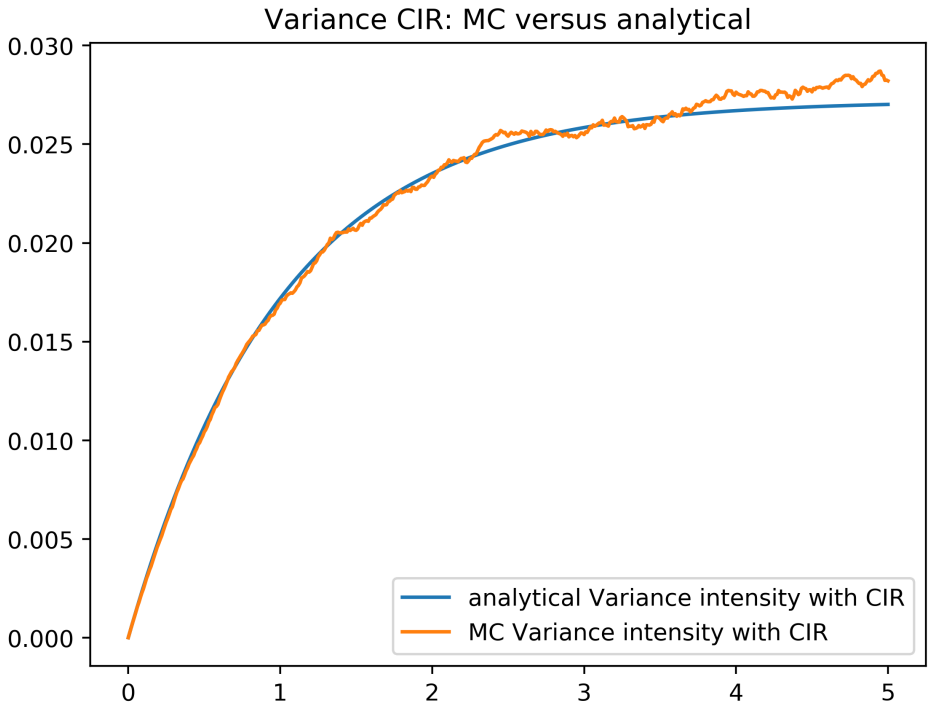

Figure 3.4: Variance of $\lambda(t)$, analytical vs. simulation

the CIR-part of the JCIR from Equation (3.3.17) can be computed as follows:

$$
\begin{aligned}
&\mathrm{COV}\Big[y_J(s)e^{-\kappa t} + \kappa\mu\int_s^t e^{-\kappa(t-u)}\mathrm{d}u + \nu\int_s^t \sqrt{y_J(u)}e^{-\kappa(t-u)}\mathrm{d}W(u), \\
&\quad \int_s^t e^{-\kappa(t-u)}J(u)\mathrm{d}X_P(u)\Big|\mathscr{F}(s)\Big] \\
&= \mathbb{E}\Big[\Big(\nu\int_s^t e^{-\kappa(t-u)}\sqrt{y_J(u)}\mathrm{d}W(u)\Big)\cdot \\
&\quad \Big(\int_s^t e^{-\kappa(t-u)}J\mathrm{d}X_P(u) - \xi\mathbb{E}[J]\mathbb{E}\Big[\int_s^t e^{-\kappa(t-u_-)}\mathrm{d}u\Big]\Big)\Big|\mathscr{F}(s)\Big] \\
&= \mathbb{E}\Big[\Big(\nu\int_s^t e^{-\kappa(t-u)}\sqrt{y(u)}\mathrm{d}W_y(u)\Big) \\
&\quad \cdot\Big(\int_s^t e^{-\kappa(t-u_-)}J\mathrm{d}X_P(u) - \xi\mathbb{E}[J]\mathbb{E}\Big[\int_s^t e^{-\kappa(t-u_-)}\mathrm{d}u\Big]\Big)\Big|\mathscr{F}(s)\Big] \\
&= \mathbb{E}\Big[\Big(\nu\int_s^t e^{-\kappa(t-u)}\sqrt{y(u)}\mathrm{d}W_y(u)\Big)\Big(\int_s^t e^{-\kappa(t-u_-)}J\mathrm{d}X_P(u)\Big)\Big|\mathscr{F}(s)\Big] \\
&\quad -\mathbb{E}\Big[\Big(\nu\int_0^t e^{-\kappa(t-u)}\sqrt{y(u)}\mathrm{d}W_y(u)\Big)\Big(\xi\mathbb{E}[J]\mathbb{E}\Big[\int_0^t e^{-\kappa(t-u_-)}\mathrm{d}u\Big]\Big)\Big|\mathscr{F}(s)\Big] \\
&= 0,
\end{aligned}
$$

where we used the independence of $J(t)$ and $X_P(t)$ and Ito's table in the final equation, giving the result of 0. This means that we can compute the variance of Equation (3.3.22) by adding the variance of the CIR-part of the JCIR process (Equation (3.3.24) to the variance of the jump term (Equation (3.3.23)):

$$
\begin{aligned}
\mathbb{V}ar\left[\, y_J(t)\middle|\mathscr{F}(s)\right] = {} & y_J(s)\frac{\nu^2}{\kappa}\left(e^{-\kappa(t-s)} - e^{-2\kappa(t-s)}\right) + \mu\frac{\nu^2}{2\kappa}\left(1-e^{-\kappa(t-s)}\right)^2 \\
& + \xi\gamma\frac{\nu^2}{2\kappa^2}\left(1-e^{-2\kappa(t-s)}\right) - \xi\gamma\frac{\nu^2}{\kappa^2}\left(e^{-\kappa(t-s)} - e^{-2\kappa(t-s)}\right) \\
& + \xi\gamma^2\frac{1}{\kappa}\left(1-e^{-2\kappa(t-s)}\right)
\end{aligned}
\tag{3.3.25}
$$

So, now we need to compute $\mathbb{E}\left[\sqrt{y_J(t)}\right]$ before we can compute the covariance in Equation (3.3.21). To find

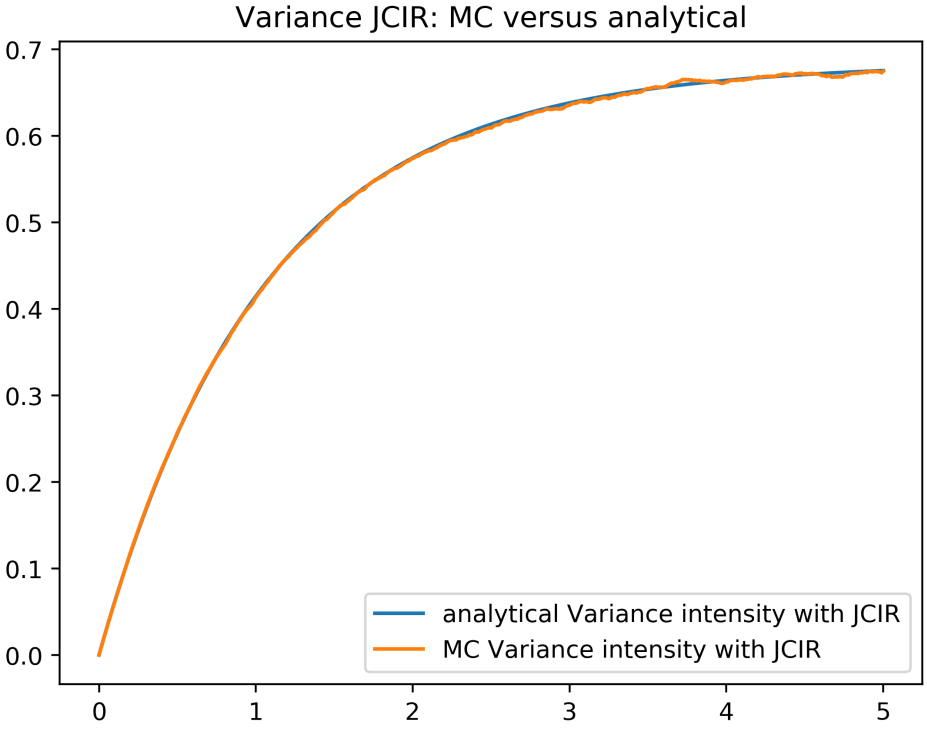

Figure 3.5: Variance of $\lambda_J(t)$, analytical vs. simulation

an approximation of $\mathbb{E}\left[\sqrt{y_J(t)}\right]$, we use the delta method [6, 40, 36]. This method uses a first-order Taylor expansion to find an approximation for the function of a random variable, given its expectation and variance. The method gives the following approximation for the expectation of $\sqrt{y_J(t)}$:

$$\mathbb{E}\left[\sqrt{y_J(t)}\right] \approx \sqrt{\mathbb{E}\left[y_J(t)\right] - \frac{1}{4}\frac{\mathbb{V}ar\left[y_J(t)\right]}{\mathbb{E}\left[y_J(t)\right]}}. \tag{3.3.26}$$

Filling in Equation (3.3.25) for the variance and Equation (3.3.19) for the expectation, this gives approximation that we use to compute the covariance in (3.3.21) and to compute the terminal correlation between the hazard rate using JCIR++ dynamics and the interest rate using HW1F dynamics. With Equations (3.3.21), (3.3.25), (3.1.8), and (3.3.11). We have all the ingredients to compute the terminal correlation. This gives the following intantaneous correlation $\rho^J(t)$ to use for the JCIR++ model:

$$\begin{aligned}\rho^J_{\text{term}}(t) &= \text{corr}(\lambda_J(t), r(t) \mid \mathscr{F}(0)) \\ &= \frac{\eta\nu\int_0^t e^{-(k+\kappa)(t-u)}\rho(u)\mathbb{E}\left[\sqrt{y_J(u)}\middle|\mathscr{F}(0)\right]\mathrm{d}u}{\sqrt{\mathbb{V}ar\left[y_J(t)\mid\mathscr{F}(0)\right]\mathbb{V}ar\left[r(t)\mid\mathscr{F}(0)\right]}} \end{aligned} \tag{3.3.27}$$

$$\implies \rho^J(t) = \frac{1}{e^{(k+\kappa)t}\mathbb{E}\left[\sqrt{y_J(t)}\right]}\frac{\mathrm{d}}{\mathrm{d}t}\left(\rho_{\text{term}}(t)\frac{\sqrt{\mathbb{V}ar[\lambda_J(t)\mid\mathscr{F}(0)]\mathbb{V}ar[r(t)\mid\mathscr{F}(0)]}}{\eta\nu e^{-(k+\kappa)t}}\right) \tag{3.3.28}$$

In Figure 3.6 the terminal correlation between simulated hazard rate $\lambda_J(t)$ and interest rate $r(t)$ can be observed, when using an instantaneous correlation of 0.5 (the blue line). It is plotted together with the analytically computed terminal correlation, using Equation (3.3.27) (the green line). It can be observed that the analytically computed terminal correlation fits the sample correlation of the MC paths well. This means that we can use Equation (3.3.28) to counter the leaking correlation happening in the JCIR model. Using Equation (3.3.28) for the instantaneous correlation, where we set the desired terminal correlation equal to 0.5,

gives a terminal sample correlation between the simulated hazard rate and interest rate paths, which can be observed in Figure 3.6 (the red line). The new terminal correlation between the simulated MC paths is approximately equal to the desired correlation. This indicates that we solved the leaking correlation problem. To be sure, we made simulations with different number of paths, to show that the terminal sample correlation converges to the desired correlation. The results are shown in Table 3.3. What is noticeable in Figure 3.6 is that the correlation with leaking correlation (the blue and the green plot) starts at a relatively low value. Instead of starting at the desired correlation such as with the CIR++ dynamics, the correlation starts at approximately 0.225. This is because of the independent jumps of the JCIR++ dynamics, which have an impact on the correlation from the first time step. The independent jumps ruin the correlation between the interest rate and the hazard rate, if the instantaneous-correlation-function Equation (3.3.28) is not used.

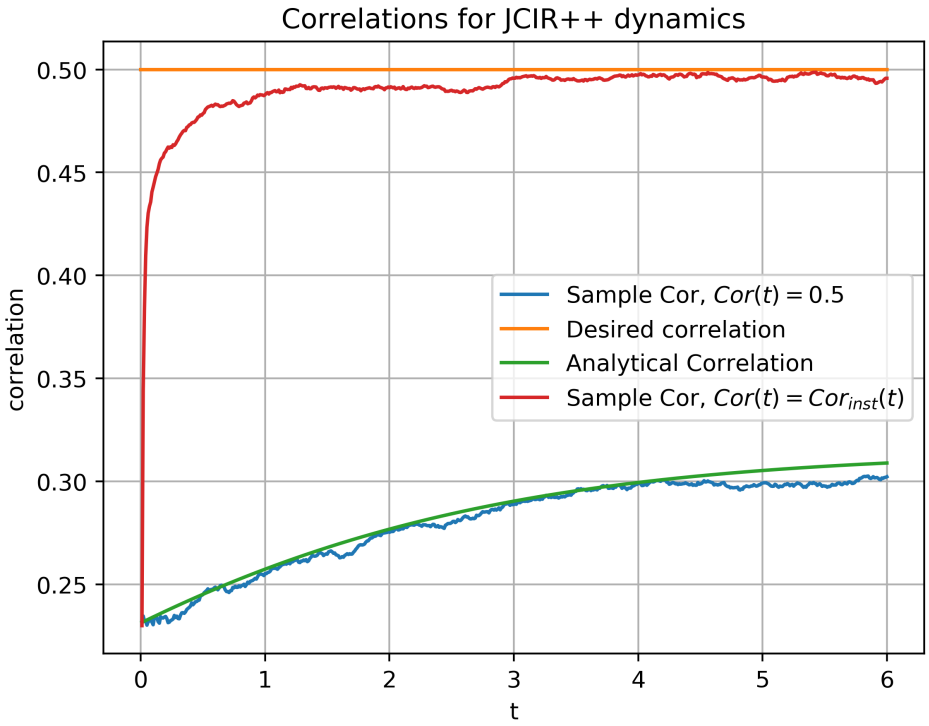

Figure 3.6: Correlation between the hazard rate and the interest rate, where we used the JCIR++ model for the hazard rate. The analytical and sample correlation when instantaneous correlation $\rho = 0.5$ can be observed. Also, using Equation (3.3.28), the sample correlation is plotted together with the desired correlation of 0.5. Used parameters: $\rho = 0.5$, $\kappa = 0.5$, $\mu = 0.17$, $\nu = 0.4$, $\lambda(0) = 0.17$, $r(0) = 0.05$, $k = 0.5$, $\eta = 0.1$, $\xi = 5$, $\gamma = 0.025$ and $0 \leq t \leq 3$.

Steps - Paths	10^2	10^3	10^4	10^5
50	$7.95341627990 \cdot 10^{-2}$	$5.023266444 \cdot 10^{-2}$	$1.0689934964 \cdot 10^{-2}$	$4.2006386773 \cdot 10^{-3}$
100	$4.30938101 \cdot 10^{-2}$	$1.61451830 \cdot 10^{-2}$	$1.115575 \cdot 10^{-2}$	$3.25605120 \cdot 10^{-3}$
200	$7.60809912157 \cdot 10^{-2}$	$2.6111051482 \cdot 10^{-2}$	$8.049784412 \cdot 10^{-3}$	$4.80418674835 \cdot 10^{-3}$

Table 3.3: Average absolute difference between desired correlation ρ and terminal correlation for $t \in [0,5]$.

Steps - $error^i / error^{i+1}$			
50	1.5833156	4.69906174	1.09920337
100	2.66914348	1.44725126	3.4261613
200	2.91374674	3.24369575	1.67557692

Table 3.4: Error decrease of terminal correlation convergence.

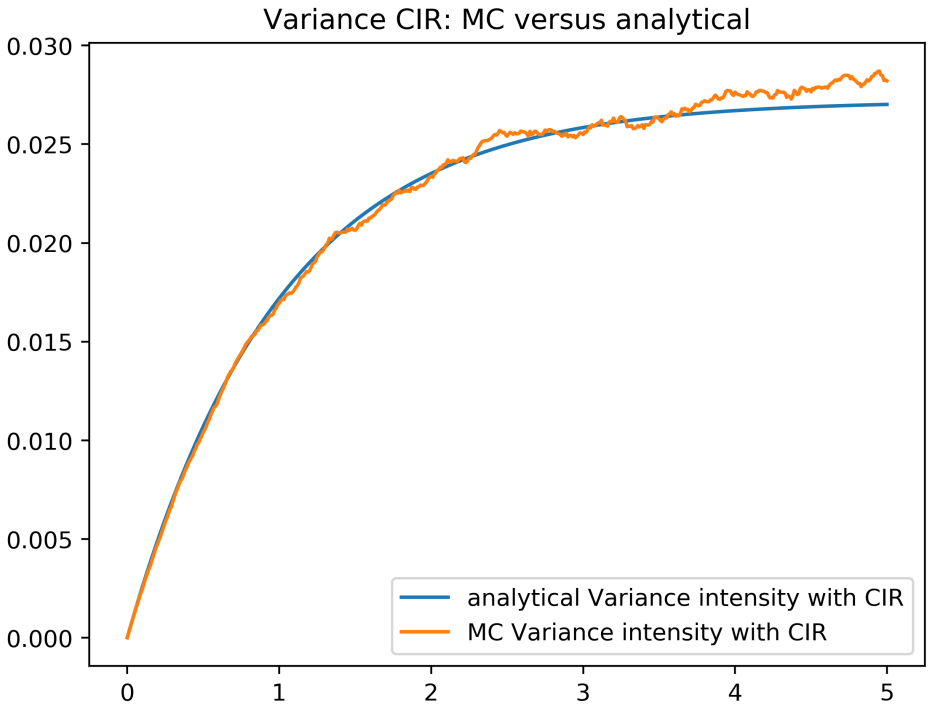

Figure 3.7: Variance of $\lambda(t)$, analytical vs. simulation

3.3.4. Method of assessing WWR on the CVA of an IRS

To asses the impact of Wrong-Way Risk on the CVA of the portfolio, we have chosen an intensity-based reduced form credit model and Hull-White one factor interest rate model to combine to make the CVA model. As we suggest in Section 3.3.1, the most suitable option to model the hazard rate of the credit model is a form of CIR processes, with or without jumps included. Therefore, we want to use both the CIR process as the JCIR process to model the hazard rate and see the influence on the CVA of the portfolio. Also, this way we can determine how much of the CVA is determined by the choice of the hazard rate process and how much by the influence of WWR.

To make objective statements about the impact of WWR, we need to calibrate the model to the market. Then we can make realistic statements about the impact. Another reason for calibrating the model is that we need to be able to fairly compare the two credit models. Calibrating both models to the market is a way to do so. Another reason for calibrating the models, especially the volatility parameter of the models, is the following. As explained in 3.3.1, the reason that the JCIR++ model might be more suitable to use than the CIR++ model, is the fact that for some situations (i.e. CDSO quotes), no realistic values of the parameters of the CIR++ can be found, because the CIR++ can not reach the high volatility in that situation. This is something we want to check ourselves.

We calibrate both models to term structure of credit rates and and we use a CDS option (CDSO) quote to calibrate the volatility parameter ν. The latter is needed since the jumps of the JCIR model create extra model volatility, compared to the CIR model. For the other parameters, we choose the same values for both models and investigate the influence of them on the CVA. Instead of calibrating both the JCIR and the CIR model to the actual market for some counterparty, we choose to use synthetic quotes. We use synthetic CDS quotes to create a credit curve to calibrate the models to. These synthetic CDS quotes are described by their tenor, loss-given-default and credit rate that makes the prices of the CDSs equal to zero. With a reduced form intensity model with piecewise constant hazard rates, we can build the credit curve from these quotes. Then we can build two functions $\psi(t)$ and $\psi_J(t)$ that we can add to the hazard rate such that the models produce the same credit curve. We explain this in more detail in Section 3.3.5. The CIR and JCIR dynamics with the added shift $\psi(t)$ is called the CIR++ and the JCIR++ model. For the volatility parameter we use a synthetic quote, generated by the JCIR++ model. This way, we have a JCIR++ model that is already perfectly calibrated and we only need to calibrate the CIR++ model. More about the calibration of the volatility parameter is described in

Section 3.3.5.

To begin the assessment, we first choose the input for the CVA model: the constant L_{GD} of the IRS, the credit curve, the parameters $\kappa, \mu, \nu, y(0)$ (see Equation (3.3.16) for the JCIR++ model, the parameters $\kappa, \mu, y(0)$ (see Equation (3.3.2) for the CIR++ model, the yield curve, the parameters k and η for the HW model (see Equation (3.1.1). Then we calibrate the credit part of the model. Hereafter we produce the discount factors, needed to produce a exposure profile of the IRS in the portfolio, after which we produce the survival probabilities, also needed for the CVA calculation. If we then assume a correlation between the hazard rate and the interest rate, we have all the elements needed to compute the CVA of the portfolio. Hence, we compute the CVA for multiple values of correlation parameter ρ, such that we can see the impact of the correlation. Since we assume the correlation parameter is historically chosen and we assume that it is the desired correlation for the future years until maturity of the portfolio, we make sure the correlation between the interest rate and the hazard rate stays the desired correlation. We do this by solving the leaking correlation problem. We describe this problem in more detail in Section 3.3.3. When we have the values of the CVA(ρ), depending on the correlation, we can compare the CVA results using a CIR++ model with the results using a JCIR++ model. Thus, we can determine how much of the impact on the CVA comes from the model choice and how much comes from wrong-way risk. Also, this gives more insight when we must decide what kind of model we want to use to determine WWR and determine the CVA of a interest rate portfolio.

3.3.5. Calibration of the default model

A benefit of the CVA model, is that the calibrations to the interest-rate market and to the credit market can be be done separately. A separate calibration is less complex and has the practical benefit that the IR desk and the XVA desk can calibrate the model separately, without needing information from each other. A side note given by [8]: usually the authors do not calibrate to option data, since CDS options and other related volatility products have wide bid-ask spreads. This means that it is difficult to find the actual value of the product that is needed for calibration.

According to [8], the instantaneous correlation between the two diffusion processes (correlating the Brownian motions) has a negligible impact on the CDS price. Therefore the calibration of the model on both the CDS prices and swaps can be done separately, even when the correlation is not zero. The authors argue that it is even the only good choice for modeling the intensity in a diffusion setting, if the properties that need to be taken into account are the need to remain positive and the analytical tractability of the process. Hence, the authors calibrate to CDS data with correlation $\rho = 0$, using the separate calibration and set ρ to a desired value after calibration.

For the calibration of the default model, we use Credit Default Swaps (CDSs) to calibrate to the term structure of the credit curve and we use Credit Default Swaptions (or Credit Default Options) to calibrate the volatility parameter of the CIR dynamics. First we explain how we construct the credit curve from the CDSs from the market. After which we show how we adjust the dynamics such that the survival probabilities from the market are equal to the survival probabilities from the model. Finally we show how we use Credit Default Swaptions to find the volatility ν of the dynamics.

Constructing the credit curve

Here we explain how the credit curve can be constructed by bootstrapping survival probabilities from a set of CDS quotes from the market, using a reduced form model and an interpolation method. We explain what Credit Default Swaps are, how we price them and how we calibrate the model to them, such that we can construct the credit curve. We use this credit curve to calibrate both the CIR++ and the JCIR++ dynamics of the hazard rate to the market.

Credit Default Swaps are contracts that are used to transfer credit default risk from one party to another. A CDS can be seen as an insurance against a defaulting counterparty that would otherwise result in missing some payments.

A CDS works in the following way. There are three parties in a CDS contract: the protection seller, the protection buyer and the reference entity. The protection buyer is the party that has a certain amount of money that needs to be insured, this will be the notional value N of the CDS. For example, he could have a portfolio of bonds of a company. We call this company the reference entity. The protection buyer of the CDS contract will pay regular interest payments with a credit rate R to the protection seller: the premium leg. In return, the protection seller agrees to pay (a part of) the notional amount and any remaining interest in case the

reference entity defaults before the maturity T of the CDS. The size of this protection leg depends on the face value N and the loss-given-default L_{GD}, which is the fraction that tells what part of the notional needs to be paid back. This loss-given-default is assumed to be a known constant.

We explain how a CDS is priced under the risk-neutral pricing framework. To value a CDS we use the theorem of arbitrage-free pricing. If the market is arbitrage-free, then there exist a unique risk-neutral measure $\mathbb{Q}$ such that there is a unique price $V(t)$ for a derivative with payoff $H(T)$. This price is equal to the discounted expectation of the payoff under the risk-neutral measure $\mathbb{Q}$. In formula:

$$V(t) = \mathbb{E}^{\mathbb{Q}}\left[\frac{B(t)}{B(T)}H(T)|\mathcal{G}(t)\right]. \tag{3.3.29}$$

Here is $\mathcal{G}(t)$ the market filtration including default monitoring. This means that this filtration represents all the information on all market variables up to t, including the information until time t on the default of the reference entity. Mathematically, $\mathcal{G}$ can be denoted as follows: $\mathcal{G}(t) = \mathcal{F}(t) \vee \sigma(\{\tau < u\}, u \leq t)$, where $\mathcal{F}(t)$ is the default free market filtration, and $\sigma(\{\tau < u\}, u \leq t)$ is the sigma algebra generated by all the sets $(\{\tau < u\}$, for which the default time τ is smaller than u and where $u < t$.

In order to construct a credit curve, we need to extract information (survival probabilities) from CDSs quoted in the market. To do so, we need the pricing formula for a CDS w.r.t the default free market filtration. So, we derive the pricing formula for a CDS w.r.t. the default free market filtration $\mathcal{F}(t)$. In the derivative pricing formula from Equation (3.3.29) the value of a CDS can be computed as an expectation with respect to filtration $\mathcal{F}(t)$ instead of $\mathcal{G}(t)$, by scaling the expectation by a normalized term, according to [11]. This would give us the following pricing formula w.r.t. $\mathcal{F}(t)$:

$$V(t) = \frac{\mathbf{1}_{\{\tau>t\}}}{\mathbb{Q}(\tau > t|\mathcal{F}(t))}\mathbb{E}\left[\frac{B(t)}{B(T)}H(T)|\mathcal{F}(t)\right]. \tag{3.3.30}$$

The value of the CDS with start date T_a and maturity date T_b is the expectation of the discounted value of the future cash flows, which depend on the default time τ of the reference entity. A CDS consists of two legs: the premium leg and the protection leg. The premium leg is paid at times $T_{a+1}, ..., T_b$ or until default time τ of the reference entity. Then also the payment that accrued from the last payment date before τ is paid. This payment date is denoted by $T_{\beta(\tau)-1}$, since $T_{\beta(\tau)}$ is denoted as the first payment after τ. If $\tau \geq \tau$, then the protection seller pays the protection buyer the premium leg: $N \cdot L_{GD}$.

In formula form, the value of a CDS, from the viewpoint of a protection seller:

$$\begin{aligned} V^{CDS}_{a,b}(t,R,L_{GD}) = &\frac{\mathbf{1}_{\{\tau>t\}}}{\mathbb{Q}(\tau > t|\mathcal{F}(t))}\Big(\mathbb{E}\Big[N\frac{B(t)}{B(\tau)}(\tau - T_{\beta(\tau)-1})R\mathbf{1}_{\{T_a<\tau<T_b\}}\Big|\mathcal{F}(t)\Big] + \\ &NR\sum_{a+1}^{b}\alpha_i\mathbb{E}\Big[\frac{B(t)}{B(T_i)}1_{\{\tau\geq T_i\}}\Big|\mathcal{F}(t)\Big] - L_{GD}\mathbb{E}\Big[N1_{\{T_a<\tau\leq T_b\}}\frac{B(t)}{B(\tau)}\Big|\mathcal{F}(t)\Big]\Big), \end{aligned} \tag{3.3.31}$$

where α_i is the year fraction between T_{i-1} and T_i, $B(t)$ and $B(T_i)$ are the values of a bank account at times t and T_i, R is the annualised CDS credit rate, N is the notional value and $\mathbf{1}_A$ denotes the indicator function of the set A. The term $\frac{\mathbf{1}_{\{\tau>t\}}}{\mathbb{Q}(\tau>t|\mathcal{F}(t))}$ comes from the filtration switching formula from [11], where we switch from the complete market filtration $\mathcal{G}(t)$ including default monitoring, to the default free market filtration $\mathcal{F}(t)$. Note that at today's date, t_0, we have $\mathbb{Q}(\tau > t_0 \mid \mathcal{F}(t_0)) = 1$ and $1_{\{\tau>t_0\}} = 1$ as well. Hence, for today's date, we do not need the filtration switching formula.

In Equation (3.3.31) we see three parts. The first two are together the premium leg. The first term is the accrued cashflow from the last payment date, where we call $\beta(t)$ the index of the first payment date that would follow t, so that $T_{\beta(\tau)-1}$ is the last payment date since the default. The second part is the summation of the cashflows that happen if the default time happens after that payment date. The last term in the equation is the protection leg, that is only paid if the default happens between the start of the CDS and the maturity date. Furthermore, in Equation (3.3.31) we are assuming that both the offered protection rate L_{GD} and the notional N to be equal to one, unless otherwise specified.

A CDS with $t < T_a$ is called a forward default swap. If $t = T_a$ we say that the CDS is a spot CDS. In the credit market spot CDSs are usually quoted through their credit rate R, such that these quotes give the CDSs zero value at inception. These rates in the premium leg that make the CDS fair are also called par rates.

CDS rates on one name (on one company) are usually quoted through their credit rates[11]. From the term structure of credit rates, information about the credit worthiness of the reference entity can be extracted. With this information, a credit curve can be constructed. A credit curve of the reference entity is a mapping from time t to $\mathbb{Q}(\tau \geq t \mid \mathscr{F}(t_0))$, which is the probability that the reference entity will survive until at least time t. In other words, the survival probability of t indicates the probability that the default time τ will happen after t. The credit curve can be calibrated on liquid market instruments and after which it can be used to price less liquid instruments. We will use the credit curve to calibrate the hazard rate process and use this to compute the CVA or the portfolio.

For constructing the credit curve, we assume a reduced form model as the default model and we assume piecewise constant hazard rates as intensity. We assume a piecewise constant hazard rates, following two reasons. Firstly, piecewise constant intensities behave better than alternatives such as piecewise linear intensities and they are numerically stable. This means that they do not magnify approximation errors. Secondly, there is no information on the intensities between CDS maturities. Piecewise constant intensities are the simplest assumption that take the term structure of credit rates into account. So, a piecewise constant method is sensible, gives an exact fit, is local and could deliver fast calibration. According [24, 35, 25], this choice is the most suitable to use, considering the available information on the reference entity and considering the described desired properties.

We use the credit rates from the market and find the values of the piecewise constant market implied hazard rate $\lambda^{\text{imp}}(t)$, that match the default probabilities implied by the model with the default probabilities implied by the CDS credit rates. For this we use a multi-dimensional Newton-Raphson method, where we use central finite differences to construct the Jacobian. Hence, we need the value of the CDS in terms of survival probabilities and hazard rates:

$$V_{a,b}^{\text{CDS}}(t_0, R, \text{L}_{\text{GD}}; \lambda^{\text{imp}}(t)) = -R \int_{T_a}^{T_b} P(t_0,u)(u - T_{\beta(u)-1}\,\text{d}\,\text{SP}(t_0,u) + R \sum_{i=a+1}^{b} P(t_0,T_i)\alpha_i\,\text{SP}(t_0,T_i) + \text{L}_{\text{GD}} \int_{T_a}^{T_b} P(t_0,u)\text{d}\,\text{SP}(t_0,u), \tag{3.3.32}$$

where we use Equation (2.2.1) for the survival probabilities and $P(t,T)$ is defined as in Equation (2.3.2). Note that since we assume that the credit curve is constructed by a piecewise constant (deterministic) intensity model, where the default is the first jump of a time homogeneous Poisson process, we make the distinction between the market implied hazard rates and the stochastic hazard rates from the CVA model with the superscript 'imp'. For the market implied hazard rates we have the following:

$$\text{SP}^{mkt}(0,t) = \mathbb{Q}(\tau \geq t \mid \mathscr{F}(0)) = \mathbb{E}\left[\exp\Big(-\int_0^t \lambda^{\text{imp}}(u)du\Big)\right] = \exp\Big(-\int_0^t \lambda^{\text{imp}}(u)du\Big).$$

Also, in Equation (3.3.32) we assumed $\rho = 0$, independence between the hazard rate and the interest rate. This is because according to [11] dependence has a negligible effect on CDS prices. Also we used the theorem of Fubini to switch the integral and the expectation.

We calibrate the intensity model on some given calibration CDSs with maturity dates $T_1, T_2, \ldots$ and this results in a particular function for the intensity:

$$\lambda^{\text{imp}}(t) = \lambda_k^{\text{imp}}, \quad \text{for } t \in [T_{k-1}, T_k).$$

With this form of the hazard rate, the survival probabilities are of the form:

$$\text{SP}(0,t) = \exp\Big(-\int_0^t \lambda^{\text{imp}}(u)du\Big) = \exp\Big(-\sum_{i=1}^{\beta(t)-1}(T_i - T_{i-1})\lambda_i^{\text{imp}} + (t - T_{\beta(t)-1})\lambda_{\beta(t)}^{\text{imp}}\Big), \tag{3.3.33}$$

with $\beta(t)$ is the index of the first payment date that follows t.

the CDS pricing formula described in Equation (3.3.32) is a function of survival probabilities, and the survival probabilities are functions of hazard rates λ_k^{imp}: $V_{a,b}^{\text{CDS}}(t, R, \text{L}_{\text{GD}}; \lambda^{\text{imp}}(t)))$. Therefore the CDS pricing function is a function of hazard rates. We write the value of a CDS at time t as: $V_{a,b}^{\text{CDS}}(t, R, \text{L}_{\text{GD}}; \lambda_k^{\text{imp}})$ and incorporate

Equation (3.3.33) in the pricing formula. This allows us to use a multidimensional Newton-Raphson method (MNR) to find the hazard rates calibrated on the quoted CDSs.

We use the MNR since it is an efficient technique for solving equations numerically. We will look at the present value (pv) of the CDSs, $pv_i := V_i(t, R, L_{GD}; \lambda^{\text{imp}}(t))$, and find for which constants λ_i^{imp} the CDSs price back to par. We use the following iteration scheme to find the hazard rates:

$$\underline{\lambda}^{\text{imp}(n+1)} = \underline{\lambda}^{\text{imp}(n)} - \mathbf{J}^{-1}(\underline{\lambda}^{\text{imp}(n)})\mathbf{pv}(\underline{\lambda}^{\text{imp}(n)}).$$

In this iteration scheme $\mathbf{pv} = [pv_1, pv_2, ..., pv_N]^T$ is the array of present values, $\mathbf{J^{-1}}$ is the inverse of the Jacobian of the present values and $\underline{\lambda}^{\text{imp}}$ is the vector containing constants λ_k^{imp}. For the Jacobian we use central finite differences to perform the derivatives. After these constant hazard rates are found, the credit curve can be constructed with Equation (3.3.36)

Calibration to the credit curve

We present how we calibrate the CIR++ dynamics such that it reproduces the credit curve. To show how we calibrate the model to market data, we first show how we can calibrate the CIR++ to the term structure of credit rates.

The relation between the survival probabilities generated by the model and the survival probabilities implied by the market is the following:

$$\text{SP}_{CIR}(t_0, t) = \mathbb{Q}(\tau > t \mid \mathscr{F}(t_0)) = \mathbb{E}\left[e^{-\int_{t_0}^t \lambda(u)\mathrm{d}u} \middle| \mathscr{F}(t_0)\right] = e^{-\int_{t_0}^t \lambda^{\text{imp}}(u)\mathrm{d}u} = \text{SP}^{mkt}(t_0, t). \tag{3.3.34}$$

We use this relation to find a function $\psi(t)$ for the hazard rate dynamics in Equation (3.3.2), such that the survival probabilities produced by the model are exactly the same as produced by the market. This way the hazard rate process is arbitrage free, just as we used $\theta(t)$ in the Hull-White model to make the process arbitrage free.

Rewriting Equation (3.3.34) gives the following:

$$\begin{aligned}
e^{-\int_{t_0}^t \lambda^{\text{imp}}(u)\mathrm{d}u} &= \mathbb{E}\left[e^{-\int_{t_0}^t \lambda(u)\mathrm{d}u}\right] \\
&= \mathbb{E}\left[e^{\int_{t_0}^t (-\psi(u) - y(u))\mathrm{d}u}\right] \\
\implies \int_{t_0}^t \psi(u)\mathrm{d}u &= \int_{t_0}^t \lambda^{\text{imp}}(u)\mathrm{d}u + \ln\left(\mathbb{E}\left[e^{-\int_{t_0}^t y(u)\mathrm{d}u}\right]\right) \qquad (3.3.35) \\
&= \int_{t_0}^t \lambda^{\text{imp}}(u)\mathrm{d}u + \ln\left(\left[\text{SP}_{\text{CIR}}(t_0, t, y_0)\right]\right), \qquad (3.3.36)
\end{aligned}$$

where $\text{SP}^{\text{CIR}}(t_0, t, y_0; \beta)$ is the survival probability formula from the basic CIR model, which has the same form as the zero-coupon bond formula of the CIR model, if it was used to model the interest rate. This formula is a closed-form analytical formula of the following form, due to the affinity of the CIR process:

$$\text{SP}_{\text{CIR}}(t, T, y(t)) = \mathbb{E}\left[e^{-\int_t^T y(s)ds} \mid \mathscr{F}(t)\right] = A(t, T)\exp\left(-B(t, T)y(t)\right), \tag{3.3.37}$$

with A and B the following deterministic functions depending on parameters κ, μ, ν, y_0:

$$\begin{aligned}
A(t, T) &= \left[\frac{2h\exp\{(\kappa + h)(T - t)/2\}}{2h + (\kappa + h)(\exp\{(T - t)h\} - 1)}\right]^{2\kappa\mu/\nu^2} \\
B(t, T) &= \frac{2(\exp\{(T - t)h\} - 1)}{2h + (\kappa + h)(\exp\{(T - t)h\} - 1)} \\
h &= \sqrt{\kappa^2 + 2\nu^2}
\end{aligned}$$

This formula can be found in [11]. Since we use the integrated form of the hazard rate, we can leave the calibration with the integrated form of $\psi(t)$.

Note that Equation (3.3.37) can only be used when $\rho = 0$. Otherwise we use Equation (3.3.35), where we use the MC paths from the CIR simulation to compute the expectation. For the JCIR++ model we apply the exact same reasoning as in Equation (3.3.34), but then we compute $\psi_J(t)$ for the JCIR++ model with $\lambda(t)$ and $y_J(t)$. The analytical survival probability formula for the basic JCIR model is also given in [10], but since we have a correlation $\rho \neq 0$ in most cases, we also use the MC paths of $y_J(t)$ to compute the expectation.

To conclude, we have a calibration of the CIR++ model, without choosing parameters κ, μ, ν and y_0. We do have to take into account the fact that the parameters κ, μ, ν, y_0 need to be chosen such that $\psi(t)$ is positive for all t and thus $\int_0^t \psi(u)\mathrm{d}u$ increasing in t. This is needed such that the intensity $\lambda(t)$ stays positive. With Equation (3.3.35) the CIR++ model is calibrated to the market implied hazard function and thus to the CDS data.

Calibration of the volatility parameter

After the calibration of the CIR and the JCIR model to the term structure of credit rates, we have the parameters κ, μ, ν and y_0 left to calibrate to the market. In this section we show how we calibrate the volatility parameter ν of the CIR++ model to a CDS option (CDSO) from the market. First we explain what a CDSO is, then we explain how we price it, after which we explain the calibration method.

For the calibration we use a CDS option, since a CDS option is dependent on the volatility of the model and the volatility parameter ν. A CDS option, also called a default swaption, gives the holder the right, but not the obligation to enter into a CDS contract, at the maturity date of the option. We use an European call option on a protection seller CDS. This maturity date is the start date T_a of the CDS contract. The credit rate that is used for contract is denoted by R_{CDS}. The credit rate that is used in the market, which is denoted by R_{mkt} is the credit rate that prices the CDS back to par. The payoff at maturity of the CDSO is the value of the CDS contract with credit rate R_{CDS} minus the value of the CDS contract with credit rate R_{mkt}, if positive. Since the market credit rate R_{mkt} makes the CDS contract fair at inception, the payoff of the CDSO is just the value of the CDS contract, if positive. Then the value of the CDSO at time t is the risk-neutral expectation of the discounted value of the CDS contract, taking into account that the default of the counterparty is not before maturity of the option. In formula form, the CDS option can be computed as follows [11]:

$$\begin{aligned} V^{CDSO}(t_0, \mathcal{T}, R_{CDS}, \text{L}_{\text{GD}}) &= 1_{\tau > t_0} \mathbb{E}^{\mathbb{Q}} \left[\frac{B(t_0)}{B(T_a)} 1_{\tau > T_a} \max\left(V^{CDS}(T_a, \mathcal{T}, R_{CDS}, \text{L}_{\text{GD}}), 0\right) \middle| \mathcal{G}(t_0) \right] \\ &= 1_{\{\tau > t_0\}} \mathbb{E}\left[\exp\left(-\int_{t_0}^{T_a} \lambda(u)\mathrm{d}u \right) \frac{B(t_0)}{B(T_a)} \max\left(V^{CDS}(T_a, \mathcal{T}, R_{CDS}, \text{L}_{\text{GD}}), 0\right) \middle| \mathcal{F}(t_0) \right], \end{aligned} \tag{3.3.38}$$

where t_0 is the valuation date, $\mathcal{T}$ is the tenor, R_{CDS} is the credit rate, L_{GD} the Loss-given-default and $\lambda(t)$ the hazard rate from the reduced form credit model. For the calibration, we need a CDSO pricer, dependent on ν and a calibration method. We use the root-finding Newton-Raphson method to find the root of function $g(\nu)$: the CDSO pricer minus the market value. Hence, we use the same method as described for the calibration to the credit curve, except we use a one-dimensional Newton-Raphson method instead of a multi-dimensional one. We write $g(\nu)$ as follows:

$$g(\nu) := V^{CDSO}(t_0, \mathcal{T}, R_{CDS}, \text{L}_{\text{GD}}; \nu) - V^{CDSO}_{mkt}(t_0),$$

where we try to find ν such that $g(\nu) = 0$. We use as initial guess for ν, the volatility parameter of the JCIR++ model ν_J and call this $\nu^{(0)}$. The superscipt between brackets stands for the iteration step of the Newton-Raphson method. The value of $\nu^{(i+1)}$ in the next step in the iteration, can be found as follows:

$$\nu^{(i+1)} = \nu^{(i)} - \frac{g(\nu^{(i)})}{g'(\nu^{(i)})}, \quad \text{for} \quad i \geq 0,$$

where $g'(\nu^{(i)})$ stands for the derivative of $g(\nu)$ w.r.t. ν. We use the central finite difference method to find the derivative. Since the market value of the CDSO is a constant,

$$g'(\nu) = \frac{\partial V^{CDSO}(t_0, \mathcal{T}, R_{CDS}, \text{L}_{\text{GD}}; \nu)}{\partial \nu}$$

holds. This is called the vega. It is important that this value does not becomes too small, otherwise we get numerical issues, since we divide by the option's vega. for deep ITM or deep OTM options, the vega is rather small [6]. Therefore, we use ATM CDSOs to calibrate to.

For the calibration, we assume a desired terminal correlation of ρ_{des} and we use the leaking correlation function of Equation (3.3.14) for the CIR model to correlate the Brownian increments of the simulated hazard rate and interest rate. To compute the value of the CDSO, with correlated dynamics, we need to simulate the hazard rate paths from 0 to T_a, for all the possible scenario's for the hazard rate at T_a. For every path, we need to find the CDS value at T_a. Since the hazard rate and the interest rate are correlated, we cannot use a fast analytical expression for the survival probabilities. Hence, for every path, we need to find the CDS value at T_a by simulating sub-paths from T_a to T_b. This is very computationally intensive. Also, according to [5], assuming a correlation not equal to zero has a negligible impact on the CDS price, since the impact is usually much smaller than the bid-ask spread of the CDS. Hence, we can simulate the Monte Carlo paths for the hazard rate until maturity date T_a of the option with a correlation equal to the leaking correlation function and then we can assume $\rho = 0$ from T_a until maturity of the CDS contract T_b. Hence, use Equation (3.3.32) for the price of the CDS contract at valuation time T_a, where independence between the hazard rate and interest rate is assumed. Then, at time T_a, everything is $F(T_a)$-measurable and we can compute every term for the CDSO price, given the simulated paths of $\lambda(t)$ and $r(t)$ from 0 to T_a. This means we only have to simulate until T_a, which makes the Monte Carlo based Newton-Raphson method faster. Because we need to simulate new paths for every NR-step, we use a seed and generate the same BM increments for every simulation. This is to make sure the NR converges.

Although we have found a analytical pricer for the CDSO in literature, we use a Monte Carlo pricer during the calibration of the CIR++ model [14]. This due to the following reasons. The goal of this research is to asses the impact of WWR on the portfolio, and to compare two models that we use to asses this impact. The results we make and conclusions we draw will not be any different using a MC pricer. Also, we are using a synthetic quote for the CDSO instead of real market data. Often, CDSO's are not liquid or they do not even exist for a certain counterparty. In that case, we also would not use a analytical pricer to calibrate directly to the market, but then a time series of historical values would be used. It is not very efficient, but no harm is done using a MC pricer instead of an analytical one, taking into account the MC standard error of the MC paths. And with the MC pricer we can calibrate the volatility parameter ν while assuming $\rho \neq 0$, instead of calibrating with $\rho = 0$. This gives us another possible way to compare the CIR++ model with the JCIR++ model.

4

Results

The main goal of this thesis is to asses the impact of WWR on the CVA of a portfolio of IRS. In this chapter we present a case study with the aim to determine the impact of WWR on a portfolio of IRS swaps in a specific case. With the case study we also show to what boundaries we can use the CVA model.

4.1. Data

As mentioned before, we use synthetic data for the case study. The reason for this is twofold. Firstly, by using synthetic data, we circumvent some of issues that arise with real market data, such as large bid-ask spreads. Secondly, since we produce the synthetic data ourselves, it is easier to use this data. Sometimes there is no real market data available, or there is a quoting mechanism that makes the data more difficult to use. Since such issues do not contribute to answering the main question, they have no impact on the conclusion we will draw. To make sure that the case study we perform is still realistic, we use data that can be found in other articles. Unless otherwise specified, the parameters used in this chapter are the parameters given in the following sections.

4.1.1. Interest date data

A portfolio of interest rate swaps with different strike rates, maturity dates, payment and frequencies, can all be converted into one swap, with a time dependent notional, credit rate and unevenly spread payment dates. We use a simplification of a portfolio of interest rate swaps and use one IRS with a constant notional, payment frequency, and strike rate. Our first case study consists of the following swap from a payer perspective:

- Payer perspective, paying the fixed rate.
- Notional $N = 1000$.
- Year fraction of payment dates $\alpha = 0.25$.
- Maturity date $T_b^{\text{IRS}} = 3$,
  hence the tenor $\mathcal{T}^{\text{IRS}} = [0, 0.25, 0.5, 0.75, 1.0, 1.25, 1.5, 1.75, 2.0, 2.25, 2.5, 2.75, 3.0\,]$.
- Strike rate $R_{\text{IRS}} = 0.04$.

For the yield curve we have assumed a simple equation, a more difficult equation does not contribute to answering the main question. The yield curve we use is the following:

$$P_{\text{mkt}} = \exp(-0.05t). \tag{4.1.1}$$

This means that $r(0) = 0.05$, since we have the following:

$$\begin{aligned} f^r(0,t) &= -\frac{\partial}{\partial t}\log P_{\text{mkt}}(0,t) \\ &= 0.05 \\ \implies r(0) &= f^r(0,0) = 0.05 \end{aligned}$$

For the other parameters of the Hull-White model we use the following values:

- Volatility parameter $\eta = 0.1$
- Speed of mean reversion parameter $k = 0.5$

4.1.2. Credit data

In the market, the normal practice is to use risk-neutral survival probabilities for the CVA. This is because the CVA is computed with the exposure of the IRS to the counterparty, which is depending on risk-neutral valuation. Therefore, the survival probabilities used for the CVA should be implied from the market and be found using the same risk-neutral valuation principle [24]. Also, from a hedging-perspective, the CVA should use risk-neutral survival probabilities, since this way the CVA can be hedged accordingly, by buying CDS contracts for to hedge the credit part. A side note: this could lead to problems since sometimes there is no data to use.

We have the following data that we use to construct the credit curve. We use CDSs that price back to par. All the CDSs have a payment frequency α equal to 0.25, a loss-given-default L_{GD} equal to 1 and a notional N equal to one. The CDSs only differ in credit rate R_i and maturity date T_b^i. The credit rates and maturity dates we use come partly from the Parmalat case study in the book of Brigo and Mercurio [11].

CDS_i	1	2	3	4	5	6	7
T_b^i	1	3	5	7	10	13	16
R_i	0.01925	0.0215	0.0225	0.0235	0.0235	0.0240	0.0242

Table 4.1: Synthetic CDS quotes.

For the calibration of the volatility parameter of the CIR++ model, we use an European call option on a protection seller CDS, with the following characteristics:

- The option is a call option on receiver CDS.
- The notional N equals 1000.
- The tenor $\mathcal{T}_{CDSO} = [2, 2.5, 3]$.
- The credit rate for the CDS is 0.022468.

The chosen credit rate is such that the CDSO is At-The-Money, such that the option's vega is not too small and we avoid numerical issues with the Newton-Raphson method (see Section 3.3.5).

For the correlation parameter we do not choose a value. First, we will calibrate the CIR++ model to the JCIR++ model with a desired correlation equal to 0. Then we simulate hazard rate paths to compute the survival probabilities used for the CVA calculations per desired correlation. This gives a good indication how the CVA models behave as a function of the desired correlation. However, to compare between the two models even better, we also calibrate the two models per desired correlation data point. In the latter case, we do for every value in the desired correlation data points $\bar{\rho}$ = [-1, -0.8, -0.6, -0.4, -0.2, 0, 0.2, 0.4, 0.6, 0.8, 1] the following. We compute the CDSO from the market per point. This is because we choose to make the JCIR++ model the market and the CDSO prices from the JCIR++ model depend on the correlation. Then for every CDSO price we calibrate the CIR++ volatility parameter. Thereafter we can compute the survival probabilities of both models and use the exposure profile we already calculated to compute the CVA values of the models per correlation value.

The CIR++ model parameters are the following:

- Initial value $y(0) = 0.005$.
- Speed of mean reversion parameter $\kappa = 0.5$.
- Long-term mean parameter $\mu = 0.015$.

The JCIR++ model parameters are the following:

- Initial value $y_J(0) = y(0) = 0.005$.

- Speed of mean reversion parameter $\kappa_J = \kappa = 0.5$.
- Long-term mean parameter $\mu_J = \mu = 0.015$.
- Volatility parameter $\nu_J = 0.03$.
- Jump rate $\xi = 0.01$.
- Jump size $\gamma = 0.005$.

We have chosen these parameters such that the model works. During the numerical experiments we found some boundaries of the credit part of the CVA model. One is that the volatility parameters cannot get too high, compared to κ and μ. When the Feller condition is satisfied, the volatility is not too high. When it is too high, an approximation for the instantaneous-correlation-function does not work anymore and then the uncorrelated hazard rate is not Chi-squared distributed anymore. This is due to the reflecting principle of the reflecting Euler scheme.

Also, we have to choose the initial value of the hazard rate, the speed of mean reversion parameter and the long-term mean parameter such that $\psi(t)$ and $\psi_J(t)$ stay positive, otherwise $\lambda + \psi(t)$ and $\lambda_J(t) + \psi_J(t)$ can become negative and then we can get negative survival probabilities and therefore a negative CVA.

Furthermore, we have to choose the jump rate and jump size not too high, because otherwise the value of the CDSO produced by the JCIR++ model, cannot be reproduced by the CIR++ model. In other words: there is an interval of CDSO prices for which the CIR++ can calibrate to the JCIR++ model. If the value is too high, then the CIR++ model needs a volatility that is too high for the CIR++ model and then we have the first problem again.

4.1.3. Other model parameters

In this thesis the L_{GD} is assumed to be constant and for the CVA calculations of this chapter we assume it to be equal to one. For the broader interpretation of WWR the L_{GD} could be assumed to be stochastic and dependent on the probability of default. However, the modelling of the L_{GD} is outside the scope of this thesis. Other model parameters are the following:

- All the Monte Carlo paths are simulated with 100 discritization steps and 10^4 paths. This means that the standard error for the interest rate paths is equal to approximately $9.9 \cdot 10^{-4}$, for the CIR++ paths it is equal to approximately $3.3 \cdot 10^{-5}$ and for the JCIR++ paths it is equal to approximately $5.8 \cdot 10^{-5}$.
- The derivatives are computed with central finite differences with a bump size of 10^{-5}.
- For the Newton-Rahpson method used in both the construction of the credit curve and the calibration of the volatility parameter we use a tolerance of 10^{-5}. This means that the Newton-Raphson terminates if a root is found, such that the function for which we want to find the root has a absolute value of at most 10^{-5}.
- To calculate integrals we use the trapezoidal integral rule with an integration step with size 10^{-4}.

4.2. Generating survival probabilities

With the synthetic quotes from Section 4.1.2 and the methods from Section 3.3.5, we build the credit curve and calibrate to the term structure of credit rates. The piecewise constant intensity model that is used gives the following market implied hazard rates $\lambda^{\text{imp}}(t)$:

$$\begin{aligned}&[\lambda_1^{\text{imp}}, \lambda_2^{\text{imp}}, \lambda_3^{\text{imp}}, \lambda_6^{\text{imp}}, \lambda_6^{\text{imp}}] \\ &= [0.01913002, 0.02260963, 0.02415067, 0.02659107, 0.02335355, 0.0265985, 0.02568033],\end{aligned} \tag{4.2.1}$$

such that

$$\lambda^{\text{imp}}(t) = \begin{cases} \lambda_1^{\text{imp}}, & \text{if } t \in [1,3), \\ \lambda_2^{\text{imp}}, & \text{if } t \in [3,5), \\ \lambda_3^{\text{imp}}, & \text{if } t \in [5,7). \\ \lambda_4^{\text{imp}}, & \text{if } t \in [7,10), \\ \lambda_5^{\text{imp}}, & \text{if } t \in [10,13), \\ \lambda_6^{\text{imp}}, & \text{if } t \in [13,16). \end{cases} \tag{4.2.2}$$

In Figure 4.1 it can be observed that the market implied hazard rates remain constant between the maturity

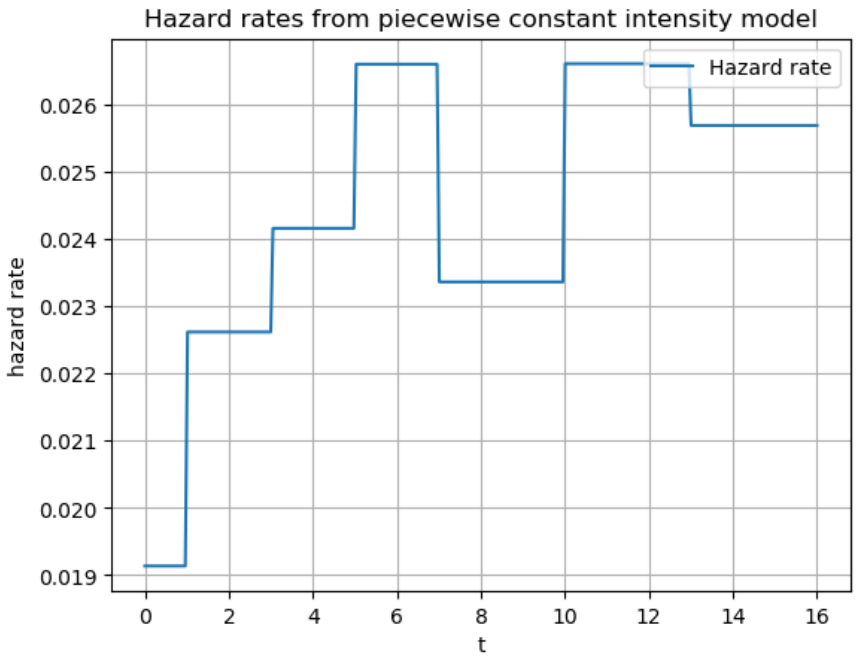

Figure 4.1: Hazard rates from the piecewise constant intensity model, extracted from the term structure of credit rates from Table 4.1.

dates of the calibration CDSs. The credit curve that these hazard rates give using a reduced form intensity model, can be observed in Figure 4.2.

We want the CIR++ and JCIR++ model calibrated to this credit curve from the synthetic market. As explained in Section 3.3.5, we use two functions $\psi(t)$ and $\psi(t)_J$. These functions need to be positive for all $t > 0$, otherwise the hazard rates $\lambda(t)$ and $\lambda_J(t)$ from the CIR++ and the JCIR++ model can become negative. This would give rise to negative survival probabilities and can lead to a negative CVA. Since the CVA can be seen as an option on the IRS, this is not possible. The functions $\psi(t)$ and $\psi_J(t)$ that are used can be observed in Figures 4.3a and 4.3b.

From this figure it can be observed that the functions $\psi(t)$ and $\psi_J(t)$ remain positive for all $t > 0$. Looking at Equation (4.2.1), the market implied hazard rates are approximately around 0.01 on average. For the $\psi_{(J)}(t)$ function to remain positive, the paths $y(t)$ and $y_J(t)$ generated by the CIR and the JCIR model respectively cannot become too large. This means, if $y(t)$ and $y_J(t)$ are on average far above the market implied hazard rates, the $\psi_{(J)}(t)$ function needs to compensate these values of $y(t)$ and $y_J(t)$ by becoming negative. In Figure 4.4 the deterministic shift functions of the CIR++ and JCIR++ model can be observed, where parameters $\mu = \mu_J = 0.4$ and $y(0) = y_J(0) = 0.5$ are too high for the credit curve from Figure 4.2. Hence, for the chosen market credit rates, we cannot choose large values for parameters μ, μ_J, $y(0)$ and $y(0)$. Thus, the $\psi_{(J)}(t)$ functions limit the model.

With these deterministic shift functions added to the MC paths, we get the CIR++ and JCIR++ dynamics, as described in Equations (3.3.2) and (3.3.16). These dynamics compute the same credit curve as shown in Figure 4.2. This can be observed in Figure 4.5 and in Figure 4.6, where in the latter figure the absolute differences between the survival probabilities $SP_{\text{mkt}}(0,t)$ from the market and survival probabilities $SP_{\text{CIR++}}(0,t)$, $SP_{\text{JCIR++}}(0,t)$ from the models are plotted.

In Figures 4.6a and 4.6b it can be observed that the differences between the survival probabilities from the market and from the CIR++ and JCIR++ are most of the time zero and sometimes they are around the value of the standard error of the MC simulations. Also, the average absolute differences decrease with the number of paths used for the MC simulation. This means, that the survival probabilities of the models are implemented correctly and we can say that they are approximately equal to the credit curve from the market.

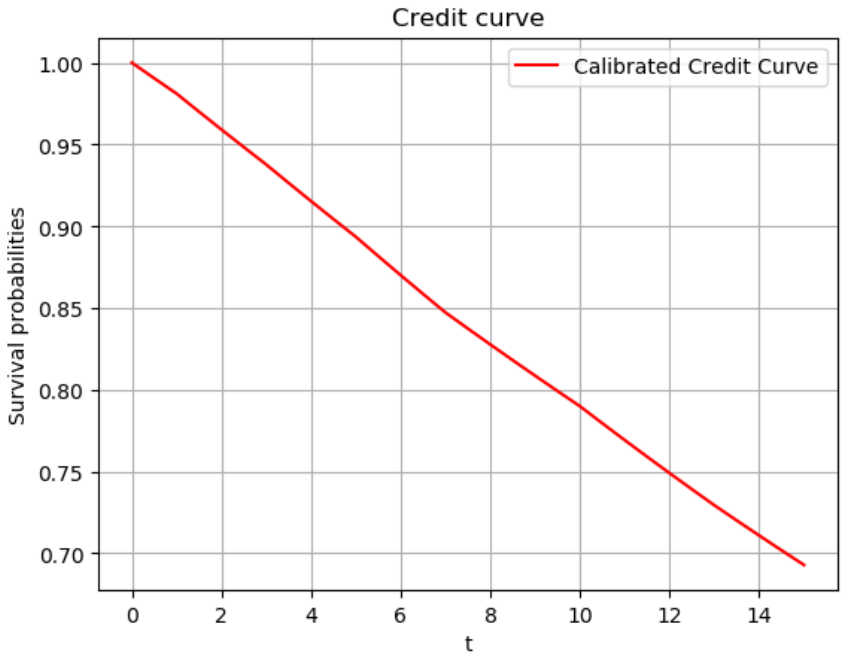

Figure 4.2: Credit Curve, constructed with the hazard rates from Equation (4.2.2) and Figure 4.1.

4.3. Leaking correlation

If we could calibrate the correlation parameter $\rho(t)$ just as the volatility parameter of the CIR++ model, we would. This would mean that we do not have to worry about leaking correlation, since $\rho(t)$ is then just a parameter. However, there are no products in that market that we can calibrate to. Hence, we need to use historical data to estimate a certain correlation for the counterparty. The statistical estimation of the correlation lies beyond the scope of this research. Therefore, we check for every $0 \leq \rho \leq 1$ what the impact of the correlation between the hazard rate and the interest rate will be.

Since we choose the correlation parameter, we want to be able to impose this correlation on the hazard rate and the interest rate. This correlation is the desired correlation. However, when using the desired correlation as instantaneous correlation parameter $\rho_{\text{inst}}(t)$, the problem of leaking correlation occurs. This means that the actual correlation between the hazard rate and the interest rate, the terminal correlation $\rho_{\text{term}}(t)$, is decreasing in absolute value. We want to be able to impose the right correlation for every time-step in the future. Therefore, we use the instantaneous-correlation-functions of Equations (3.3.14) $\rho^{\text{CIR}}(t)$ and (3.3.28) $\rho^{\text{J}}(t)$. With these functions, we put the time dependent instantaneous correlation parameters $\rho_{\text{inst}}(t) = \rho^{\text{CIR}}(t)$ or $\rho_{\text{inst}}(t) = \rho^{\text{J}}(t)$ in the simulation, such that for every time-step, the terminal correlation is equal to the desired correlation for both the CIR++ and the JCIR++ models.

To simulate the paths of the hazard rate and the interest rate, we use a Monte Carlo simulation, with Brownian increments. The increments of the Brownian motions are normally distributed. Hence, a combination of the Brownian increments of the interest rate and the Brownian increments of the hazard rate is normally distributed as well. This normal distribution is dependent on time, and the variance of that normal distribution grows over time. This means that for any value for the correlation between the two Brownian increments except for one, the variance of this distribution increases over time. The variance of the correlated Brownian increments increase over time, which means that the correlation disappears over time. Hence, for the long-term, we need a system that holds the hazard rate and the interest rate together and that counters this leaking correlation effect. The system that we use, is the instantaneous-correlation-functions $\rho^{\text{CIR}}(t)$ and $\rho^{\text{J}}(t)$ described by Equations (3.3.14) and (3.3.28) for the CIR++ and the JCIR++ model respectively.

Equations (3.3.14) and (3.3.28) are created as follows: First we find out what the analytically computed terminal correlation $\rho_{\text{term}}(t)$ would be if we use an instantaneous correlation function $\rho_{\text{inst}}(t)$. Then we rewrite

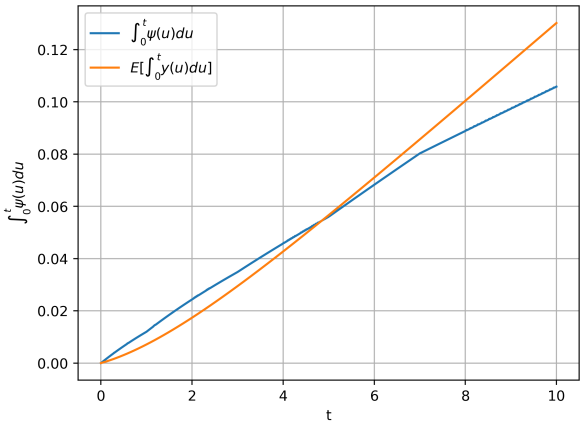

(a) $\psi(t)$ for the CIR model, plotted together with the average of the MC paths $y(t)$, for $0 \le t \le 10$.

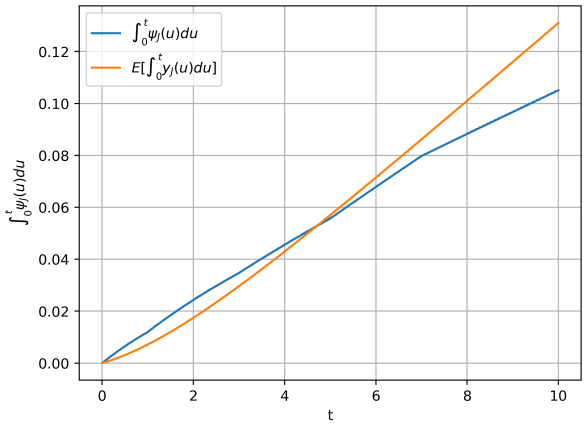

(b) $\psi(t)$ for the JCIR model, plotted together with the average of the MC paths $y_J(t)$, for $0 \le t \le 10$.

Figure 4.3: The deterministic shift functions $\psi_{(J)}(t)$ for the calibrated credit models.

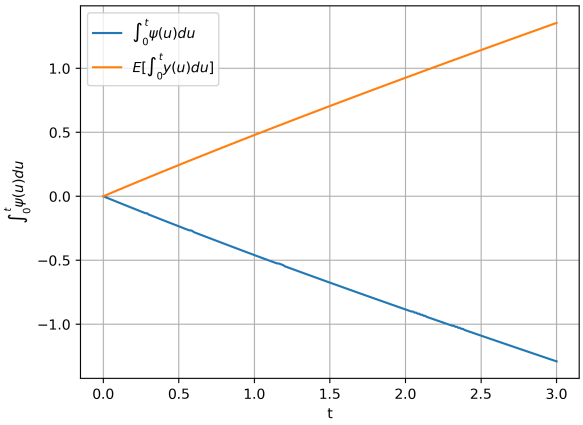

(a) $\psi(t)$ for the a CIR model and the average of the MC paths $y(t)$, for $\mu = 0.4$ and $y(0) = 0.5$.

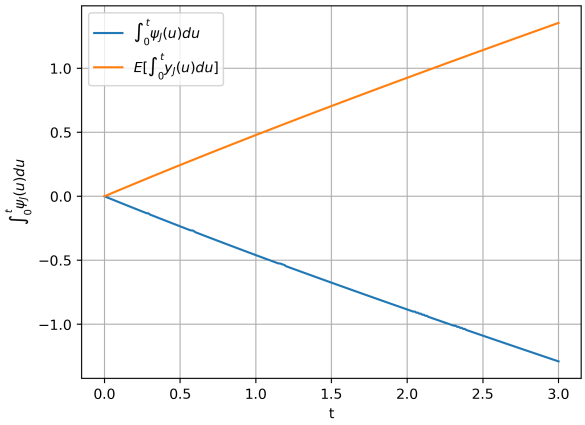

(b) $\psi(t)$ for the JCIR model and the average of the MC paths $y(t)$, with $\mu_J = 0.4$ and $y_J(0) = 0.5$.

Figure 4.4: The deterministic shift functions $\psi_J(t)$ for the calibrated credit models.

the found equation, such that we have the instantaneous correlation in terms of the terminal correlation: Equations (3.3.14) and (3.3.28). Then we set $\rho_{\text{term}}(t)$ in the equations equal to $\rho_{\text{des}}(t)$. This should result in a terminal correlation equal to the desired correlations. Unfortunately, we show that this is not always the case.

With the input from Section 4.1 we run the simulations of the hazard rate and the interest rate, with and without leaking correlations. For both the CIR++ and the JCIR++ model we compare the two, to see whether instantaneous-correlation-functions have a positive influence on the terminal correlation (i.e. if the terminal correlation is closer to the desired correlation). We investigate how much the terminal correlation with leaking correlation differs from the one without. We use the term *with leaking correlation* (wlc) if the hazard rate is simulated without the use of Equations (3.3.14) and (3.3.28) and we say *without leaking correlation* if Equations (3.3.14) and (3.3.28) are used as instantaneous correlation. Also, we investigate what influence the parameters of the (J)CIR++ dynamics have on leaking correlations. Furthermore, in Section 4.6, we show the impact of leaking correlation and using Equations (3.3.14) and (3.3.28) on the CVA of the portfolio.

To establish a baseline, we first show the terminal correlation of the CIR++ and the JCIR++ models with the interest rate with a desired correlation of 0. This gives an indication how the terminal correlation of the MC paths (the sample correlation) behave and this way we can put the values of the leaking correlation and of the improvement of the terminal correlation of the models in perspective. The terminal correlations for $\rho_{\text{des}}(t) = 0$ can be observed in Figure 4.7. Figure shows that although $r(t)$ is simulated independently from $\lambda(t)$ and $\lambda_J(t)$, the terminal correlation from the simulations is not equal to zero. The average abs difference

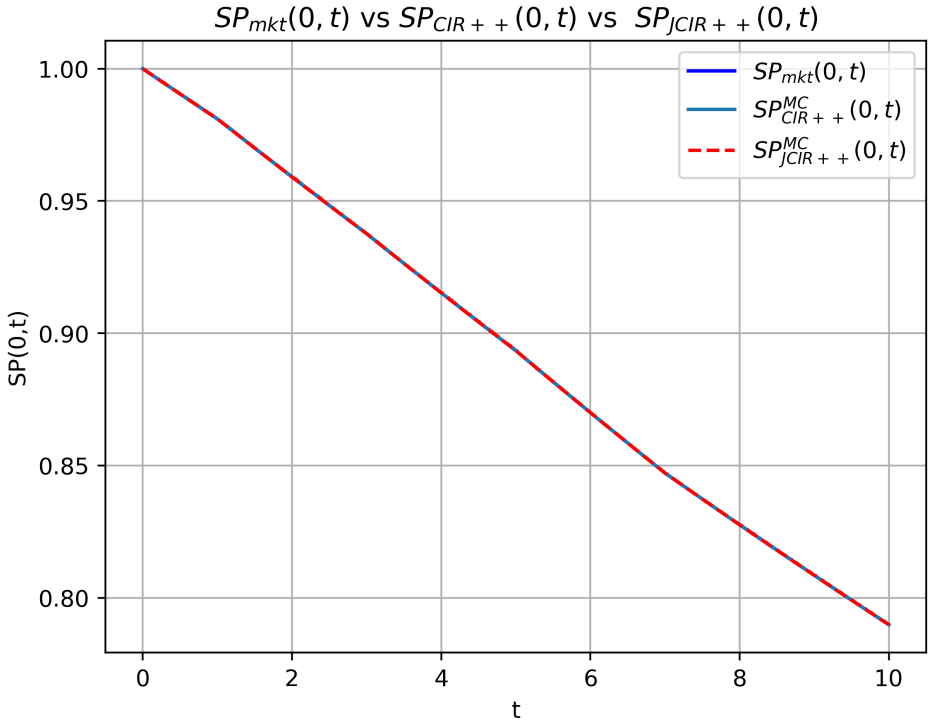

Figure 4.5: The credit curve and the survival probabilities generated by both the CIR++ and the JCIR++ model.

between $\rho_{\text{des}}(t)$ and $\rho_{\text{term}}(t)$ for $\rho_{\text{inst}}(t) = \rho_{\text{des}}(t) = 0$ for the CIR++ model is equal to 0.00449695 and for the JCIR++ is equal to 0.00456143. Analytically this should be equal to zero, but due to numerical methods it is not.

In what follows we analyse cases of $\rho_{\text{des}} \neq 0$. In Figures 4.9a, 4.9b, 4.8a, 4.8b we take $\rho_{\text{des}}(t)$ to be equal to 0.2, 0.6, -0.2 and -0.6 respectively, to compare high values (in absolute sense) of correlations with low values of correlations. In the Figures the desired correlation (in orange) is plotted together with the terminal correlations with (blue) and without (red) leaking correlation, for the CIR++ model. Also the analytically calculated terminal correlation (with leaking) is plotted (in green). It can be observed that the influence from the MC paths (i.e. the fluctuations) have more influence on the terminal correlations than the use of function $\rho^{\text{CIR}}(t)$. We compute the average absolute differences between $\rho_{\text{des}}(t)$ and $\rho_{\text{term}}(t)$ with and without leaking correlation, to determine whether the function ρ^{CIR} was an improvement. We did the same for the JCIR++ model, these results can be observed in Figures 4.12a, 4.12b, 4.11a and 4.11b. Thus, for the CIR++ model, we have the following:

- With leaking correlation: For $\rho_{\text{des}}(t) = 0.2$, $\frac{1}{M}\sum_{i=1}^{M} |\rho_{\text{des}}(t_i) - \rho_{\text{term}}(t_i)| = 0.0094599$. Without leaking correlation $\frac{1}{M}\sum_{i=1}^{M} |\rho_{\text{des}}(t_i) - \rho_{\text{term}}(t_i)| = 0.0111917$. Improvement = - 18.3059 %.
- With leaking correlation: For $\rho_{\text{des}}(t) = 0.6$, $\frac{1}{M}\sum_{i=1}^{M} |\rho_{\text{des}}(t_i) - \rho_{\text{term}}(t_i)| = 0.0044969$. Without leaking correlation $\frac{1}{M}\sum_{i=1}^{M} |\rho_{\text{des}}(t_i) - \rho_{\text{term}}(t_i)| = 0.0040580$. Improvement = 9.7589 %.
- With leaking correlation: For $\rho_{\text{des}}(t) = -0.2$, $\frac{1}{M}\sum_{i=1}^{M} |\rho_{\text{des}}(t_i) - \rho_{\text{term}}(t_i)| = 0.0104532$. Without leaking correlation $\frac{1}{M}\sum_{i=1}^{M} |\rho_{\text{des}}(t_i) - \rho_{\text{term}}(t_i)| = 0.01182044$. Improvement = -13.0787 %.
- With leaking correlation: For $\rho_{\text{des}}(t) = -0.6$, $\frac{1}{M}\sum_{i=1}^{M} |\rho_{\text{des}}(t_i) - \rho_{\text{term}}(t_i)| = 0.00899064$. Without leaking correlation $\frac{1}{M}\sum_{i=1}^{M} |\rho_{\text{des}}(t_i) - \rho_{\text{term}}(t_i)| = 0.00841863$. Improvement = 6.3623 %.

The leaking correlations differ from the desired correlations approximately as much as the baseline ($\rho = 0$). Hence, there is not much leaking correlation to solve with the used parameter set. Also, the improvement for the CIR++ is not significant and sometimes there is a deterioration. Hence it will not have much impact on the CVA computations. For the JCIR++ model we have the following values:

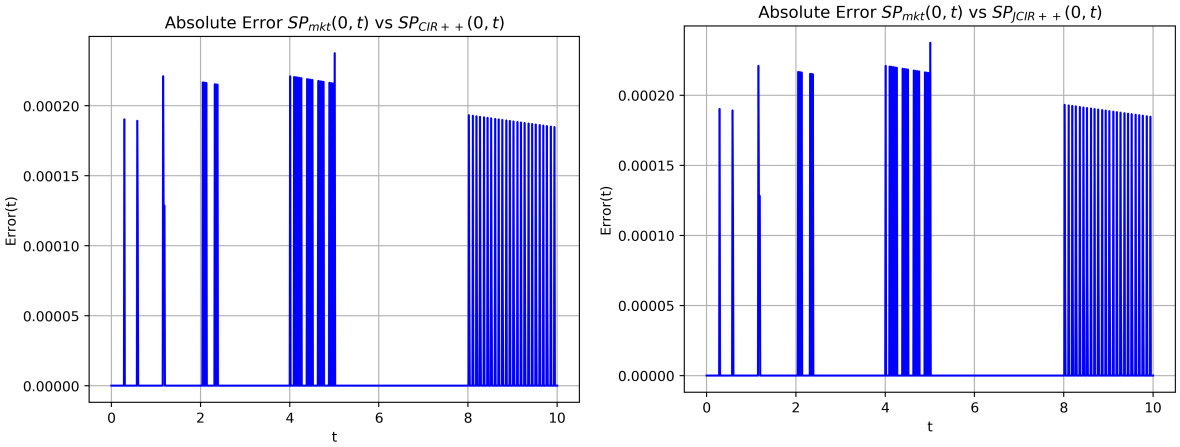

(a) The absolute difference between $SP_{\text{mkt}}(0,t)$ and $SP_{CIR}(t)$.

(b) The absolute difference between $SP_{\text{mkt}}(0,t)$ and $SP_{JCIR}(t)$.

Figure 4.6: Error plots for survival probabilities.

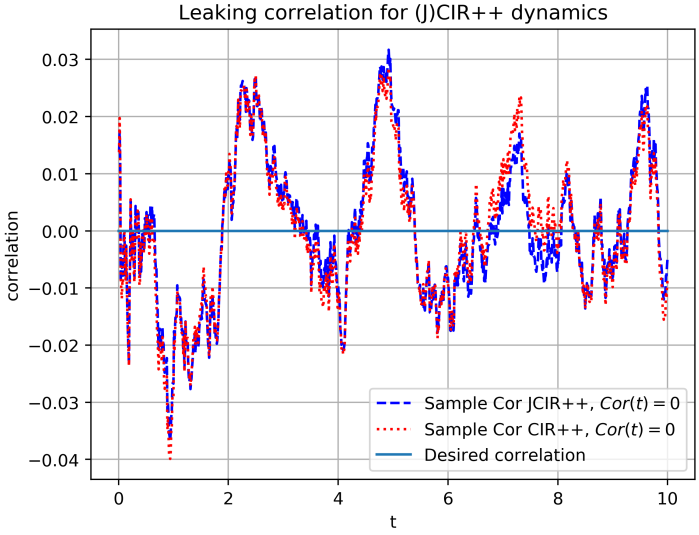

Figure 4.7: Terminal correlations between $r(t)$ and $\lambda(t)$ (red) and between $r(t)$ and $\lambda_J(t)$ (blue).

- With leaking correlation: For $\rho_{\text{des}}(t) = 0.2$, $\frac{1}{M}\sum_{i=1}^{M}|\rho_{\text{des}}(t_i) - \rho_{\text{term}}(t_i)| = 0.0108456$. Without leaking correlation $\frac{1}{M}\sum_{i=1}^{M}|\rho_{\text{des}}(t_i) - \rho_{\text{term}}(t_i)| = 0.01073656$. Improvement = 1.0061 %.
- With leaking correlation: For $\rho_{\text{des}}(t) = 0.6$, $\frac{1}{M}\sum_{i=1}^{M}|\rho_{\text{des}}(t_i) - \rho_{\text{term}}(t_i)| = 0.0045614$. Without leaking correlation $\frac{1}{M}\sum_{i=1}^{M}|\rho_{\text{des}}(t_i) - \rho_{\text{term}}(t_i)| = 0.00386655$. Improvement =15.233 %.
- With leaking correlation: For $\rho_{\text{des}}(t) = -0.2$, $\frac{1}{M}\sum_{i=1}^{M}|\rho_{\text{des}}(t_i) - \rho_{\text{term}}(t_i)| = 0.01091836$. Without leaking correlation $\frac{1}{M}\sum_{i=1}^{M}|\rho_{\text{des}}(t_i) - \rho_{\text{term}}(t_i)| = 0.00994262$. Improvement = 8.9367%.
- With leaking correlation: For $\rho_{\text{des}}(t) = -0.6$, $\frac{1}{M}\sum_{i=1}^{M}|\rho_{\text{des}}(t_i) - \rho_{\text{term}}(t_i)| = 0.01713667$. Without leaking correlation $\frac{1}{M}\sum_{i=1}^{M}|\rho_{\text{des}}(t_i) - \rho_{\text{term}}(t_i)| = 0.00695910$. Improvement = 59.3906 %.

In Figures 4.12a and 4.11a we see the same as for the CIR++ model: the MC simulation has more impact on the correlations than the instantaneous-correlation function ρ^{J}. However, in Figures 4.12b and 4.11b we can observe a larger change in the terminal correlation. We notice that when function $\rho^{\text{J}}(t)$ is used, the terminal correlation is in absolute value higher. Also, it can be observed that after the first time step - correlation at $t = 0$ is not plotted - the terminal correlation is already much less in absolute value than the instantaneous correlation. This is because the jumps are assumed independent and therefore make the hazard rate in total

less correlated to the interest rate.

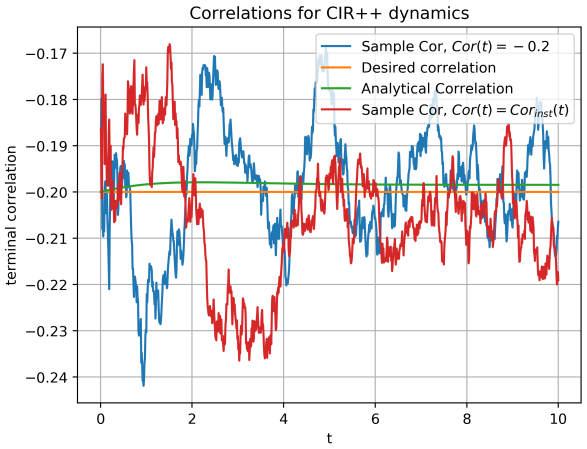

(a) Desired and terminal correlations from the CIR++ model, for $\rho_{\text{des}}(t) = -0.2$ (in orange). The analytically calculated terminal correlation with leaking correlation is in green, the terminal correlation from the MC paths with leaking correlation is blue and without in red.

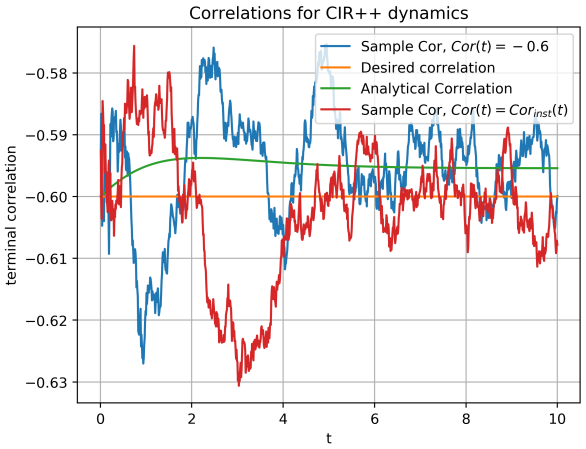

(b) Desired and terminal correlations from the CIR++ model, for $\rho_{\text{des}}(t) = -0.6$ (in orange). The analytically calculated terminal correlation with leaking correlation is in green, the terminal correlation from the MC paths with leaking correlation is blue and without in red.

Figure 4.8

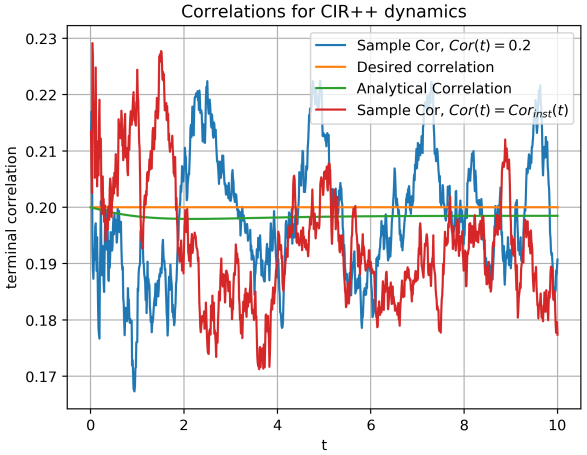

(a) Desired and terminal correlations from the CIR++ model, for $\rho_{\text{des}}(t) = 0.2$ (in orange). The analytically calculated terminal correlation with leaking correlation is in green, the terminal correlation from the MC paths with leaking correlation is blue and without in red.

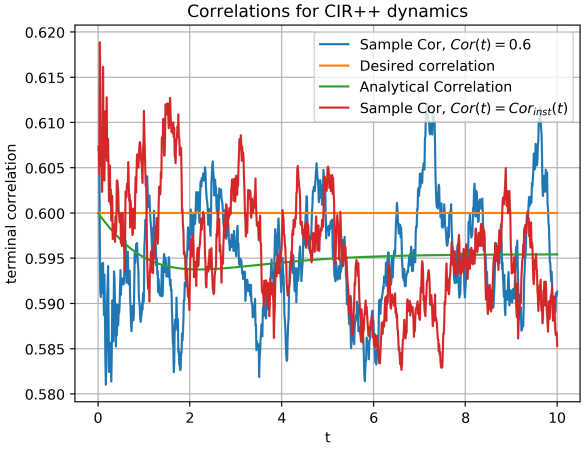

(b) Desired and terminal correlations from the CIR++ model, for $\rho_{\text{des}}(t) = 0.6$ (in orange). The analytically calculated terminal correlation with leaking correlation is in green, the terminal correlation from the MC paths with leaking correlation is blue and without in red.

Figure 4.9

We have noticed that the problem is of more significance for a high volatility value and for a high desired correlation. Leaking correlation increases with an increased volatility parameter, because the volatility parameter amplifies the Brownian increment of the simulation. In Figure 4.10a the terminal correlations between $r(t)$ and $\lambda(t)$ can be observed, with a higher value for the volatility parameter: $\nu = 0.4$. For this value of ν the leaking correlation is much more significant. It can also be observed that with a value of ν this high, the jumps have less impact on the terminal correlation. With higher values for the jump rate $\xi = 0.1$ and $\gamma = 0.005$ the jumps have more impact. In Figure 4.10b the same can be observed as Figures 4.12a, 4.12b, 4.11a and 4.11b: the terminal correlation starts at a much lower value than the instantaneous correlation, because after one time step the independent jumps have already deteriorated the correlation between the interest rate and the hazard rate. With the chosen value for the volatility, it is not possible to determine whether functions ρ^{CIR} and ρ^{J} are an improvement. This is because of the following. If we have the same parameters, but with a large volatility, then the feller condition is not satisfied and then we have two problems with the simulations.

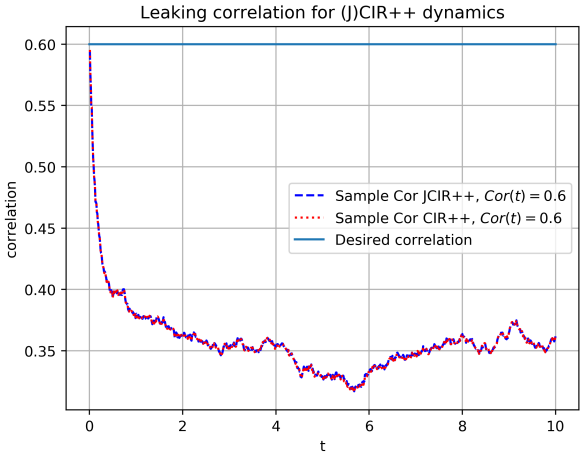

(a) Terminal correlations for the CIR++ and JCIR++ model, simulated with leaking correlation. The instantaneous correlation equals 0.6 and the volatility parameters ν and ν_J equal 0.4.

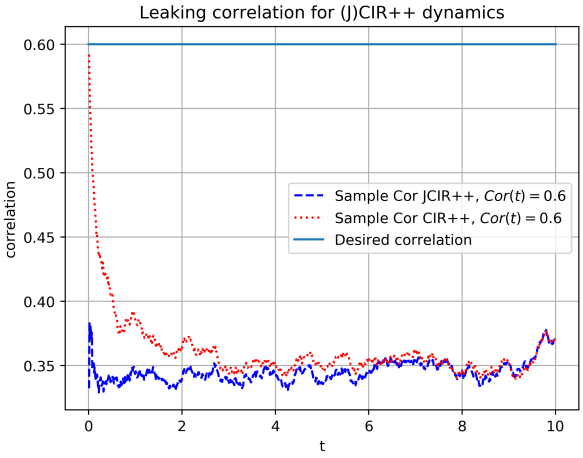

(b) Terminal correlations for the CIR++ and JCIR++ model, simulated with leaking correlation. The instantaneous correlation equals 0.6. Computed with $\nu = \nu_J = 0.4$, $\xi = 0.1$ and $\gamma = 0.05$, instead of $\nu = 0.03$, $\xi = 0.01$, $\gamma = 0.005$

Figure 4.10

The approximation of $E\left[\sqrt{y(t)}\middle|\mathcal{F}(0)\right]$ does not work anymore. Therefore, the instantaneous-correlation-function (3.3.14) does not work and we cannot counter the leaking correlation. Also, with a volatility value that is too high, we see that we have problems with the MC simulations. The uncorrelated $y(t)$ paths from the CIR++ model are not Chi-squared distributed anymore and therefore the survival probabilities made from the MC paths do not agree with the analytically calculated survival probabilities $SP_{\text{CIR}}(0,t)$ anymore. For the JCIR++ model we see the same problem. The reason for this problem is the reflecting Euler scheme. If the volatility parameter is too high compared to μ and κ, then much of the MC paths reach the origin and then the reflecting principle influences the distribution too much. Hence, we have found another limitation of the model: the value of the volatility parameter cannot be too high compared to the values of μ and κ. When the Feller condition is satisfied, then we are still within the boundaries of the model.

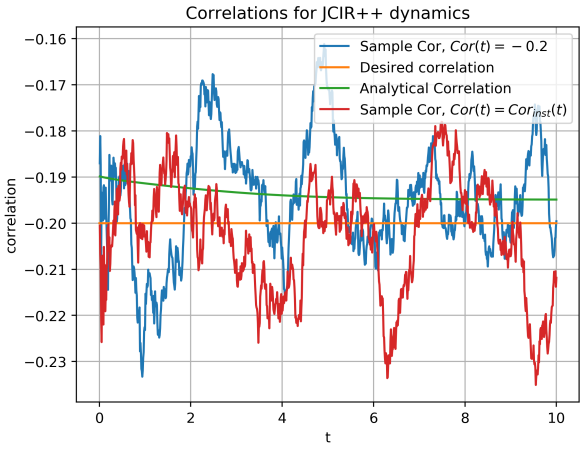

(a) Desired and terminal correlations from the JCIR++ model, for $\rho_{\text{des}}(t) = -0.2$ (in orange). The analytically calculated terminal correlation with leaking correlation is in green, the terminal correlation from the MC paths with leaking correlation is blue and without in red.

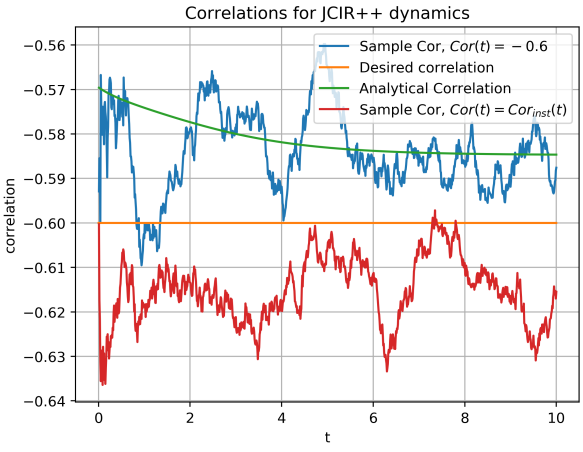

(b) Desired and terminal correlations from the JCIR++ model, for $\rho_{\text{des}}(t) = -0.6$ (in orange). The analytically calculated terminal correlation with leaking correlation is in green, the terminal correlation from the MC paths with leaking correlation is blue and without in red.

Figure 4.11

An example parameter set, parameter set B, for which the instantaneous-correlation-functions do have impact, is the following:

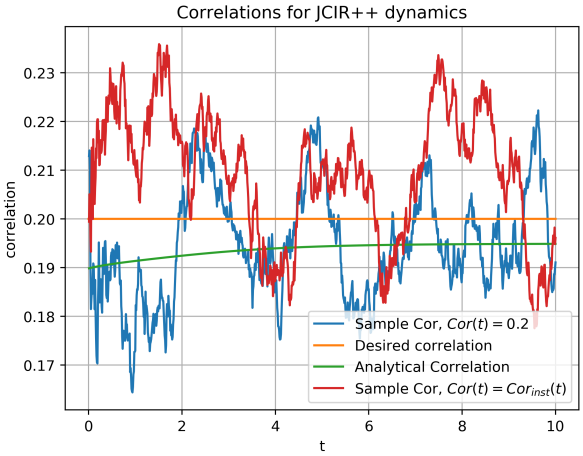

(a) Desired and terminal correlations from the JCIR++ model, for $\rho_{\text{des}}(t) = 0.2$ (in orange). The analytically calculated terminal correlation with leaking correlation is in green, the terminal correlation from the MC paths with leaking correlation is blue and without in red.

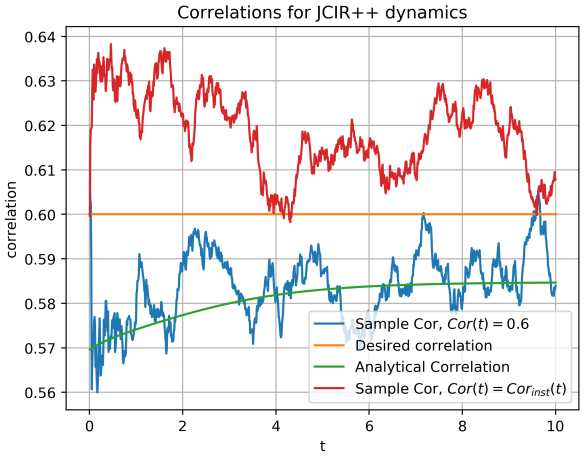

(b) Desired and terminal correlations from the JCIR++ model, for $\rho_{\text{des}}(t) = 0.6$ (in orange). The analytically calculated terminal correlation with leaking correlation is in green, the terminal correlation from the MC paths with leaking correlation is blue and without in red.

Figure 4.12

- $y(0) = y_J(0) = 0.17$.
- $\kappa = \kappa_J = 0.5$.
- $\mu = \mu_J = 0.17$.
- $\nu = \nu_J = 0.4$.
- $\xi = 0.01$, $\gamma = 0.005$ (Figures 4.14a, 4.14b), $\xi = 0.1$, $\gamma = 0.05$ (Figures 4.15a, 4.15b).
- $\rho_{\text{des}} = 0.6$ (Figures 4.13a, 4.14a, 4.15a), $\rho_{\text{des}}(t) = -0.6$ (Figures 4.13b, 4.14b, 4.15b).

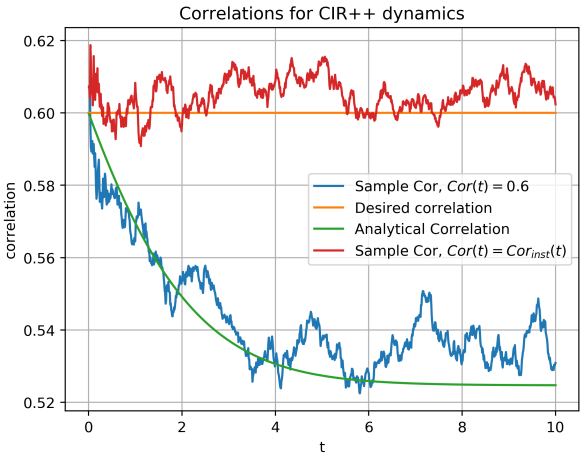

(a) $\rho_{\text{des}}(t) = 0.6$ (in orange). Terminal correlations from the CIR++ model. The analytically calculated terminal correlation with leaking correlation is in green, the terminal correlation from the MC paths with leaking correlation is blue and without in red. $y(0) = 0.17$, $\kappa = 0.5$, $\mu = 0.17$, $\nu = 0.4$.

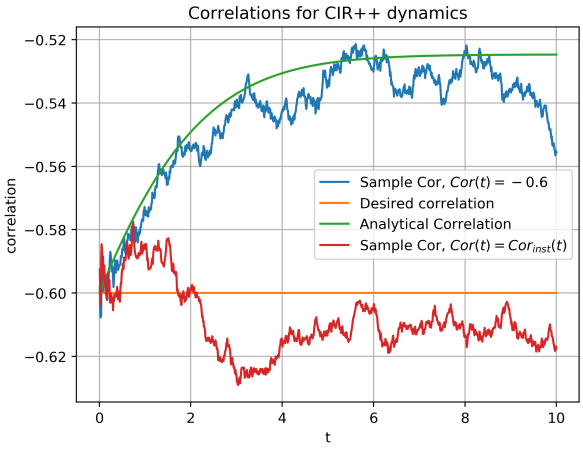

(b) $\rho_{\text{des}}(t) = -0.6$ (in orange). Terminal correlations from the CIR++ model. The analytically calculated terminal correlation with leaking correlation is in green, the terminal correlation from the MC paths with leaking correlation is blue and without in red. $y(0) = 0.17$, $\kappa = 0.5$, $\mu = 0.17$, $\nu = 0.4$.

Figure 4.13

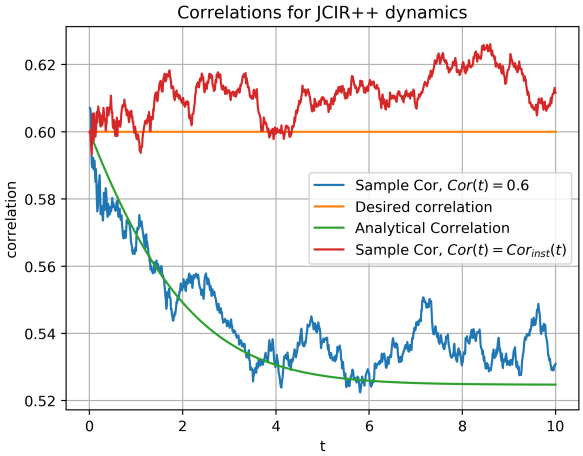

(a) $\rho_{\text{des}}(t) = 0.6$ (in orange). Terminal correlations from the JCIR++ model. The analytically calculated terminal correlation with leaking correlation is in green, the terminal correlation from the MC paths with leaking correlation is blue and without in red. $y_J(0) = 0.17$, $\kappa_J = 0.5$, $\mu_J = 0.17$, $\nu_J = 0.4$, $\xi = 0.01$, $\gamma = 0.005$

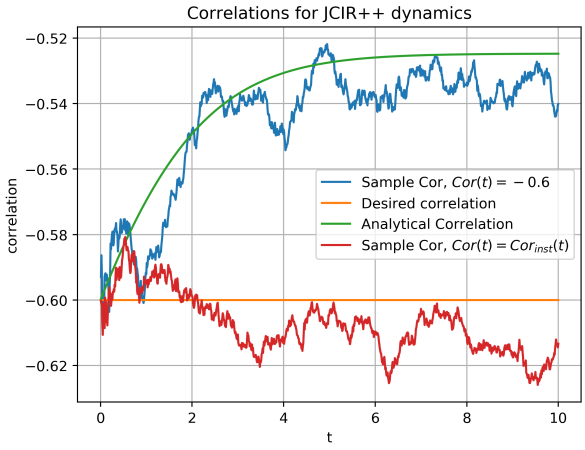

(b) $\rho_{\text{des}}(t) = -0.6$ (in orange). Terminal correlations from the JCIR++ model. The analytically calculated terminal correlation with leaking correlation is in green, the terminal correlation from the MC paths with leaking correlation is blue and without in red. $y_J(0) = 0.17$, $\kappa_J = 0.5$, $\mu_J = 0.17$, $\nu_J = 0.4$, $\xi = 0.01$, $\gamma = 0.005$

Figure 4.14

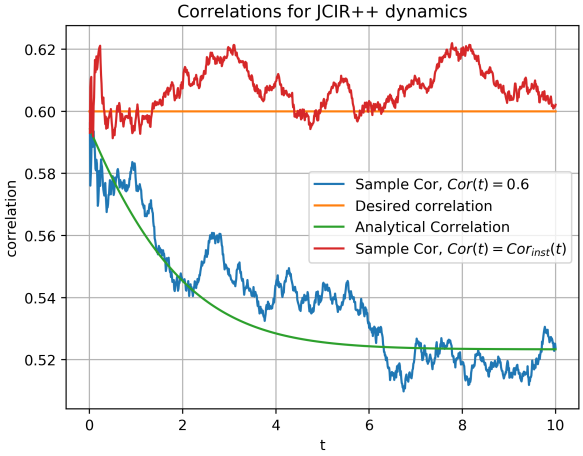

(a) $\rho_{\text{des}}(t) = 0.6$ (in orange). Terminal correlations from the JCIR++ model. The analytically calculated terminal correlation with leaking correlation is in green, the terminal correlation from the MC paths with leaking correlation is blue and without in red. $y_J(0) = 0.17, \kappa_J = 0.5, \mu_J = 0.17, \nu_J = 0.4, \xi = 0.1, \gamma = 0.05$

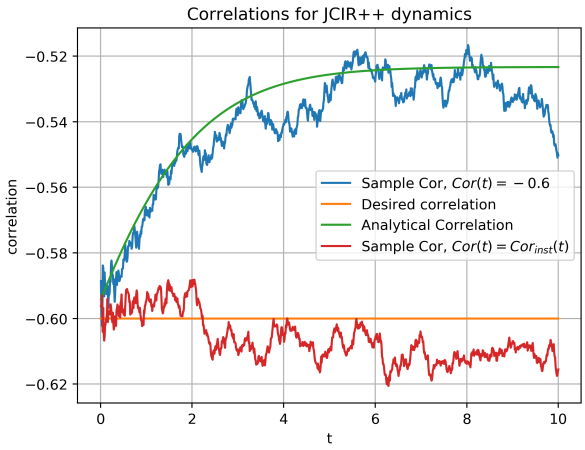

(b) $\rho_{\text{des}}(t) = -0.6$ (in orange). Terminal correlations from the CIR++ model. The analytically calculated terminal correlation with leaking correlation is in green, the terminal correlation from the MC paths with leaking correlation is blue and without in red. $y_J(0) = 0.17, \kappa_J = 0.5, \mu_J = 0.17, \nu_J = 0.4, \xi = 0.1, \gamma = 0.05$

Figure 4.15

In Figures 4.13a, 4.13b, 4.14a, 4.14b, 4.15a and 4.15b it can be observed that without the use of Equations (3.3.14) and (3.3.28), there is some leaking correlation. However, with the use of the functions, we see a terminal correlation that is more constant, around the value of the desired correlation. Although this parameter set cannot be used with the current credit curve, it does show that there are parameter sets for which Equations (3.3.14) and (3.3.28) have impact on the terminal correlation. With the parameters from parameter set B, we have the following average absolute differences between the desired correlation and the terminal correlation, with and without leaking correlation:

- For the CIR++ model in Figure 4.13a with $\rho_{\text{des}}(t) = 0.6$, $\frac{1}{M}\sum_{i=1}^{M} |\rho_{\text{des}}(t_i) - \rho_{\text{term}}(t_i)| = 0.05732150$. Without leaking correlation $\frac{1}{M}\sum_{i=1}^{M} |\rho_{\text{des}}(t_i) - \rho_{\text{term}}(t_i)| = 0.006324699$. Improvement =88.96627%.
- For the CIR++ model in Figure 4.13b with $\rho_{\text{des}}(t) = -0.6$, $\frac{1}{M}\sum_{i=1}^{M} |\rho_{\text{des}}(t_i) - \rho_{\text{term}}(t_i)| = 0.05557393$.

Without leaking correlation $\frac{1}{M}\sum_{i=1}^{M}|\rho_{\text{des}}(t_i)-\rho_{\text{term}}(t_i)| = 0.012902632$. Improvement =76.78294%.

- For the JCIR++ model in Figure 4.14a with $\rho_{\text{des}}(t) = 0.6$, $\frac{1}{M}\sum_{i=1}^{M}|\rho_{\text{des}}(t_i)-\rho_{\text{term}}(t_i)| = 0.0572940166$. Without leaking correlation $\frac{1}{M}\sum_{i=1}^{M}|\rho_{\text{des}}(t_i)-\rho_{\text{term}}(t_i)| = 0.011911852$. Improvement =79.20925%.
- For the JCIR++ model in Figure 4.14b with $\rho_{\text{des}}(t) = -0.6$, $\frac{1}{M}\sum_{i=1}^{M}|\rho_{\text{des}}(t_i)-\rho_{\text{term}}(t_i)| = 0.05554800$. Without leaking correlation $\frac{1}{M}\sum_{i=1}^{M}|\rho_{\text{des}}(t_i)-\rho_{\text{term}}(t_i)| = 0.0105973$. Improvement = 80.9222%.
- For the JCIR++ model in Figure 4.14a with $\xi = 0.1$, $\gamma = 0.05$, $\rho_{\text{des}}(t) = 0.6$, $\frac{1}{M}\sum_{i=1}^{M}|\rho_{\text{des}}(t_i)-\rho_{\text{term}}(t_i)| = 0.06163222$. Without leaking correlation $\frac{1}{M}\sum_{i=1}^{M}|\rho_{\text{des}}(t_i)-\rho_{\text{term}}(t_i)| = 0.008690$. Improvement =85.900%.
- For the JCIR++ model in Figure 4.14b with $\xi = 0.1$, $\gamma = 0.05$, $\rho_{\text{des}}(t) = -0.6$, $\frac{1}{M}\sum_{i=1}^{M}|\rho_{\text{des}}(t_i)-\rho_{\text{term}}(t_i)| = 0.0604294855$. Without leaking correlation $\frac{1}{M}\sum_{i=1}^{M}|\rho_{\text{des}}(t_i)-\rho_{\text{term}}(t_i)| = 0.0091050309$. Improvement = 84.9328007%.

Hence, with the parameter set B we see that the terminal correlation has improved by approximately 80% if we compare the terminal correlations with and without leaking correlation. We have done the same experiments for multiple values of desired correlation and we see that for a higher absolute desired correlation, there is a higher decay of terminal correlation (more leaking correlation) and thus there is more advantage in using the instantaneous-correlation-functions, Equations (3.3.14) and (3.3.28). For example, for $\rho_{\text{des}}(t) = 0.2$ we have an improvement of approximately 60% and for a $\rho_{\text{des}}(t) = 0.9$ of approximately 90%, In Section 4.6 we show the impact of using Equations (3.3.14) and (3.3.28) against leaking correlation on the CVA values. First, we show the results of calibrating the volatility parameter of the CIR++ dynamics to a CDS option in Section 4.4.

4.4. Volatility calibration

Since the CDSO from the synthetic market is produced by the JCIR++ model, the value is dependent on the correlation between the hazard rate and the interest rate. First we compute the CVA values with the calibrated CIR++ model using a correlation equal to zero. For the calibration of the volatility parameter ν for the CIR++ model we use the CDSO described in Section 4.1.2. We keep the parameters of the JCIR++ model fixed and compute the CDSO market value. We have to find a value for ν such that the CIR++ model computes $CDSO_{\text{CIR++}}(\nu)$ equal to this market value. Keeping the other parameters fixed, we compute for multiple values of ν the $CDSO_{\text{CIR++}}$ prices, they are given in Figure 4.16a. $CDSO_{\text{mkt}}$ is dependent on the value of ν_J, however, we have plotted the value as a constant line in Figure 4.16a to give a graphic display of the calibration. We search for value of ν for which the value of the $CDSO_{\text{mkt}}$ intersects the value of $CDSO_{\text{CIR++}}(\nu)$.

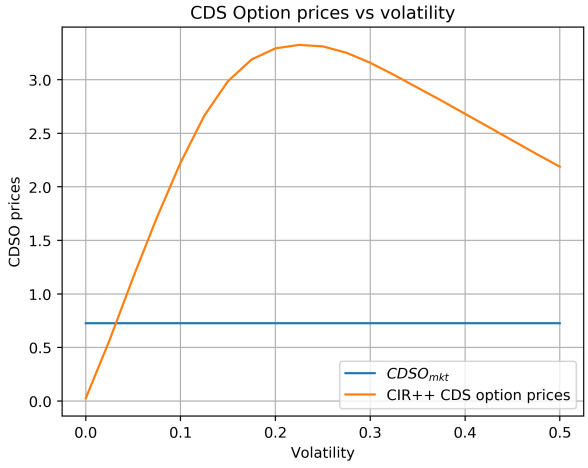

(a) In blue: the CDSO price from the market. In orange: the CDSO values computed by the CIR++ model, dependent on the volatility parameter ν.

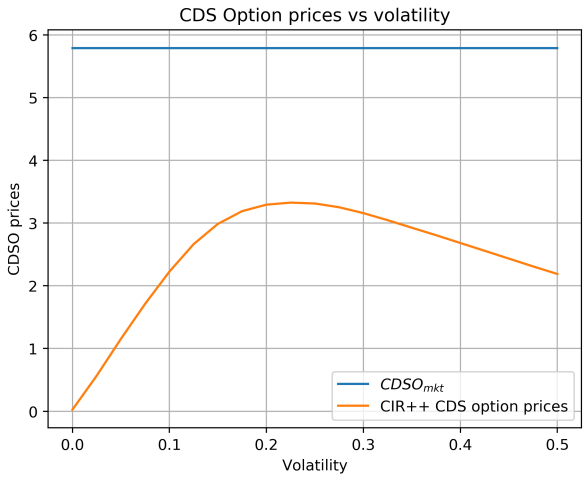

(b) In blue: the CDSO price from the market. In orange: the CDSO values computed by the CIR++ model, dependent on the volatility parameter ν. For this $CDSO_{\text{mkt}}$ value, the CIR++ cannot calibrate to the market.

Figure 4.16

In 4.16a it can be observed that for $\rho_{\text{des}} = 0$, $CDSO_{\text{mkt}} = 0.58126$, such that $\nu = 0.031705$. Hence, $CDSO_{\text{mkt}}$

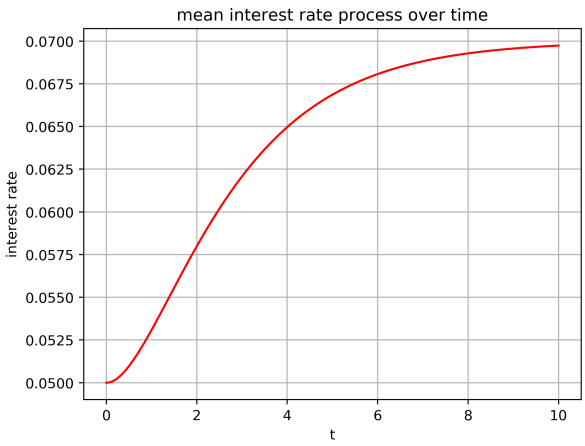

(a) Expected interest rate.

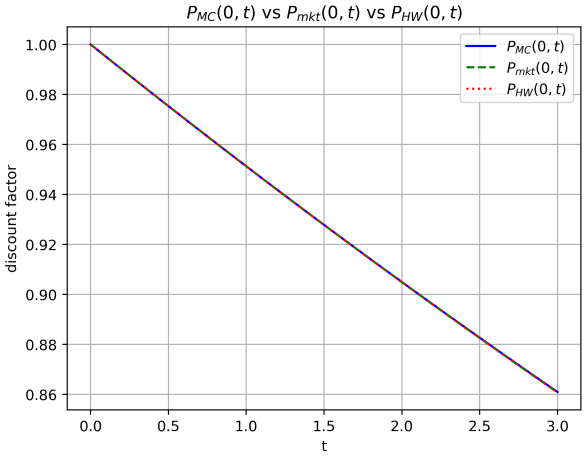

(b) The yield curve from the market, calculated with MC paths and with the analytical zero-coupon bond price formula.

Figure 4.17

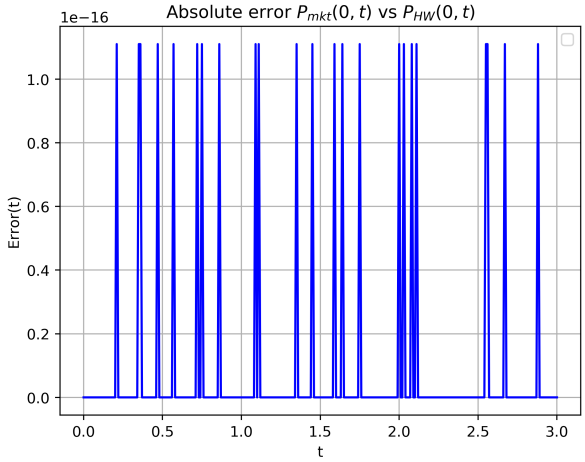

(a) Absolute difference between the analytically computed discount factors and discount factors from the market.

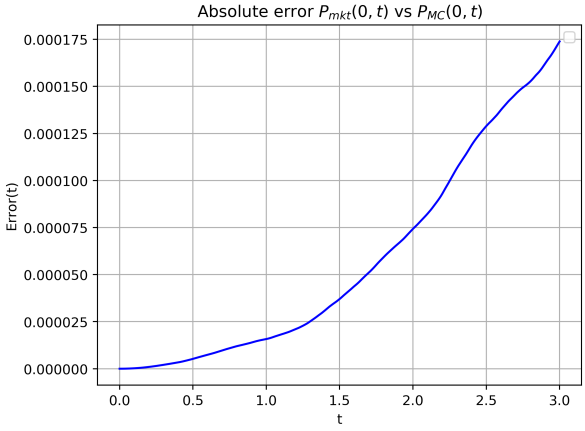

(b) Absolute difference between the Expected discount factors from the Monte Carlo simulation and discount factors from the market.

Figure 4.18

falls within the interval for which the CIR++ model can calibrate to the JCIR++ model. Compared to the volatility parameter v_J of the JCIR++ model, we notice that for the jumps with a jump rate $\xi = 0.01$ and jump size $\gamma = 0.005$ the CIR++ needs extra volatility to compensate for the lack of jumps: $v - v_J = 0.03107 - 0.03 = 0.00107$. We have compared multiple values of v_J, ξ and γ with the calibrated value of v and see that for higher values of ξ and γ, we need a higher value of v. The model is limited by approximations and not all values v can be used. Thus, for high values of ξ and γ, the CIR++ model cannot be calibrated anymore. This can be observed in Figure 4.16b: the value of $CDSO_{\text{CIR++}}(v)$ is lower than the value of $CDSO_{\text{mkt}}$ for all values of v. The value of $CDSO_{\text{CIR++}}(v)$ should be increasing in v, however, it decreases after v is approximately equal to 0.22. This is because for a high value of v compared to κ and μ, many hazard rate paths will reach the origin. Then the actual volatility of the hazard rate decreases because of the reflecting principle of the discritization scheme.

4.5. Exposures

For the input presented in Section 4.1, the expected interest rate can be observed in Figure 4.17a. Just as the $\psi(t)$ for the CIR++ model, we use function $\theta(t)$ (see Equation (3.1.4)) to make sure that the interest rate model is calibrated to the yield curve (Equation (4.1.1). In Figure 4.17b it can be observed that the errors

between $P_{\text{HW}}(0,t)$ and $P_{\text{mkt}}(0,t)$ are approximately zero. The errors $P_{\text{MC}}(0,t)$ and $P_{\text{mkt}}(0,t)$ are of the order of the MC standard error (approximately $9.9 \cdot 10^{-4}$). We have simulated the discount factors $P_{\text{MC}}(0,t)$ from the MC simulation with multiple number of paths and noticed that the error converges to zero for an increasing number of paths. Hence, all discount factors are approximately equal to the market. For more information, see Appendix **??**. Using these discount factors we compute the exposure profile of the IRS in the portfolio, see Figure 4.19.

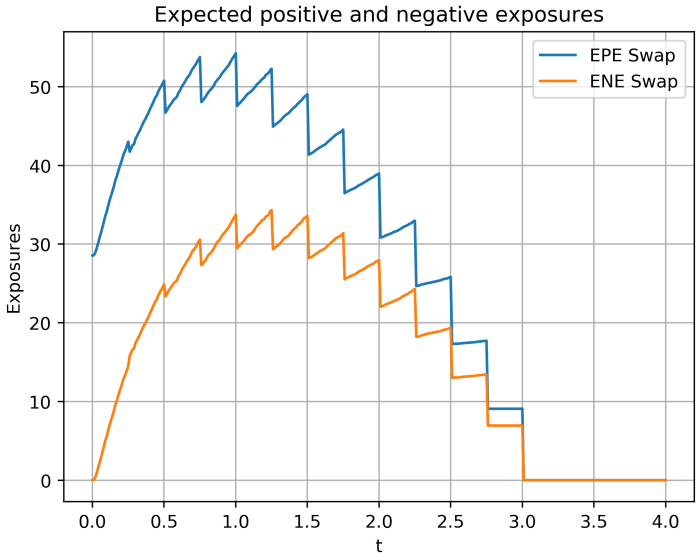

Figure 4.19: The Expected positive Exposure and the Expected negative Exposure. $EPE(t) = \mathbf{E}^{\mathbb{Q}}\left[\frac{B(0)}{B(t)}\max\left(V^{\text{IRS}}(t),0\right)\middle|\mathscr{F}(0)\right]$, $ENE(t) = \mathbf{E}^{\mathbb{Q}}\left[\frac{B(0)}{B(t)}\max\left(-V^{\text{IRS}}(t),0\right)\middle|\mathscr{F}(0)\right]$. Strike rate is 0.04.

We plotted only until $t = 4$, since the IRS has zero value after maturity date $T = 3$. The swap in Figure 4.19 has a start value of 25.5534 at start date $t_0 = 0$. This is because the fair strike rate would be 0.0503, thus the payer IRS is ITM for a strike rate of 0.04. It can be observed that both the $EPE(t)$ and the $ENE(t)$ first increase with time and then decrease with time. This is because of the uncertainty of the interest rate increases with time. At the same time, payments are made, which decrease the value of the swap. At first the uncertainty is higher: the short-rate can increase (decrease) much which gives a high ENE (EPE) for the IRS. But as t approaches the maturity date, the payments have more effect on the exposure than the uncertainty has. The payments decrease the exposure of the swap and the value of the swap converges to 0. After the last payment there is no exposure since the swap contract has ended. With the exposure profile, the survival probabilities and the L_{GD}, we can compute the CVA values.

4.6. CVA

Recall Equation (2.1.3) for the computation of the CVA. We need the L_{GD}, the survival probabilities from the credit model and the discount factors and exposures from the interest rate model. With the input from Sections 4.1 and the results from Sections 4.2, 4.2, 4.4 and 4.5, we can compute the CVA as function of desired correlation $\rho_{\text{des}}(t)$.

First we assume $\rho_{\text{des}}(t) = 0$. We calibrate the CIR++ model to the JCIR++ model and with that volatility parameter, we compute the $\text{CVA}^{\text{C}}(\rho_{\text{des}})$ and $\text{CVA}^{\text{J}}(\rho_{\text{des}})$ of both models. In this way we can see how the CVA behaves under influence of the correlation. Comparing the results of the CVA with $\rho_{\text{des}}(t) = 0$ with $\rho_{\text{des}}(t) \neq 0$, gives a mixed result: the difference depends not only on impact of the correlation, but also on the choice of the model. Hence, using two calibrated models, we can put the results into better perspective by comparing the two different models for each value of ρ_{des}. To get better results, we compute the $\text{CVA}(\rho_{\text{des}})$ values where we calibrate the CIR++ model to the JCIR++ model for each value of ρ_{des}. This way there should be less impact of the model on the CVA computations. Also, we show the impact of using Equations (3.3.14) and (3.3.28) to solve the leaking correlation problem on the CVA value. We also show whether there is more impact of WWR

on the CVA of the portfolio when the maturity date of the IRS is further away in the future.

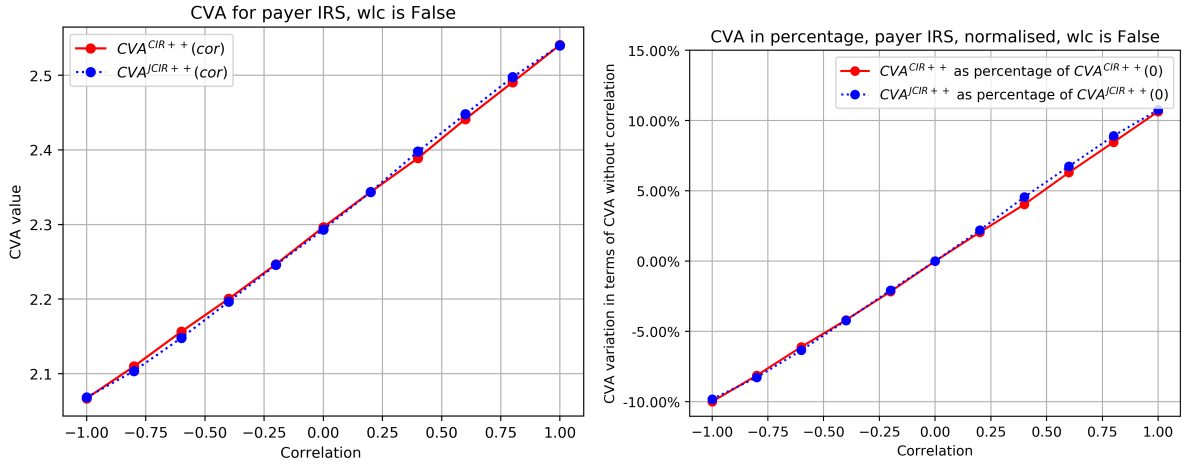

(a) Absolute CVA values, simulated without leaking correlation and calibrated for $\rho_{\text{des}}(t) = 0$.

(b) Relative CVA changes, w. r. t. CVA

Figure 4.20

Using $\rho_{\text{des}}(t) = 0$ for the calibration of the volatility parameter, we have a volatility ν for the CIR++ model equal to 0.031705. In Tables 4.2 and 4.3 the results can be found of the computed CVA values for both the CIR++ and the JCIR++ models. These values can also be observed in Figure 4.20a. The CVA values do not differ significantly. This was expected since the volatility parameters of the models do not differ significantly either. In Figure 4.20b and Tables 4.4 and 4.5 the values w.r.t. $\text{CVA}^i(0)$ are given, so that the increase is not dependent on the notional of the portfolio.

ρ	-1	-0.8	-0.6	-0.4	-0.2
$\text{CVA}^C(\rho)$	2.067	2.110	2.156	2.200	2.247
$\text{CVA}^J(\rho)$	2.068	2.104	2.148	2.196	2.246
$\text{CVA}^C(\rho) - \text{CVA}^J(\rho)$	$-1.28 \cdot 10^{-3}$	$6.19 \cdot 10^{-3}$	$8.45 \cdot 10^{-3}$	$3.84 \cdot 10^{-3}$	$9.09 \cdot 10^{-4}$
Rel. dif. w.r.t. $\text{CVA}^J(\rho)$	$-6.27 \cdot 10^{-4}$	$2.94 \cdot 10^{-3}$	$3.93 \cdot 10^{-3}$	$1.75 \cdot 10^{-3}$	$4.05 \cdot 10^{-4}$

Table 4.2: Absolute CVA values, simulated without leaking correlation and calibrated for $\rho_{\text{des}}(t) = 0$.

ρ	0	0.2	0.4	0.6	0.8	1
$\text{CVA}^C(\rho)$	2.296	2.343	2.389	2.441	2.491	2.541
$\text{CVA}^J(\rho)$	2.293	2.344	2.398	2.448	2.498	2.540
$\text{CVA}^C(\rho) - \text{CVA}^J(\rho)$	$3.17 \cdot 10^{-3}$	$-1.60 \cdot 10^{-4}$	$-8.81 \cdot 10^{-3}$	$-6.64 \cdot 10^{-3}$	$-6.89 \cdot 10^{-3}$	$7.81 \cdot 10^{-4}$
Rel. dif. w.r.t. $\text{CVA}^J(\rho)$	$1.38 \cdot 10^{-3}$	$-6.83 \cdot 10^{-5}$	$-3.683 \cdot 10^{-3}$	$-2.71 \cdot 10^{-3}$	$-2.76 \cdot 10^{-3}$	$3.07 \cdot 10^{-4}$

Table 4.3: Absolute CVA values, simulated without leaking correlation and calibrated for $\rho_{\text{des}}(t) = 0$.

ρ	-1	-0.8	-0.6	-0.4	-0.2
$\text{CVA}^C(\rho)/\text{CVA}^C(0)$	-0.09993734	-0.08127554	-0.06100047	-0.04184867	-0.02164047
$\text{CVA}^J(\rho)/\text{CVA}^J(0)$	-0.09812816	-0.08270535	-0.06338682	-0.04220005	-0.02068519

Table 4.4: Relative CVA changes, w. r. t. $\text{CVA}^{\text{CIR++}}(0)$ and $\text{CVA}^{\text{JCIR++}}(0)$ for the CIR++ and the JCIR++ model respectively. Simulated without leaking correlation and calibrated for $\rho_{\text{des}}(t) = 0$.

When $\rho_{\text{des}}(t) = 0$, it means that the counterparty is independent from market risk. In this case we can compare the two models and see what the model risk is: $\text{CVA}^C(0) - \text{CVA}^J(0) = 3.17 \cdot 10^{-3}$. This is larger than the MC standard error, which means that there is some model risk. Knowing this value, we can put the other values

ρ	0.2	0.4	0.6	0.8	1
$\text{CVA}^C(\rho)/\text{CVA}^C(0)$	0.02052499	0.04034051	0.06310634	0.08466132	0.10647435
$\text{CVA}^J(\rho)/\text{CVA}^J(0)$	0.02200478	0.04562129	0.06746997	0.08916359	0.10766257]

Table 4.5: Relative CVA changes, w. r. t. $\text{CVA}^{\text{CIR++}}(0)$ and $\text{CVA}^{\text{JCIR++}}(0)$ for the CIR++ and the JCIR++ model respectively. Simulated without leaking correlation and calibrated for $\rho_{\text{des}}(t) = 0$.

in better perspective. Considering that for some values of ρ_{des} the difference is approximately as much as the MC standard error and that for some values the difference is more, it is difficult to say whether the models give the same CVA values or not. In section 4.6.2 we compare the models while we calibrate per value of ρ. This gives better insight in the difference per models.

For a IRS payer position, a negative correlation has a right-way risk effect and a positive correlation has a WWR effect on the CVA: for a negative correlation the CVA decreases and with a positive correlation the CVA increases with respect to $\rho_{\text{des}} = 0$. This was expected: for an increasing interest rate, the exposure decreases from a payer position. For a negative correlation, an increase of the interest rate means a decrease in hazard rate and therefore a decrease in the CVA. This is a RWR situation, since there is a favourable relation between the exposure and the creditworthiness. The other way around, with a positive correlation, we see a WWR effect on the CVA. With a positive correlation, an increase of the interest rate means an increase in the hazard rate and therefore an increase in the CVA. For a IRS receiver position a negative correlation has a WWR effect on the CVA and a positive correlation a RWR effect. For the exposure, holding a payer position is most risky with a positive correlation and holding a receiver position is most risky with a negative correlation.

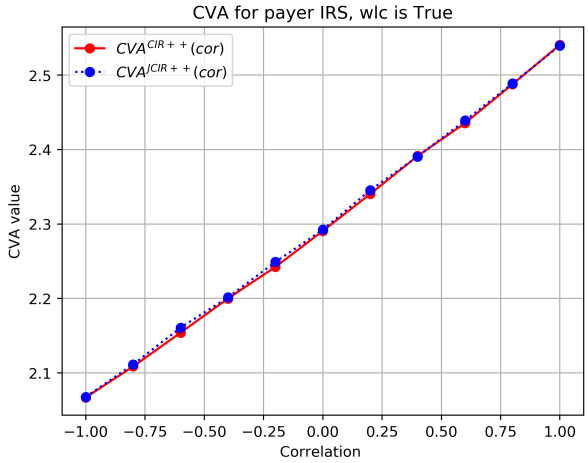

(a) Absolute CVA values, simulated with leaking correlation and calibrated for $\rho_{\text{des}}(t) = 0$.

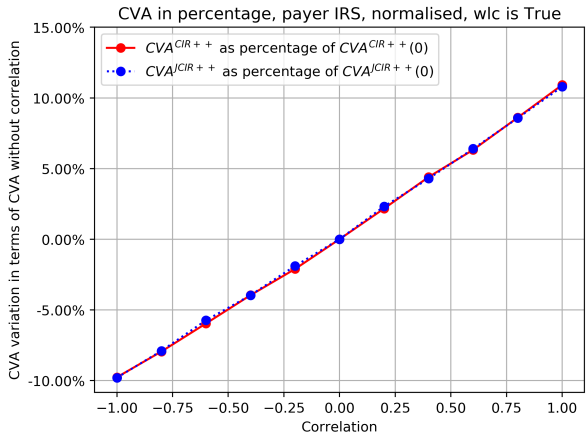

(b) Relative CVA changes, w. r. t. $\text{CVA}^{\text{C}}(0)$ and $\text{CVA}^{\text{J}}(0)$ for the CIR++ and the JCIR++ model respectively. Simulated with leaking correlation and calibrated with $\rho_{\text{des}}(t) = 0$

Figure 4.21

The effect of WWR is mathematically significant for both models with the parameters from Section 4.1, since the CVA increases and decreases up to 10% for a respectively positive or negative correlation, w. r. t. a correlation equal to zero.

4.6.1. Longer IRS tenor

The IRS in the portfolio from Section 4.1, has a maturity date $T_b^{\text{IRS}} = 3$. Keeping the other parameters the same, we analysed the results of a IRS swap with $T_b^{\text{IRS}} = 9$. The results are similar in a qualitative way and can be observed in Figures 4.22a and 4.22b. The figures show that the CVA increases in absolute value, but the relative CVA variation due to the correlation stays the same.

In Figures 4.21a and 4.21b the absolute and relative CVA values can be observed when the hazard rate paths are simulated with leaking correlation and using the parameters of Section 4.1 ($T_b^{\text{IRS}} = 3$). In Section 4.3 we showed that the using Equations (3.3.14) and (3.3.28) do not have much impact with the parameter set that is used. Hence, there is not much difference in the CVA values. The same holds for a IRS swap with $T_b^{\text{IRS}} = 9$).

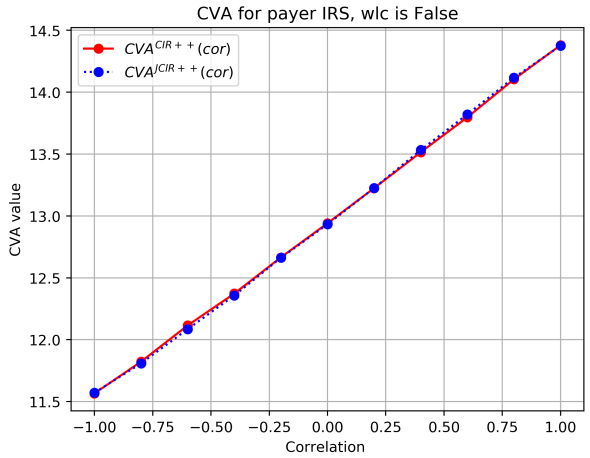

(a) Absolute CVA values, simulated without leaking correlation and calibrated for $\rho_{\text{des}}(t) = 0$. $T_b^{\text{IRS}} = 9$.

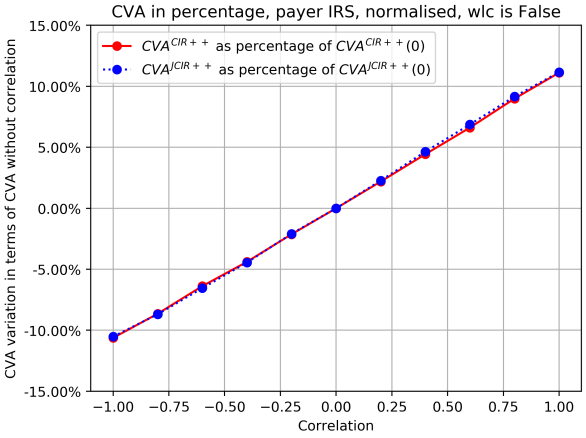

(b) Relative CVA changes, w. r. t. $\text{CVA}^{\text{C}}(0)$ and $\text{CVA}^{\text{J}}(0)$ for the CIR++ and the JCIR++ model respectively. Simulated without leaking correlation and calibrated for $\rho_{\text{des}}(t) = 0$. $T_b^{\text{IRS}} = 9$.

Figure 4.22

4.6.2. Calibration per ρ-value

We analyse the results of the CVA values when we calibrate the CIR++ model to the JCIR++ model per value for $\rho_{\text{des}}(t)$. We use the following values for the desired correlation:

$$\rho_{\text{des}}(t) = [-1, 0.8, 0.6, 0.4, 0.2, 0, 0.2, 0.4, 0.6, 0.8, 1].$$

Per value of ρ_{des} we calculate the $CDSO_{\text{mkt}}$ value and the value for ν, depending on the correlation. The values for ν per ρ_{des} can be found in Tables 4.6, 4.7. The values of the volatility do not differ much, therefore the CVA values computed with these values for ν, in Figures 4.23a and 4.23b, do not differ much from the values in Figure 4.20a and 4.20b. However, a small change can be observed: there is more difference between the models. Especially with an absolute high value for ρ_{des}, we see that the CVA^{J} values are less impacted by the correlation, compared to the values of CVA^{C}. This is because the terminal volatility of the CIR++ model is purely dependent on the instantaneous volatility parameter ν and the correlation parameter ρ_{des}, but for the JCIR++ model the terminal volatility is also partly dependent on the independent jumps. The instantaneous volatility parameter ν_J is for the JCIR++ model smaller than for the CIR++ model, therefore it is less affected by the correlation. We want to further analyse the impact of a larger jump component in the JCIR++ model,

ρ_{des}^i	-1	0.8	0.6	0.4	0.2	0
ν	0.03207	0.03159	0.03190	0.03211	0.03218	0.03226

Table 4.6: Values of ν, calibrated to the market per value of correlation. Calibrated without leaking correlation.

ρ_{des}^i	0.2	0.4	0.6	0.8	1
ν	0.03234	0.03247	0.03247	0.03232	0.03208

Table 4.7: Values of ν, calibrated to the market per value of correlation. Calibrated without leaking correlation.

therefore in the next section we use a different parameter set.

4.6.3. JCIR++: more jumps, less instantaneous volatility

In this section the following parameters are used for the JCIR++ model: jump rate $\xi = 0.1$ and volatility $\nu_J = 0.01$. The other parameters stay the same. To make a distinction, we call the parameter set from Section 4.1 parameter set A and the new parameter set is called parameter set J. We choose to use more jumps, such that the difference between ν and ν_J will be higher after calibration of ν. Also we choose a low value for ν_J, such that the CIR++ model is still able to calibrate to the JCIR++ model. With $\rho_{\text{des}} = \rho_{\text{inst}} = 0$, $CDSO_{\text{mkt}} = 0.4800347$ and after calibration, we have ν is equal to 0.027234. This shows that there is more difference

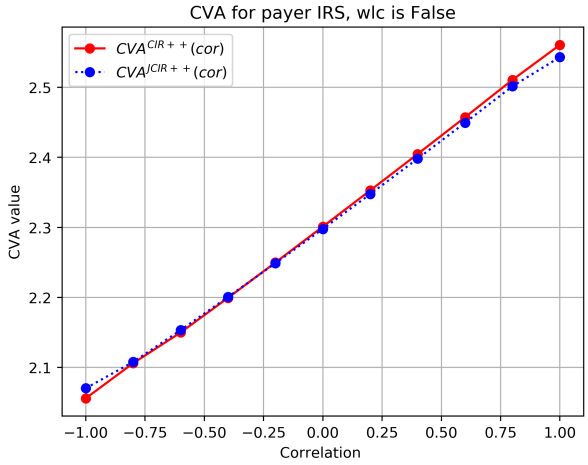

(a) Absolute CVA values, simulated without leaking correlation and calibrated per value of ρ^i_{des}.

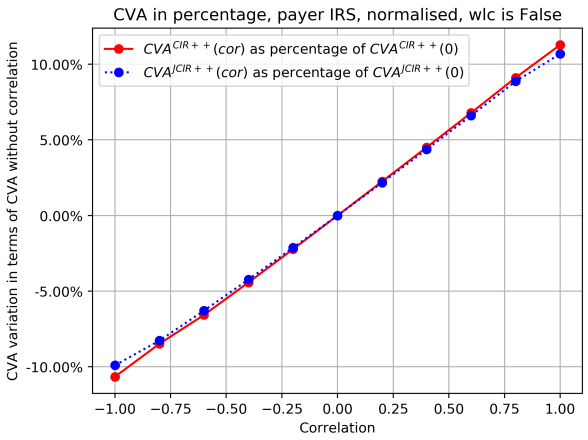

(b) Relative CVA changes, w. r. t. $\text{CVA}^{\text{C}}(0)$ and $\text{CVA}^{\text{J}}(0)$ for the CIR++ and the JCIR++ model respectively. Simulated without leaking correlation and calibrated per value of ρ^i_{des}.

Figure 4.23

between the instantaneous volatilities of the model. For parameter set A there was a difference of 0.0017, now the difference equals $v - v_J = 0.027234 - 0.01 = 0.017234$.

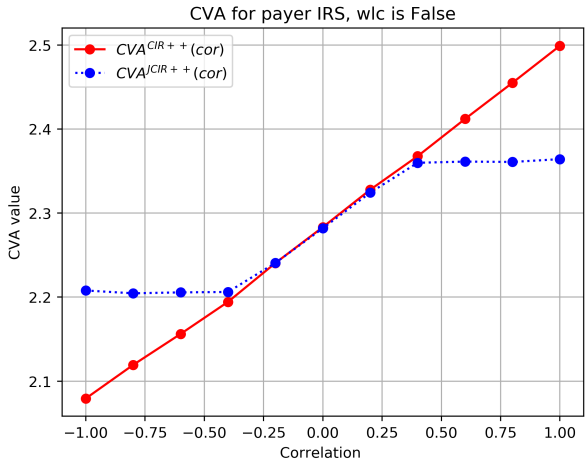

(a) Absolute CVA values, simulated without leaking correlation and calibrated with $\rho_{\text{des}}(t) = 0$.

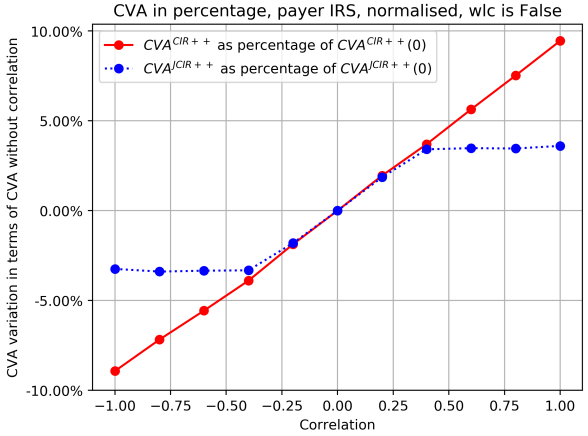

(b) Relative CVA changes, w. r. t. $\text{CVA}^{\text{C}}(0)$ and $\text{CVA}^{\text{J}}(0)$ for the CIR++ and the JCIR++ model respectively. Simulated without leaking correlation and calibrated with $\rho_{\text{des}}(t) = 0$.

Figure 4.24: CVA values of a IRS payer position.

In Figure 4.24a the absolute values of $\text{CVA}^{\text{C}}(\rho_{\text{des}})$ and $\text{CVA}^{\text{J}}(\rho_{\text{des}})$ are shown. It can be observed that the CVA^{C} values are lower than the CVA^{C} values from Figure 4.20a. This was expected, since the volatility v from parameter set A is higher than the volatility from parameter set J. In Figures 4.25a and 4.25b the values of CVA^{C} and CVA^{J} can be observed, for a calibration that is done per value of ρ_{des}. Comparing the values of CVA^{C} from parameter set A to those of parameter set J, there is not much difference. However, comparing the values of CVA^{J} of parameter set A the values of CVA^{J} to parameter set J, there is a significant difference. Hence, for parameter set J, the difference between the values of CVA^{C} and CVA^{J} are significant. So, there is indeed more difference between the CVA values of the models for a higher difference between v and v_J. Also, we notice a different shape in the CVA^{J} values. If the desired correlation is in absolute value higher than approximately 0.37, then the CVA^{J} do not depend on $\rho_{\text{des}}(t)$ anymore. If the jump rate is high (or jumps are large) in combination with a high desired correlation, then the instantaneous-correlation-function $\rho^{\text{J}}(t)$ cannot counter the leaking correlation. Then the difference between the desired correlation and the terminal correlation mainly comes from the jumps. An example of this, for $\rho_{\text{des}}(t) = 0.8$, can be observed in Figures 4.26a and 4.26b. Although the analytically calculated correlation fits the leaking correlation well, the instantaneous-correlation-

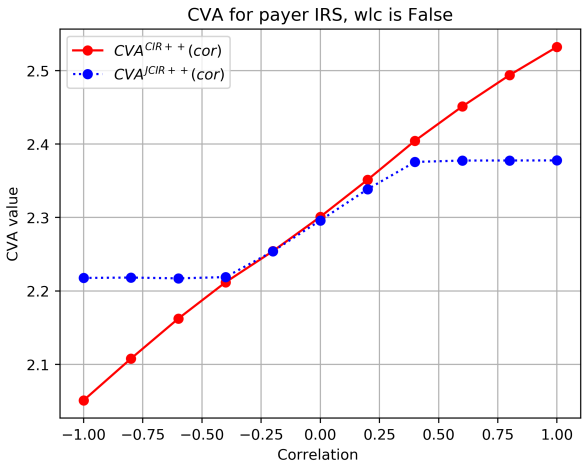

(a) Absolute CVA values. Calibrated to the market per value of correlation. Calibrated without leaking correlation.

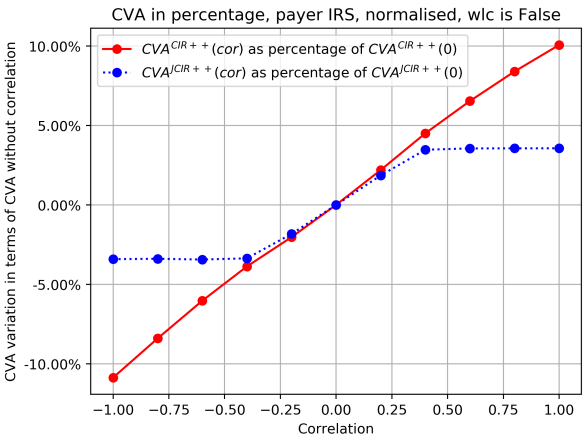

(b) Relative CVA changes, w. r. t. $\text{CVA}^{\text{C}}(0)$ and $\text{CVA}^{\text{J}}(0)$ for the CIR++ and the JCIR++ model respectively. Calibrated to the market per value of correlation. Calibrated without leaking correlation.

Figure 4.25: CVA values for an IRS payer position.

function ρ^{J} cannot use this properly to counter the leaking correlation. To counter it, ρ^{J} has to become larger than one. However, due to the use of a Cholesky decomposition to correlation the Brownian increments of the hazard rate and the interest rate, $\rho^{\text{J}}(t)$ cannot become larger than one (see Figure 4.26b). Hence, if $\rho_{\text{des}}(t)$ is larger than approximately 0.37, then $\rho_{\text{inst}}(t) = \rho^{\text{J}}(t) = 1$ for all t and hence CVA^{J} stays constant. For the CIR++ model, the instantaneous-correlation-function $\rho^{\text{CIR}}(t)$ does give a terminal correlation closer to the desired correlation for all t and hence CVA^{C} is still dependent on $\rho_{\text{des}}(t)$. To give a better comparison, we

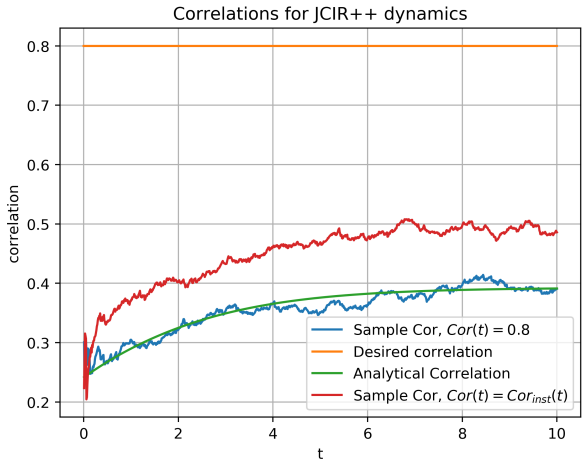

(a) $\rho_{\text{des}} = 0.8$. Terminal correlations from the CIR++ model. The analytically calculated terminal correlation with leaking correlation is in green, the terminal correlation from the MC paths with leaking correlation is blue and without in red. Parameter set J.

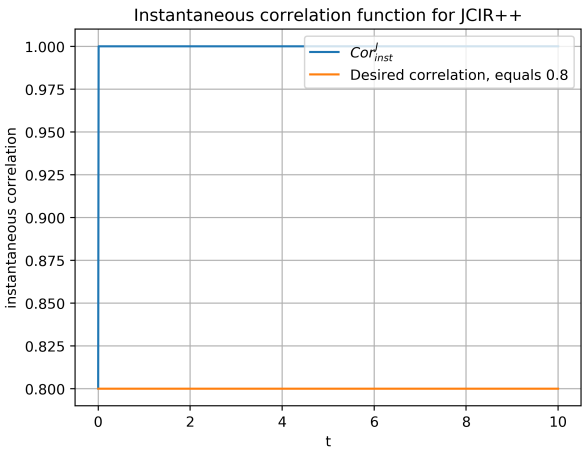

(b) Instantaneous correlation function ρ^{J} for $\rho_{\text{des}}(t) = 0.8$ and parameter set J.

Figure 4.26: Correlations.

have also computed the CVA values with leaking correlation for parameter set J. The absolute values can be found in Figure 4.27a and the relative values can be found in Figure 4.27b. Compared to Figures 4.21a and 4.21b, there is a more distinctive difference between $\text{CVA}^{\text{C}}(\rho_{\text{des}})$ and $\text{CVA}^{\text{J}}(\rho_{\text{des}})$. Also these figures confirm that the impact of WWR is dependent on the value of $\rho_{\text{inst}}(t)$ and the value of the instantaneous volatility parameter. Since there is a larger difference between ν and ν_J, there is a larger difference between $\text{CVA}^{\text{C}}(\rho_{\text{des}})$ and $\text{CVA}^{\text{J}}(\rho_{\text{des}})$ per value of ρ_{des}.

So, does leaking correlation have impact on the CVA of the portfolio, or is it unnecessary to use the instantaneous-

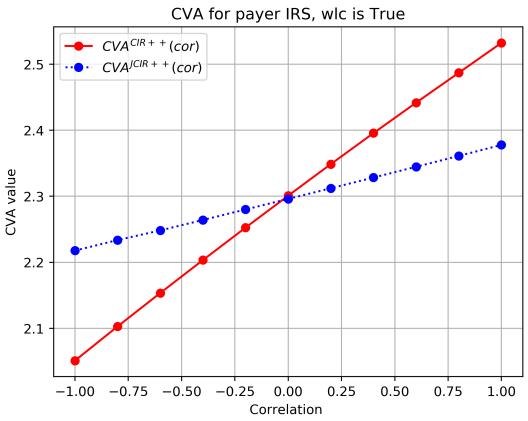

(a) Absolute CVA values, simulated wit leaking correlation and calibrated to the market per value of correlation.

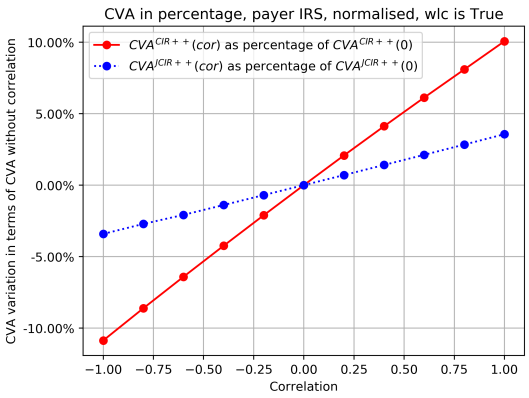

(b) Relative CVA changes, w. r. t. $\text{CVA}^{\text{C}}(0)$ and $\text{CVA}^{\text{J}}(0)$ for the CIR++ and the JCIR++ model respectively. Simulated with leaking correlation and calibrated to the market per value of correlation.

Figure 4.27

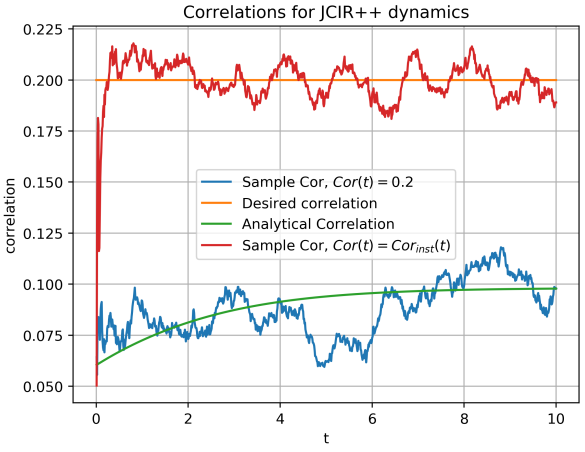

(a) $\rho_{\text{des}} = 0.2$. Terminal correlations from the CIR++ model. The analytically calculated terminal correlation with leaking correlation is in green, the terminal correlation from the MC paths with leaking correlation is blue and without in red. Parameter set J.

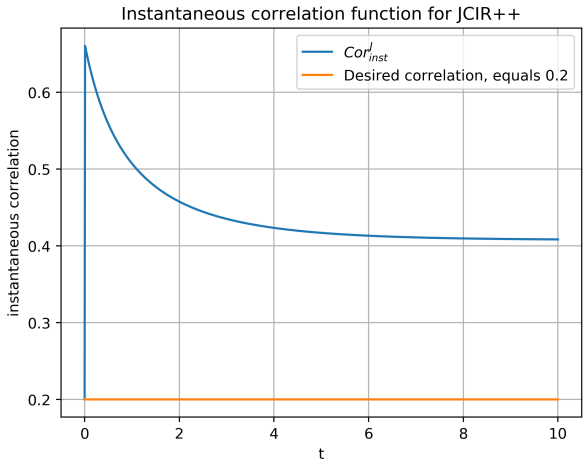

(b) Instantaneous-correlation-function ρ^{J} for $\rho_{\text{des}}(t) = 0.2$ and parameter set J.

Figure 4.28

correlation-functions. We see some difference in correlation in Figures 4.28a and 4.26a, but we take a look at the following CVA results to see if there is also a difference in CVA value.

For $\rho_{\text{des}} = 0.8$ we have the following for the CIR++ model:

1. Average difference between the desired correlation and the terminal correlation is 0.006190346097700139 with leaking correlation and 0.004418275006184927 without. Although absolute small, a relative improvement of 28.62 %.
2. CVA with leaking: 2.44970957, without leaking: 2.44970957. A difference of the size of the MC standard error: so insignificant.
3. Hence, the difference CVA values as fraction of the portfolio values is also insignificant.

So indeed, for the CVA of the IRS with the CIR++ model, with the used parameters, solving leaking correlation has no significant impact. For the JCIR++ we have the following. For $\rho_{\text{des}} = 0.8$:

1. Average difference between the desired correlation and the terminal correlation is 0.44501599 with leaking correlation and 0.351848192967 without. The difference is relatively large and there is a rel-

ative improvement of 20.9358 %.

2. CVA with leaking: 2.34421804, without leaking:2.360855. A difference of 0.01663769. So, CVA value is 0.709733 percent higher without leaking correlation. This could be significant, when the notional becomes very large.

3. The CVA with leaking correlation has a value which is 8.209939 % of the portfolio value (28.5534). The CVA without leaking correlation: 8.2682082 %. This is a difference of approximately 6 basis points, which could be significant for large nominal values of the IRS.

For the JCIR++ model with $\rho_{\text{des}} = 0.2$

1. Average difference between the desired correlation and the terminal correlation is 0.11295663 with leaking correlation and 00.007512238 without. The difference is relatively large and there is a relative improvement of 93.349 %.

2. CVA with leaking: 2.29902093, without leaking: 2.32436. A difference of 0.02534469. So, CVA value is 1.1024 percent higher without leaking correlation. This could be significant, when the notional becomes very large.

3. The CVA with leaking correlation has a value which is 8.05165 % of the portfolio value (28.5534). The CVA without leaking correlation: 8.15763 %. This is a difference of approximately 10 basis points, which could be significant for large nominal values of the IRS.

Therefore, for parameter set J, using the instantaneous-correlation-function $\rho^{\text{J}}(t)$ has a significant impact on the CVA, for both low and high values of desired correlation. For the CVA of the CIR++ model, we see less impact.

5

Conclusion, discussion and future research

In this research we investigated the impact of wrong-way risk (WWR) on the Credit Value Adjustment (CVA) of a portfolio of Interest Rate Swaps (IRSs). The main goal was to quantify it. During the research we found two suitable credit models and finding out what the most suitable credit model is, became a sub-goal. A CVA model, using a Monte Carlo (MC) framework with stochastic differential equations and a reduced form model, was developed to model WWR in the portfolio of IRSs. The model was partly calibrated to a synthetic market and partly parameters were chosen historically. This has led to another sub goal: solving the leaking correlation problem and investigating the impact of leaking correlation on the CVA. In this chapter, first a summary of the research is given in Section 5.1, after which we conclude with an answer for the main question of this research in Section 5.2. In Section 5.3 we discuss the limits of our CVA model and in Section 5.4 of this chapter we discuss possible topics for future research.

5.1. Summary

Within the MC framework we used Hull-White one factor (HW1F) dynamics to model the interest rate. For the credit part of the CVA model we used a reduced form model and modeled its hazard rate with both Cox Ingersoll Ross (CIR) dynamics and CIR dynamics with jumps (JCIR). To create dependence between the interest rate part and the credit part of the CVA model, we used a correlation parameter to correlate the Brownian increments of the dynamics. We used synthetic data set of suitable Credit Default Swaps (CDSs) to calibrate the credit models to the term structure of credit rates and called the calibrated models 'CIR++' and 'JCIR++'. We assumed the JCIR++ to be the market, computed for multiple parameter sets suitable Credit Default Swaptions (CDSOs) and calibrated the volatility parameter of the CIR++ model to the CDSOs. We chose the other parameters of the models and created multiple parameter sets to investigate the WWR in the IRS portfolio. When simulating the correlated paths of the interest rate and hazard rate, we came across a phenomenon called 'leaking correlation'. Due to the choice of using a historical chosen correlation parameter, We built instantaneous-correlation functions to tackle the leaking correlation problem, for as far as the used approximations and numerical method allow it. We used two parameter sets, one with a high jump rate and low volatility parameter for the JCIR++ model and one with a low jump rate and a higher volatility parameter. We investigated the impact of the correlation on the value of the CVA of the portfolio, including and excluding the instantaneous-correlation-functions and investigated the impact on a IRS with a maturity date further away in the future. We investigated the impact of both the credit models, to separate the influence of the model choice from the impact of WWR and to investigate which model is more suitable to model WWR.

5.2. Conclusion

During our research we came across the problem of leaking correlation, because of the use of a correlation parameter based on historical data. Leaking correlation is increased for higher values of instantaneous correlation and higher values of instantaneous volatility. For the CIR++ model, using a parameter set with small values of volatility, the built instantaneous-correlation-function has little impact on the terminal correlation itself and therefore also little impact on the CVA. For higher values of instantaneous volatility, both models show a significant impact on the terminal correlation. In the JCIR++ model, the jumps destroy partly

the terminal correlation between the interest rate and the hazard rate. Therefore, using the instantaneous-correlation-function does have a non-negligible impact, even for small values of instantaneous volatility. It also noticeably changes the value of the CVA for the IRS. Unfortunately, for a jump rate of jump size too large, the instantaneous-correlation-function cannot compensate for the independent jumps and it cannot bring the terminal correlation to the desired correlation. However, it still has an not negligible impact on the value of the CVA of the IRS. Whether the changes of the CVA are significant, depends on the size of the exposure.

Wrong-way risk has an significant impact on the CVA of a portfolio of IRS. The size of the impact and in which direction depends on multiple factors, such as the size of the exposure and the position of the IRS, the yield curve and the credit curve. Calibrated to the synthetic data, the model shows changes of the CVA up to 10% in both directions, therefore the impact of WWR has mathematical significance and is at least not negligible. A longer tenor of the IRS has an impact on the absolute value of the CVA, not on the relative change caused by WWR. A negative correlation has a right-way-risk (RWR) effect and a positive correlation a WWR effect on the CVA of a IRS payer position. For a receiver position a negative correlation has a WWR effect on the CVA and a positive correlation a RWR effect on the CVA. Since there is a non-negligible impact on the CVA, WWR needs to be taken into account to correctly price and hedge the CVA of an IRS.

To determine which credit model should be used to determine the CVA and the WWR of a portfolio of IRSs, the following need to be taken into account. Considering CDSOs from the market, there is a possibility that the CIR++ dynamics cannot attain the high levels of volatility. In that case, the JCIR++ dynamics are the obvious choice. Assuming we can use both models, then the impact of WWR can be taken into account. When only correlating the Brownian increments of the credit model with the interest rate level, then it can be observed that the JCIR++ model generates a lower impact of WWR on the CVA of the portfolio. This is due to the independent jumps and due to the fact that the JCIR++ dynamics use a lower value of instantaneous volatility, to reach the same volatility as the CIR++ dynamics. Only when the difference in instantaneous volatility parameter is large enough, this lower impact on the CVA is not negligible. The difference can also be dependent on the calibration data and on the products in the portfolio, for a more exotic product this could be different.

Knowing that there is a difference between the models, the choice for one or the other depends on multiple factors. The risk appetite of the bank for example. If a riskier appetite is preferred, the JCIR++ model can be used, if more risk averse, the CIR++ model. Also, since the CIR++ models gives larger CVA values, using the CIR++ model could mean that the bank is less competitive in its CVA calculations. But using the JCIR++ model leads to other problems: calibrating the jumps of the JCIR++ model could be more difficult and finding products to calibrate to as well. Analysing how each model behaves in different situations, helps making a choice. Either way, the degree of the impact of WWR on the CVA is model dependent. We only analysed a portfolio of IRSs, maybe for different products a different conclusion will be drawn. Using a CIR++ model or a JCIR++ model, either way, for the bank it is worth the trouble to look into WWR.

5.3. Limitations

It is important to not only consider the results, but also the assumptions and the limitations of the research. In creating the CVA model, we encountered several boundaries. They are listed below:

- To calibrate the credit part to the term structure of credit rates, we used a deterministic shift. This $\psi_{(J)}$-function is dependent on the parameters of the CIR and JCIR dynamics. It bounds the parameters, since the function needs to remain positive. Otherwise the CVA could become negative. The $\psi_{(J)}$-function remains positive for values of $y_{(J)}(0)$ and $\mu_{(J)}$, such that the mean of the $y_{(J)}$ paths is not much higher than the market implied hazard rates.
- We came across a limitation for the volatility parameter using this CVA model. It cannot be too high compared to κ and μ, otherwise too many $y_{(J)}$-paths hit the origin. Then the volatility of the paths decrease and hence the CIR++ model cannot be calibrated to the CDSO from the market. Also, when many paths hit the origin, the reflecting principle of the reflecting Euler discritization changes the distribution. The paths are no longer Chi-squared distributed and therefore the analytically computed survival probabilities $SP_{\text{CIR}}(t,T)$ and $SP_{\text{JCIR}}(t,T)$ are not equal to the survival probabilities computed by the MC simulation. These analytically computed survival probabilities are used for computing CDSs, used for calibrating the credit curve and in the CDSO prices. Satisfying the Feller condition guarantees that the volatility is not too high.

- Another problem arises when the volatility is too high compared to κ and μ: the approximations of $\mathbf{E}^{\mathbb{Q}}\left[\sqrt{y_{(J)}(t)}\middle|\mathscr{F}(0)\right]$ used for the instantaneous-correlation-functions, can not be computed. The approximations use a square root, however, the expression under the square root can become negative for a volatility value that is too high. The square root is well defined when the Feller condition is satisfied or when $8\kappa\mu/\nu^2$ is valid [6].
- We argued to use an ATM CDS option to calibrate the volatility parameter to, because then the vega of the option is not too large and we avoid numerical issues with the Newton-Raphson. However, the CDS option market is not very liquid. Since most options in the market are out of the money, finding an ATM option is even more difficult.
- For smaller counterparties, CDSs to calibrate to are not always available. Then other methods should be used to construct survival probabilities. CDS index derivatives can be used, or historical data is needed.
- Due to limited memory on our computer, computing more than 10^4 paths for maturity dates $T > 6$ was an issue. A higher accuracy can be achieved for the MC experiments by simulating more paths.

5.4. Future research

Unfortunately, time for this thesis is not infinite, and there are multiple extensions of this research that are worthwhile. In this section we mention some of those possibilities for future research.

- In the used CVA model there were numerical methods and other model choices that were not investigated thoroughly and that could be improved. Using the reflecting Euler scheme limited the use of the model. Investigating which discritization method works best could greatly improve the model.
- WWR is interpreted as the adverse relationship between the exposure to and the creditworthiness of the counterparty. The loss-given-default is a factor that influences the exposure at default and therefore, in the broader sense of WWR, it should be taken into account in a more realistic manner. Not only assuming that the exposure and the creditworthiness are stochastic quantities, but also the L_{GD}, is a realistic extension of the current CVA model. The Brownian increments of the stochastic process that defines the L_{GD} could be correlated with both the interest rate and the hazard rate.
- This research only investigated the correlation between the interest rate level and the hazard rate. In times of crisis, the volatility of the interest rate increases. This could be modeled as well, by choosing a stochastic process for the volatility of the interest rate and correlating this quantity with the hazard rate.
- This thesis uses synthetic data. To quantify WWR in the CVA even better, real market data could be used. Also calibrating the other required parameters, would be an interesting extension.
- Investigating a portfolio including more advanced derivatives, or when collateral is involved is a logical next step. Investigating whether this model can easily be extended to take into account the credit risk of the bank (DVA) next to the counterparty as well.
- The goal of this research was to asses the impact of WWR on the CVA of a portfolio of IRSs. This goal is important for correctly pricing and hedging the CVA. Hence, the next step of the research should be to investigate how WWR in the CVA is hedged best.

A

Hull-White experiments

A.1. Implementation of the HW1F model

Guarantee of a Robust Monte Carlo Method

We check our Monte Carlo method by computing the standard error of the Monte Carlo method and we check the convergence error of the used discritization method.

Accuracy of the Monte Carlo Method

As said before, the result of a Monte Carlo simulation is a random number and therefore the solution that is given by the simulation has a variance. Since the MC simulation is based on the central limit theorem and the law of large numbers, an increasing number of paths should decrease the error made by the MC simulation by decreasing the variance [6]. Therefore, we can achieve the desired accuracy for our simulation if we use the right amount of paths.

We simulate M Monte Carlo paths under the risk-neutral measure and then we approximate the short-rate by taking the average over all the paths.

$$\mathbb{E}^{\mathbb{Q}}[r(t_i)] \approx \bar{r}_M(t_i) := \frac{1}{M}\sum_{j=1}^{M} r_j(t_i), \tag{A.1.1}$$

where M is the number of paths used and r_j is the j^{th} path. By the strong law of large numbers, we know that for $M \to \infty$,

$$\lim_{M\to\infty} \bar{r}_M(t_i) = \mathbb{E}^{\mathbb{Q}}[r(t_i)], \tag{A.1.2}$$

with probability 1 [6]. We determine the error that comes from using a finite number of MC paths. This error at time T is the variance the approximation $\bar{r}_M(T)$ and it can be approximated by the sample variance $\bar{v}^2_M$. This is an unbiased estimator, which means that the expected value of the sample variance is equal to the expected value of the variance of our approximation [6]. So:

$$\mathbb{E}\left[\bar{v}^2_M\right] = \mathbb{E}\left[\mathbb{V}ar\left[\bar{r}_M\right]\right]$$

The sample variance at time T is defined as follows:

$$\bar{v}^2_M(T) := \frac{1}{M-1}\sum_{j=1}^{M}\left(r_j(T) - \bar{r}_M(T)\right)^2,$$

where $r_j(T)$ is the value of the j^{th} path at time T. The standard error $\epsilon_N(T)$ is defined as:

$$\epsilon_M(T) := \frac{\bar{v}^2_M(T)}{\sqrt{M}}.$$

We have computed the standard error of the short-rate at time $T = 3$ for multiple numbers of paths M. The results can be found in Table A.1. Theoretically, from the definition of the standard error, we see that for an increase of the number of paths by a factor of 10, the error decreases by a factor of $\sqrt{10} \approx 3.16$. We have computed factor that decreases the standard error in the same table. It can be observed that the standard error indeed decreases with a factor of approximately $\sqrt{10}$ when we increase the number of paths by 10.

M	$\epsilon_M(T)$	reduction factor
10^2	$6.81 \cdot 10^{-3}$	
10^3	$2.23 \cdot 10^{-3}$	3.13
10^4	$7.23 \cdot 10^{-4}$	3.09
10^5	$2.31 \cdot 10^{-4}$	3.05

Table A.1: Standard error short-rate, for a Monte Carlo simulation of the short-rate with the following parameters: $T = 3$, $\eta = 0.1$, $r_0 = 0.05$, $k = 0.5$ and 400 steps per year.

Accuracy of the Discritization Method.
We use the Euler discitization scheme and we check the convergence error of the used discritization scheme. We show that the solution of our discrete simulation converges to the analytical computed solution.

For the convergence error we compute a exact solution of the short-rate. We can do this for every time-step t_k in the MC simulation. For every time t_k from the Monte Carlo simulation we take a sample from a normal distribution with a mean of Equation (3.1.7) and a variance from Equation (3.1.8). This sampling method is called semi-exact, since in general we still need to perform the integral in Equation (3.1.7) numerically. In our particular case, with Equation (A.1.7) as assumption for the market, we can perform the integral analytically. So, when we compute the convergence error, we use the analytical form of Equations (3.1.7) and (3.1.8), since then we do not have a integration error that needs to be taken into account.

However, we also implement a general method such that we do not need to adjust the function for analytical sampling when we adjust the parameters of the model. In that case we perform the integral numerically, which makes the sampling semi-analytic. Integrals are approximated numerically with the trapezoidal rule.

As a sanity check we can compare the densities of the MC simulation and the analytical-sampling method. Both the distribution of the MC simulation and the analytic distribution at time $T = 3$ are plotted in Figure A.1. In this figure we plot the analytical computed density and the density obtained by the MC method. The latter is plotted using histogram. It can be observed that the densities are almost the same. We investigate the differences more accurately by numerically comparing the mean and the variance of the densities and computing the convergence error of the discritization.

To compare the simulation with an analytical solution, we compute use the analytical mean and variance from Equations (A.1.3) and (3.1.8). With our chosen assumptions and analytical form of $\theta(t)$ from Equation (A.1.8), we can derive the following formula for the mean of the short-rate at time t:

$$\begin{aligned}\mathbb{E}[r(t)|\mathscr{F}(t_0)] &= \mathrm{e}^{-kt} r_0 + k \int_0^t \theta(z) \mathrm{e}^{-k(t-z)} \mathrm{d}z \\ &= \mathrm{e}^{-kt} r_0 + k \int_0^t \left(0.05 + \frac{\eta^2}{2k^2} \cdot (1 - \mathrm{e}^{-2kt})\right) \mathrm{e}^{-k(t-z)} \mathrm{d}z \\ &= 0.05 + \frac{\eta^2}{2k^2} - \frac{\eta^2}{k^2} \mathrm{e}^{-kt} + \frac{\eta^2}{2k^2} \mathrm{e}^{-2kt} \end{aligned} \tag{A.1.3}$$

We check the convergence of the MC discritization used (Euler), by computing the weak convergence error: at every time-step t_k we compute the absolute difference between the mean of the realisation from the MC simulation and the samples $R_j(T)$ from the analytical sampling method.We obtain the mean of the short-rate numerically by using Equation (A.1.1) and analytically by using samples from the normal distribution with mean and variance from Equations (A.1.3) and (3.1.8). Then we compute the weak convergence error $\epsilon^w(\Delta t)$ for a simulation until T as follows:

$$\epsilon^w(\Delta t; T) = \left| \frac{1}{M} \sum_{j=1}^{M} R_j(T) - \frac{1}{M} \sum_{j=1}^{M} r_j(T) \right|, \tag{A.1.4}$$

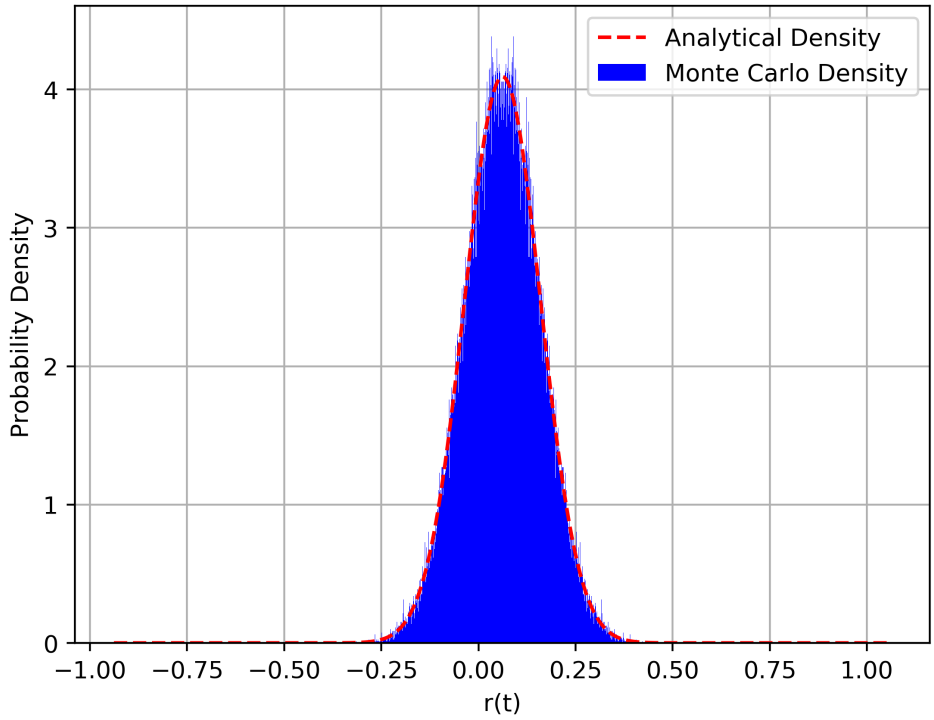

Figure A.1: Density of MC simulation and density of exact simulation at T=3 with 10^6 paths and 400 steps per year. Parameters of the model are $\theta(t)$ as described in Equation (A.1.8), $\eta = 0.1$, $r_0 = 0.05$ and $k = 0.5$.

where $R_j(T)$ is defined as a sample from the analytical sampling method of the short-rate at time T, index j indicates the paths number, M is the number of paths and $r_j(T)$ are realisations of the MC simulation at time T.

As the Euler method has a weak convergence order of 1, we expect our convergence error to decrease by a factor 2 when we increase the number of MC simulation steps by a factor 2. As this should hold for every time t_k with $0 \leq t_k \leq T$, we also computed the average of the convergence error over time. The results of the convergence error for multiple values of N (MC simulation steps per year) can be found in Table A.2. The decreasing factor is shown in this table as well.

N	$\epsilon^w(\Delta t; T)$	reduction factor	$\frac{1}{T \cdot N} \sum_{j=0}^{T \cdot N} \epsilon^w(\Delta t; t_j)$	
50	$2.48 \cdot 10^{-6}$		$2.17 \cdot 10^{-5}$	
100	$1.21 \cdot 10^{-6}$	2.05	$1.08 \cdot 10^{-5}$	2.00
200	$6.04 \cdot 10^{-7}$	2.00	$5.39 \cdot 10^{-6}$	2.00
400	$3.01 \cdot 10^{-7}$	2.01	$2.69 \cdot 10^{-6}$	2.00

Table A.2: Convergence error short-rate, for a Monte Carlo simulation with Euler scheme of the short-rate with the following parameters: $T = 3$, $\eta = 0.1$, $r_0 = 0.05$, $k = 0.5$ and $M = 10^5$.

As expected, we see that the convergence error decreases by a factor of approximately 2 for an increase in the number of steps per year (and thus also total number of steps) by a factor 2. This holds both at T and for the average over time, which means it holds for every t_k with $0 \leq t_k \leq T$.

The weak convergence errors are also visualised in Figure A.2.

After simulating the interest rate we compute risk-free prices of ZCBs with the Hull-White Characteristic

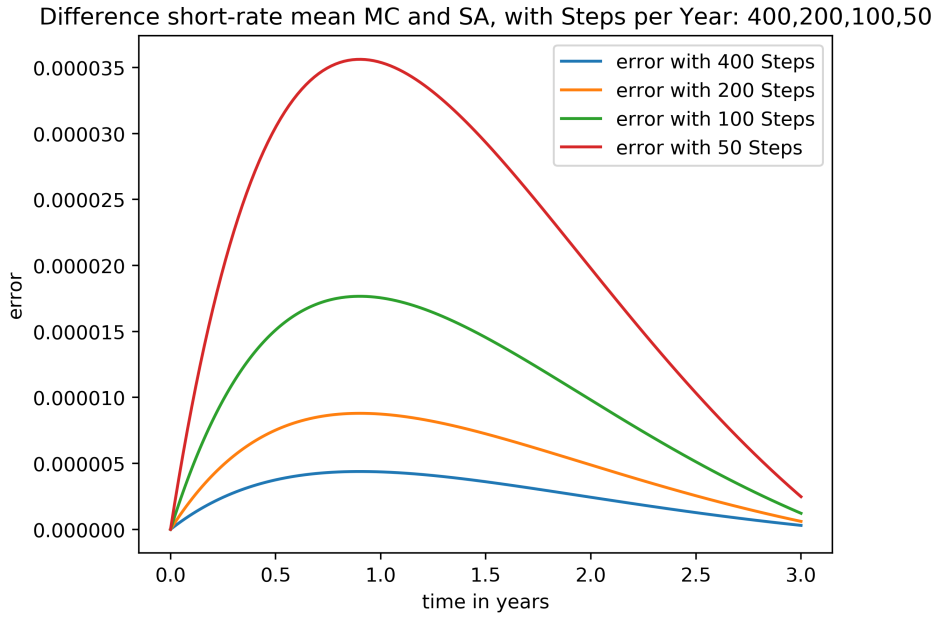

Figure A.2: Weak convergence error of the short-rate with parameter values: $T = 3$, $\eta = 0.1$, $r_0 = 0.05$, $k = 0.5$ and 10^5 MC paths

Function $\phi_{HW}(0;t,T)$. We use the following equations for the zero-coupon bond price [6]:

$$P_{HW}(t,T) = \phi_{HW}(0;t,T) = \mathbb{E}^{\mathbb{Q}}\left[e^{-\int_t^T r(z)dz} \cdot 1 | \mathscr{F}(t)\right] \tag{A.1.5}$$

$$= \exp\left(\bar{A}(\delta) + \bar{B}(\delta) r(t)\right), \tag{A.1.6}$$

where $\bar{A}(0,\delta)$, $\bar{B}(0,\delta)$ and δ are defined as follows:

$$\begin{aligned}
\delta &= T - t, \\
\bar{A}(0,\delta) &= k\int_0^\delta \theta(T-z)e^{-k(t-z)}dz + \frac{\eta^2}{4k^3}\left(e^{-2k\delta}\left(4e^{k\delta}-1\right)-3\right) + \frac{\eta^2\delta}{2k^2}, \\
\bar{B}(0,\delta) &= -\frac{1}{k}(1-e^{-k\delta}),
\end{aligned}$$

We have an assumed market:

$$P_{mkt}(0,t) = \exp(-0.05t), \tag{A.1.7}$$

which gives the following function for $\theta(t)$:

$$\theta(t) = 0.05 + \frac{\eta^2}{2k^2} \cdot (1 - \exp(-2kt)). \tag{A.1.8}$$

With Equation (A.1.8), we can compute $\bar{A}(0,\delta)$ analytically. So, only for this choice of θ, we compute $P_{HW}(t,T)$ analytically. This way our ZCB has no computational error that influences the value of our interest rate products. For other choices $\theta(t)$ we approximate $\bar{A}(0,\delta)$ numerically with a trapezoidal integral rule.

So far we have introduced three kinds of formula's for ZCBs. Recall the ZCB calculated with the Hull-White model : $P_{HW}(0,T)$ in Equation (A.1.6), the ZCBs from the market: $P_{mkt}(0,T)$ in Equation (A.1.7) and the definition of a ZCB, Equation (A.1.5), approximated with MC paths:

$$P_{MC}(0,t) = \frac{1}{M}\sum_{h=0}^{M} e^{-\int_0^t r_j(s)ds}, \tag{A.1.9}$$

with M the number of MC paths and $r_j(s)$ is the j^{th} simulated MC short-rate path at time s. We approximate the integral over the short-rate numerically by using the trapezoidal integral rule at every time step of the MC simulation.

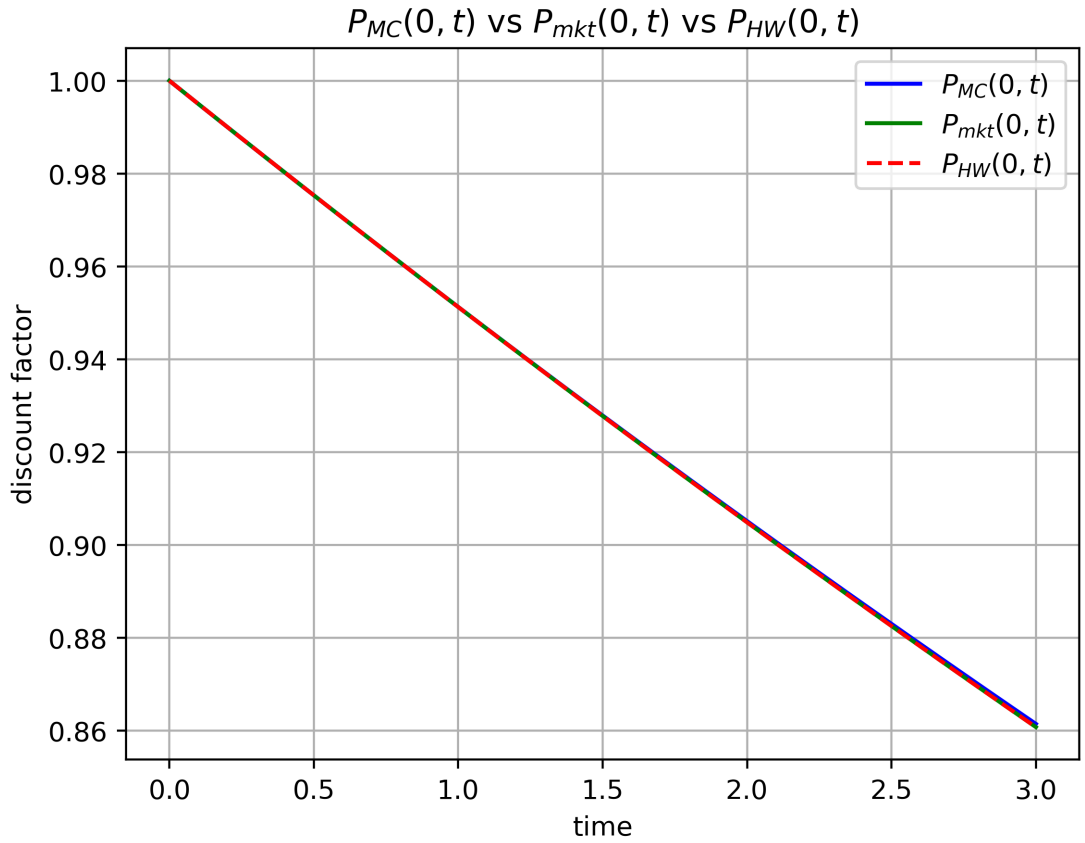

Figure A.3: $P_{mkt}(0,t)$, $P_{MC}(0,t)$ and $P_{HW}(0,t)$, calculated with $N = 400$ steps per year, $M = 10^5$ paths, $\eta = 0.1$, $k = 0.5$ and $r_0 = 0.05$, until $T = 3$ years.

As a sanity check we calculate for $0 < t < T$ these three ZCBs in Figure A.3, where T is the final simulation date. In this figure it can be observed that the ZCBs are close to each other at every time step. This is what was expected if the ZCBs were implemented correctly. We calculate the average absolute differences between $P_{HW}(0,t)$ and $P_{MC}(0,t)$ for $0 < t < T$, presented in Table A.3.

In this table it can be observed that $P_{MC}(0,t)$ converges to $P_{HW}(0,t)$ for an increasing number of paths. This was expected, since we approximate the expectation with the average of the paths. This approximation improves for an increased number of paths.

Since we can calculate $P_{HW}(0,t)$ analytically, the value of $P_{mkt}(0,t) = P_{HW}(0,t)$ for all t. If we calculate $P_{HW}(0,t)$ numerically, the only difference comes from the accuracy of the integral in formula for $P_{HW}(0,t)$.

In Table A.3 it can be observed that the difference between $P_{HW}(0,t)$ and $P_{MC}(0,t)$ converges to zero when increasing the number of paths. This means that the accuracy of $P_{MC}(0,t)$ increases with the number of paths.

M	10^3	10^4	10^5
Average Absolute Diff	$2.942 \cdot 10^{-4}$	$1.963 \cdot 10^{-4}$	$1.514 \cdot 10^{-5}$

Table A.3: Average absolute difference Between $P_{HW}(0,t)$ and $P_{MC}(0,t)$, simulated with 400 steps per year, $r_0 = 0.05$, $k = 0.5$ and $\eta = 0.1$. End of simulation date $T = 3$.

Exposure Profile

For a given swap, we calculate the (positive) exposure $E(t) := \max(V(t), 0)$ and the discounted expected (positive) exposure (EPE):

$$EE(t_0,t) = \mathbb{E}^{\mathbb{Q}}\left[\frac{B(t_0)}{B(t)}E(t)\middle|\mathscr{F}(t_0)\right], \tag{A.1.10}$$

where $B(t)$ represents the bank account. We use the implemented Monte Carlo engine and simulate the interest rate paths. For every path h at every time step t_k of the Monte Carlo simulation, we calculate the value of the swap. For all these time steps, we take the discounted value of the exposure and take the average over all the paths. This gives us the value of the discounted expected positive exposure. Using negative exposure $NE(t) := \max(-V(t), 0)$ instead of $E(t)$ gives the discounted expected negative exposure ($ENE(t)$)

At these time steps t_k, we only know the short-rate paths until t_k. Therefore, in the calculation of the discounted expected exposure of the swaps, we need two types of discount factors: the discount factors that discounts the cashflows of the swap that occur at future times T_i to time t_k and we need a discount factor to discount the exposure of the swap at future times t_k to today, time t_0.

For the former we use the discount factors $P^h_{HW}(t_k, T_i)$, since we do not know the short-rate in the future. The superscript h indicates that the discount factor is path dependent, it depends on the simulated short-rate value $r_j(t_k)$ of path j.

For the latter, we have the paths of the short-rate until t_k. So, for each path we have a value of the swap and for each path we use the discount factor $\frac{B(t_0)}{B(t_k)}$ to discount the swap to t_0, where we use realised paths of the short-rate and the definition of the bank account:

$$\frac{B(t_0)}{B(t_k)} = \exp\left(-\int_{t_0}^{t_k} r_j(s)\mathrm{d}s\right). \tag{A.1.11}$$

We approximate the integral numerically by using the trapezoidal integral rule.

For the value of the swap at each time step t_k we use Equation (2.3.1) and Equation (A.1.6). The paths of these IRSs can be found in Figure A.4. Here we see the future values of an Payer Interest Rate Swap (IRS), computed with the simulated short-rate paths, with the following characteristics: start date $T_a = t_0 = 0$ is today, maturity $T_b = 3$ (years) and with payments each half year. Also, the strike rate K is the par rate, which means that the price of the IRS is zero at inception.

After the start of the IRS, the swap values deviate from the value at the start date. This is due to the value of the short-rate: if the short-rate increases, the forward-rates increase and therefore the cashflows have a positive value from a payer perspective (see Equation (2.3.1)). The other way around: if the short-rate decreases then the forward-rates decrease and the cashflows will have a negative value.

In Figure A.4 the payment dates of the IRS can be observed by looking at the values of the swaps. We see jumps in the values of the IRS at the payment dates. If a payment has been made, the value of the swap becomes smaller in absolute terms, since less future cashflows need to be considered.

Also the last part of the IRS values are notable. After the second-last payment, the value of the swap is no longer dependent on the forward-rate, since the forward-rate resets at the beginning of a payment date. Therefore, between the second-last and the final payment, the future IRS swap value is no longer dependent on forward rates, except for the fixed forward rate that resets second-late payment date. The value of the swap is still dependent on the interest rate through discounting of the last cashflow.

In Figure A.5 the same with the same parameters can be observed, except for the fact that we use 400 steps per year instead of 40.

To find the discounted expected positive exposure of the IRS at each time step t_k, we use Equation (A.1.10). First we determine the discount factor $P_j(t_0, t) = \frac{B(t_0)}{B(t_k)} = \exp\left(-\int_{t_0}^{t} r_j(s)\mathrm{d}s\right)$ for each path j at each time step t_k. For every path we multiply $P_j(t_0, t)$ with the exposure at each time step of every path. We can not use $P_{HW}(t_0, t_k)$ since the value of the swap and the discount factor are not independent. After which we take the expectation by taking the average over all the paths at every time step. So in formulae:

$$\begin{aligned} EE(t_0, t) &= \mathbb{E}^{\mathbb{Q}}\left[\frac{B(t_0)}{B(t)}E(t)\middle|\mathscr{F}(t_0)\right] \\ &= \frac{1}{M}\sum_{j=1}^{M}\left[\exp\left(-\int_{t_0}^{t_k} r_j(s)\mathrm{d}s\right)\cdot\max\left(V_j^{IRS}(t), 0\right)\right] \end{aligned} \tag{A.1.12}$$

In Figure A.6 the mean of the swap values, the mean of the discounted swap values, the discounted expected positive exposure and the discounted negative exposure can be observed. The swap in Figure A.6 has a start

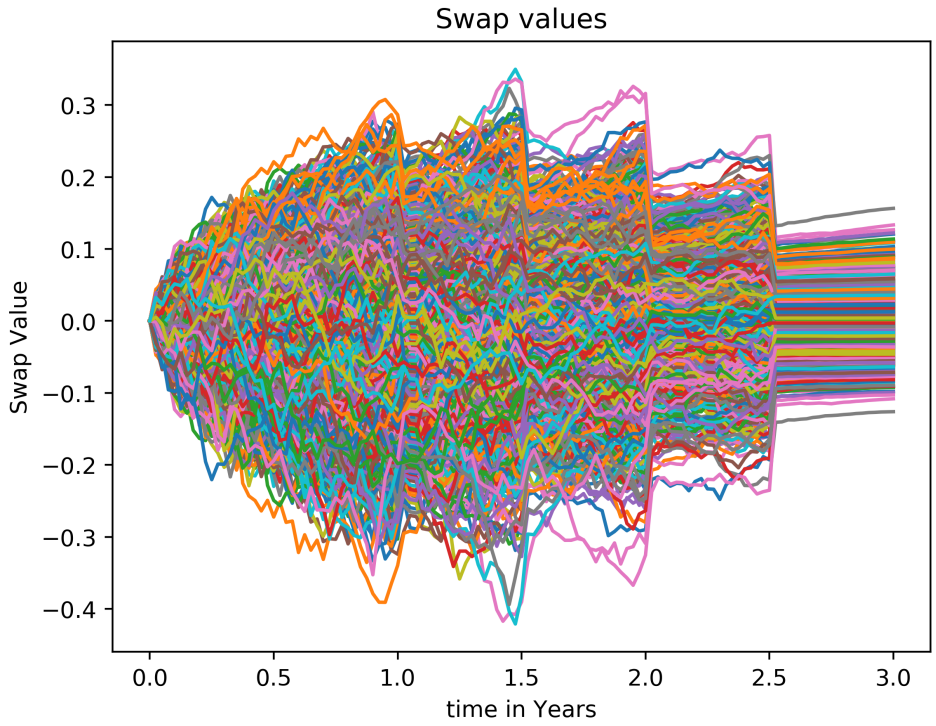

Figure A.4: MC simulation of an IRS with start date $T_a = 0$, maturity $T_b = 3$ and with payments each year. 10^3 Paths and 40 steps per year are used for the simulation. Parameters of the Hull-White model are: $r_0 = 0.05$, $k = 0.5$ and $\eta = 0.1$.

value of 0 at start date t_0. We observe that the exposure grows with the expectation of an increasing interest rate. This is because the IRS is a payer swap and we choose the strike rate to be the par rate. At the same time, payments are made, which decrease the value of the swap. At first the uncertainty is higher: the short-rate can increase a lot which gives high IRS exposures. But as t approaches T_b, the payments have more effect on the exposure than the uncertainty has. The payments decrease the exposure of the swap and the value of the swap converges to 0. After the last payment there is no exposure since the swap contract has ended.

Rewriting Equation (A.1.10) for a interest rate swap, tells us that the exposure profile can be found in closed-form. Substituting the formula for the swap value, Equation (2.3.1), into Equation (A.1.10) of the expected exposure, gives us the following:

$$\begin{aligned} EE(t_0,t) &= \mathbb{E}^{\mathbb{Q}}\left[\frac{B(t_0)}{B(t)}\max\left(V^{IRS}(t),0\right)\middle|\mathscr{F}(t_0)\right] \\ &= \mathbb{E}^{\mathbb{Q}}\left[\frac{B(t_0)}{B(t)}\max\left(N\sum_{i=a+1}^{b}P(t,T_i)\left(\ell(t,T_{i-1},T_i)-K\right),0\right)\middle|\mathscr{F}(t_0)\right] \\ &= \mathbb{E}^{\mathbb{Q}}\left[\frac{B(t_0)}{B(t)}V^{\text{Swpt}}(t,K)\middle|\mathscr{F}(t_0)\right], \end{aligned}$$

where $V^{\text{Swpt}}(t,K)$ is the value of a swaption with strike price K. So, the exposure profile of a swap is equal to today's discounted value of a swaption with the same strike rate K and a maturity time t.

A (European) swaption is a swap option: an option to enter into an interest rate swap agreement on a specified future date and predetermined strike rate K. Just as with a option on stock, the buyer of the swaption has the right, but not the obligation to exercise this option in exchange for an option premium. There are payer and receiver swaptions: options to enter into an IRS agreement as the payer of the fixed leg or the floating leg. Swaptions can be used to calibrate volatility of the Hull-White model to the volatility of the market.

In the figure it can be observed that the mean of the discounted swap values is lower than the undiscounted swap values. In fact, the mean of the discounted swap values is around zero. This is what was expected. Due to the fundamental theorem of asset pricing, the discounted expected value of the swap should be equal to

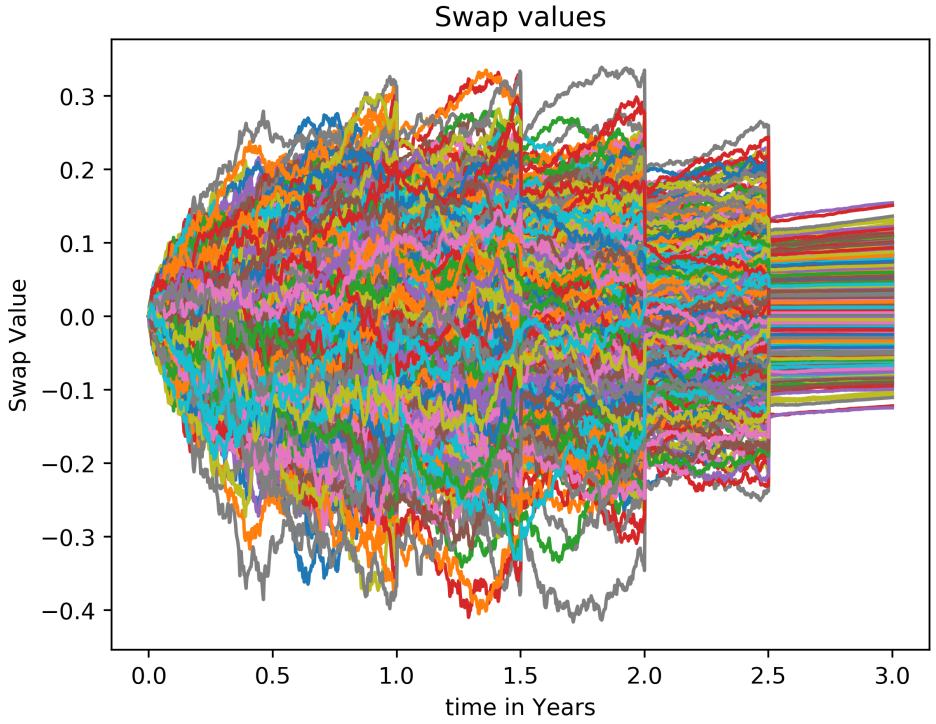

Figure A.5: MC simulation of an IRS with start date $T_a = 0$, maturity $T_b = 3$ and with payments each year. Strike rate K is the par rate of the swap. 10^3 Paths and 400 steps per year are used for the simulation. Parameters of the Hull-White model are: $r_0 = 0.05$, $k = 0.5$ and $\eta = 0.1$.

the price at inception (today, t_0). Theoretically, the discounted IRS should be a martingale under the risk-neutral measure:

$$\frac{V^S(t_0)}{B(t_0)} = \mathbb{E}^{\mathbb{Q}}\left[\left.\frac{V^S(t)}{B(t)}\right|\mathscr{F}(t_0)\right], \quad \text{for } t_0 < t. \tag{A.1.13}$$

Note that only the 'whole' swap, including every cashflow, is a martingale. You could say that the swap is not the same swap anymore after a payment is done. Therefore, at every time-step, we have checked the martingale value (MV) of the swap. We define the martingale value of the swap as the expectation of the discounted swap value, including the paid cashflows discounted to today:

$$\begin{aligned}\mathrm{MV}(t) &= \mathbb{E}^{\mathbb{Q}}\left[\left.\frac{B(t_0)}{B(t)}\left(V^S(t) + \sum_{i=1}^{k}\frac{B(t)}{B(T_i)}(\ell(T_{i-1},T_{i-1},T_i) - K)\right)\right|\mathscr{F}(t_0)\right] \\ &= \mathbb{E}^{\mathbb{Q}}\left[\left.\frac{B(t_0)}{B(t)}V^S(t) + \sum_{i=1}^{k}\frac{B(t_0)}{B(T_i)}(\ell(T_{i-1},T_{i-1},T_i) - K)\right|\mathscr{F}(t_0)\right],\end{aligned}$$

where $V^S(t)$ is the forward swap value at time t, $\frac{B(t)}{B(T_i)}$ is used to get the forward value of the payment $\ell(T_{i-1},T_{i-1},T_i) - K$, where $\ell(T_{i-1},T_{i-1},T_i)$ is the Libor forward rate for the period $[T_{i-1},T_i]$ with reset date T_{i-1} and K is the strike date.

In theory the MV is zero, but in practice, we are dealing with Monte Carlo error and the error of calculating the integral over the short-rate for $P_{MC}(0,t_k)$. In our case, we calculate $\theta(t)$ and $P_{HW}(t_k,T_i)$ exact, so that our error is only dependent on the MC parameters M and N for the number of paths and time-steps respectively. The Monte Carlo error is per value of N dependent on the value of M. The integral error is only dependent on N since the number of time-steps determines the time-step size $\mathrm{d}t$ in the formula of the trapezoidal rule.

If the IRS is a martingale, then the discounted expectation of the IRS value should be equal to the value at inception. We use IRSs with a fixed rate that is equal to the par rate, such that the IRS has value of zero at inception. This means that we want the martingale value of the IRS to converge to zero.

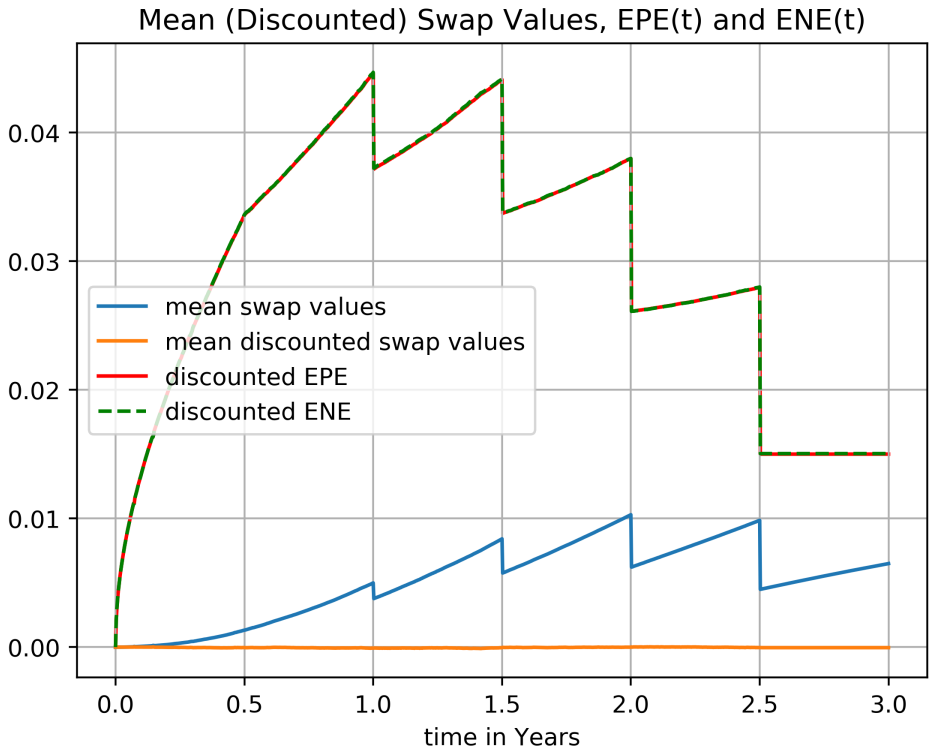

Figure A.6: MC simulation of an IRS with start date $T_a = 0$, maturity $T_b = 3$ and with 2 payments each year. 10^5 Paths and 400 steps per year are used for the simulation. Parameters of the Hull-White model are: $r_0 = 0.05$, $k = 0.5$ and $\eta = 0.1$. The Discounted Expected Positive Exposure (green), the Discounted Negative Expected Exposure (red), the mean of the swap values (blue) and the discounted mean of the swap values (orange) can be observed.

If we look at IRSs that have a fixed rate not equal to the par rate, then we look at the MV of the swap minus the value of the swap at inception. We call this value the martingale error (ME):

$$\mathrm{ME}(t) = \mathrm{MV}(t) - V^S(t_0). \tag{A.1.14}$$

So, the IRS is a martingale if the MV converges to the value of the IRS at inception or if the ME converges to zero. This scaling, using ME, makes sure that we can observe a value from what we know what the value should be: zero.

If we want to show that our IRS is a martingale, we need to show that the martingale error converges to zero when we increase our number of paths. We show with multiple parameter values and IRSs that the swap is a martingale.

Instead of looking at the ME at every time-step of the MC simulation, we take the average of the ME. Since at every time-step the ME should converge to zero, the average should converge to zero as well.

Since we calculate the ME by taking the average over all the values of the swaps at every path, the error can be seen as the variance of the collection of random variables $V_h^S(t)$. The mean of the ME together with a 95% confidence interval can be observed in Figure A.7.

To see that the martingale error goes to zero, we show the martingale errors for the number of paths is $10^3, 10^4$ and 10^5. These plots can be observed in Figure A.8. The martingale errors together with their 95% confidence intervals are plotted. The martingale values are converging to zero: the martingale value of a plot with a higher number of paths is closer to zero than the martingale values with where a lower number of paths is used.

To see this more clearly, we calculate the average over time of the MEs for the different values of M and different values of the volatility parameter η in Table A.4 .

It is clear to see that with an increasing number of paths, the martingale error decreases. If the short-rate was

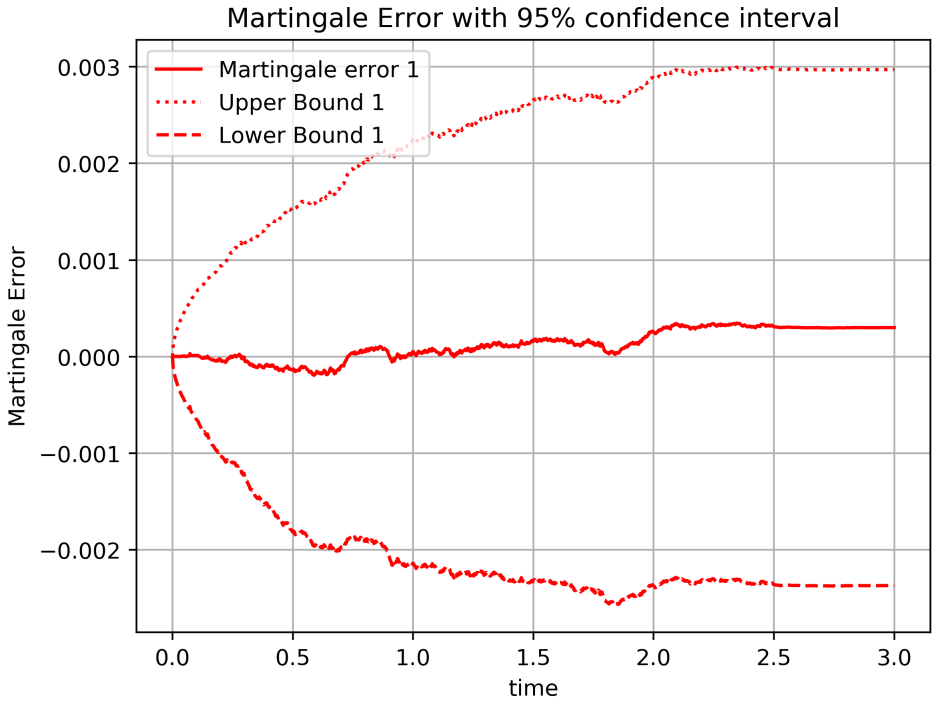

Figure A.7: Martingale Error with a 95% confidence interval and with parameters $\eta = 0.1$, $k = 0.5$, $r_0 = 0.05$, 400 steps per year, for a swap with $T_a = 0$, $T_b = 3$, 2 payments per year, notional = 1 and a fair strike rate $K = 0.05127$.

totally deterministic, we would only have a integration error, and no Monte Carlo error. So, with an increasing volatility, the we have a larger MC error and thus a larger ME. This can be observed in the Table.

M	10^3	10^4	10^5	10^6
$\eta = 0.01$	$1.75679 \cdot 10^{-6}$	$3.9455 \cdot 10^{-6}$	$6.2753 \cdot 10^{-7}$	$5.07983 \cdot 10^{-7}$
$\eta = 0.1$	$1.0127 \cdot 10^{-3}$	$3.6637 \cdot 10^{-4}$	$3.8701 \cdot 10^{-5}$	$3.3171 \cdot 10^{-5}$
$\eta = 0.3$	$1.7206 \cdot 10^{-3}$	$1.2777 \cdot 10^{-3}$	$3.2470 \cdot 10^{-4}$	$4.3782 \cdot 10^{-4}$
$\eta = 0.5$	$5.98661 \cdot 10^{-2}$	$1.05035 \cdot 10^{-2}$	$1.48622 \cdot 10^{-3}$	$1.11081 \cdot 10^{-3}$

Table A.4: Absolute martingale errors with parameters $\eta = 0.01, 0.1, 0.3, 0.5$, $k = 0.5$, $r_0 = 0.05$, $M = 10^3, 10^4, 10^5, 10^6$, 100 steps per year, for a swap with $T_a = 0$, $T_b = 3$, yearly payments and a fair strike rate $K = 0.05127$.

In Figure A.9 the martingale errors can be observed on a loglog-scale, for $M = 10^3, 10^4, 10^5, 10^6$ and for volatility values $\eta = 0.01, 0.1, 0.3, 0.5$. The figure shows that for a fixed value of η, the MEs converge to zero. Also, for a fixed number of paths, a smaller value for η gives a smaller ME. Both these observation show that the calculated error comes from a Monte Carlo error. This indicates that our code is implemented correctly and that we have a robust MC engine for the short-rate.

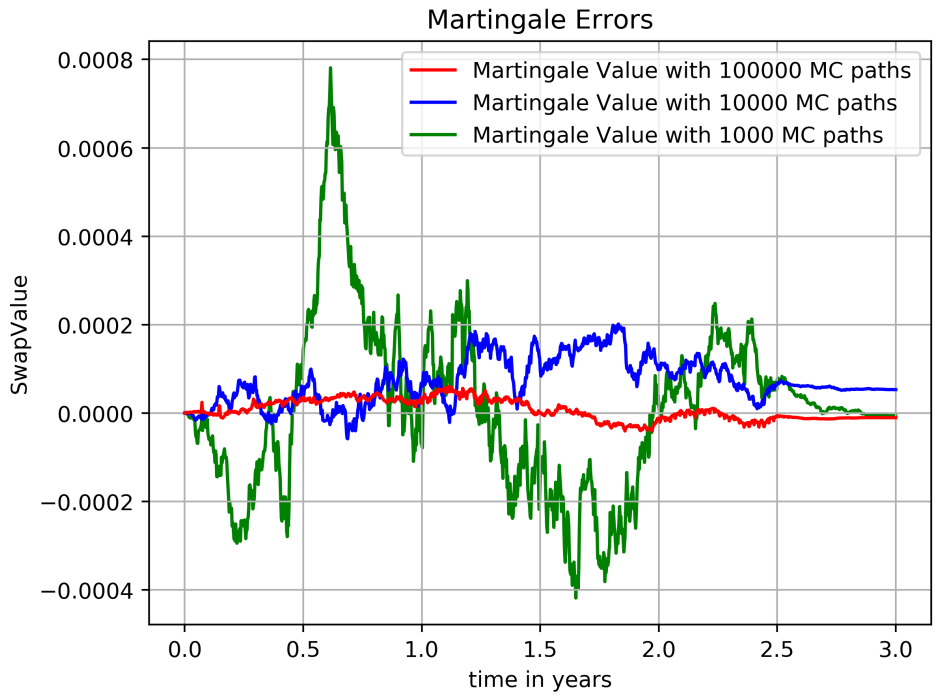

Figure A.8: Martingale Errors with parameters $\eta = 0.1$, $k = 0.5$, $r_0 = 0.05$, 400 steps per year, for a swap with $T_a = 0$, $T_b = 3$, 2 payments per year, notional = 1 and a fair strike rate $K = 0.05127$.

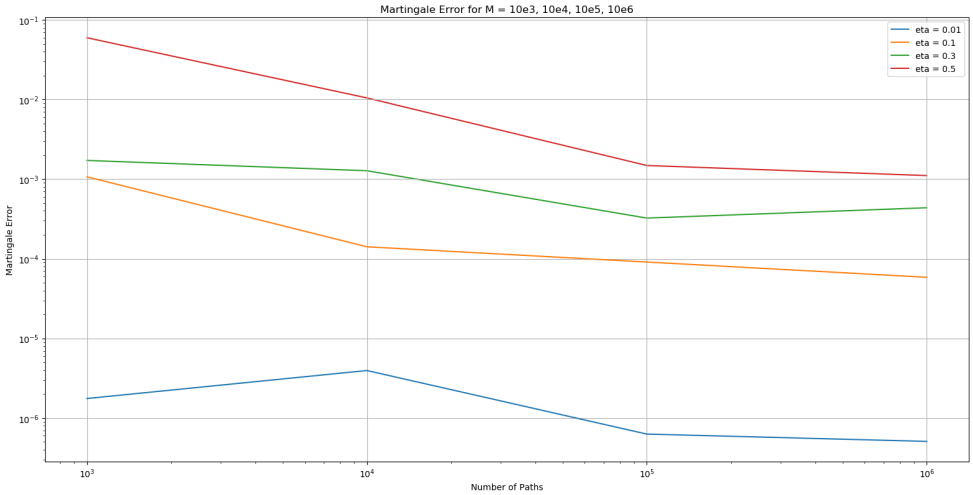

Figure A.9: Martingale Errors on a log-log-scale with parameters $\eta = 0.01, 0.1, 0.3, 0.5$, $k = 0.5$, $r_0 = 0.05$, $M = 10^3, 10^4, 10^5, 10^6$, 100 steps per year, for a swap with $T_a = 0$, $T_b = 3$, yearly payments, notional = 1 and a fair strike rate $K = 0.05127$.

Bibliography

[1] E. Alos et al. “CVA and Vulnerable Options in Stochastic Volatility Models”. In: *Working paper, available at SSRN 3429088* (2019).

[2] Van Son Lai Ayoub Gargouri. “Revisiting Interest Rate Swap Valuation With Counterparty Risk, Wrong-Way Risk and OIS Discount”. In: *Forthcoming, Journal of Fixed Income* (2016).

[3] P. Brémaud. “Markov chains”. In: *Texts in Applied Mathematics* 31 (1999).

[4] D. Brigo. “Market Models For CDS Options and Callable Floaters”. In: *Risk* 18.1 (2005), pp. 89–94.

[5] D. Brigo and A. Alfonsi. “A two-dimensional cir++ shifted diffusion model with automatic calibration to credit default swaps and interest rate derivatives data.” In: *The 6-th Columbia-JAFEE International Conference* (2003).

[6] L. Grzelak C. Oosterlee. *Mathematical Modeling and Computation in Finance*. World Scientific Publishing Europe Ltd., 2020.

[7] Umberto Cherubini. “Credit Valuation Adjustment and Wrong Way Risk”. In: *Quantitative Finance Letters* 1.1 (2013), pp. 9–15.

[8] A. Alfonsi D. Brigo. “Credit Default Swaps Calibration and Option Pricing with the SSRD Stochastic Intensity and Interest-Rate Model”. In: *Finance Stochastics* IX.1 (2005).

[9] A. Pallavicini D. Brigo. “Counterparty risk and Contingent CDS valuation under correlation between interest-rates and default”. In: *Risk Magazine* (2006).

[10] F. Mercurio D. Brigo. “A deterministic-shift extension of analytically-tractable and time-homogeneous short rate models”. In: *Finance Stochastics* 5.3 (2001), pp. 369–388.

[11] F. Mercurio D. Brigo. *Interest Rate Models - Theory and Practice*. Springer Finance, 2006.

[12] F. Vrins D. Brigo. “Disentangling wrong-way risk: pricing CVA via change of measures and drift adjustment”. In: *European Journal of Operational Research* 269.3 (2018), pp. 1154–1164.

[13] L. Cousot D. Brigo. “A Comparison between the SSRD Model and the market model for CDS options pricing”. In: *International Journal of Theoretical and Applied Finance* 9.3 (2006), pp. 315–339.

[14] N. El-Bachir D. Brigo. “An exact formula for default swaptions’ pricing in the SSRJD stochastic intensity model”. In: *Mathematical Finance* 20.3 (2008), pp. 365–382.

[15] N. El-Bachir D. Brigo. “Credit Derivatives Pricing with a Smile-Extended Jump Stochastic Intensity Model”. Available at SSRN: Available at SSRN: https://ssrn.com/abstract=950208. 2006.

[16] V. Papatheodorou D. Brigo A. Pallavicini. “Bilateral counterparty risk valuation for interest-rate”. In: *Working Paper, arXiv:0911.3331v3* (2008).

[17] Z. Wiener D. Galai A. Raviv. “Liquidation Triggers and The Valuation of Equity and Debt”. In: *EFA 2005 Moscow Meetings Paper* School of Business Administration, The Hebrew University of Jerusalem (2005).

[18] E. Morellec D. Hackbarth J. Miao. “Capital Structure, Credit Risk, and Macroeconomic Conditions”. In: *FAME Research Paper* 125 (2004).

[19] A. Elizalde. *Credit risk models II: structural models*. 2006.

[20] Abel Elizalde. “From Basel I to Basel II: An Analysis of the Three Pillars”. In: *Documentos de Trabajo (CEMFI)* 4 (2007), p. 1.

[21] E. S. Schwartz F. A. Longstaff. “A Simple Approach to Valuing Risky Fixed and Floating Rate Debt”. In: *Journal of Finance* 50 (1998), pp. 789–819.

[22] J. C. Cox F. Black. “Valuing Corporate Securities: Some Effects of Bond Indenture Provisions”. In: *Joural of Finance* 31 (2005).

[23] J. Yang G. R. Harris T. L. Wu. “The Relation Between Counterparty Default and Interest Rate Volatility, and Its Impact on the Credit Risk of Interest Rate Derivatives”. In: *Journal of Credit Risk* 11.1 (2015), pp. 93–127.

[24] Andrew Green. *XVA: Credit, Funding and Capital Valuation Adjustments*. Wiley Finance Series, 2016.

[25] J. Gregory. *Counterparty Credit Risk and credit value adjustment*. John Wiley Sons, 2012.

[26] E. Errais H. Ben Ameur D. Brigo. “Pricing credit default swaps Bermudan options: An approximate dynamic programming approach”. Working paper. Available at SSRN: https://ssrn.com/abstract=715801. 2005.

[27] P. Del Boca I. Ruiz R. Pachon. “Optimal Right and Wrong Wary Risk”. Working paper, Available at SSRN: http://ssrn.com/abstract=2248705. 2013.
[28] Bank for International Settlements. *Statistical release: OTC derivatives statistics at end June 2020*. URL: https://www.bis.org/publ/otc_hy2011.pdf. accessed: 2021-01-02.
[29] Jr.; S. A. Ross J. C. Cox J. E. Ingersoll. “A Theory of the Term Structure of Interest Rates”. In: *Econometrica* 53.2 (1985), pp. 385–408.
[30] B. Goldstein J. Casassus P. Collin-Dufresne. “Unspanned stochastic volatility and fixed income derivatives pricing”. In: *Journal of Banking Finance* 29 (2005), pp. 2723–2749.
[31] J. Witzany J. Černý. “Interest Rate Credit Valuation Adjustment”. In: *The Journal of Derivatives Winter* 23.2 (2015), pp. 24–35. DOI: https://doi.org/10.3905/jod.2015.23.2.024.
[32] J. Witzany J. Černý. “Wrong-Way Risk - Correlation Coefficient Calibration”. Information bulletin Czech statistic, 1-2-2015, Available at https://ssrn.com/abstract=2599427. 2015.
[33] A. White J. Hull. “CVA and Wrong Way Risk”. In: *Financial Analyst Journal* 68.5 (2012), pp. 58–69.
[34] R. Merton. “On the Pricing of Corporate Debt: the Risk Structure of Interest Rates”. In: *Journal of Finance* 29 (1974), pp. 449–470.
[35] Dominic O’Kane. *Modelling single-name and multi-name credit derivatives*. Wiley Finance, 2008.
[36] G.W. Oehlert. “A note on the delta method.” In: *American Statistician* 46 (1992), pp. 27–29.
[37] N. Privault. “Stochastic Calculus in Finance II Lecture Notes”. Version June 27, 2020. Can be found on https://www.ntu.edu.sg/home/nprivault/indext.html.
[38] C. W. Oosterlee Q. Feng. “Wrong Way Risk Modeling and Computation in Credit Valuation Adjustment for European and Bermudan Options”. In: *International Journal of Theoretical and Applied Finance*. 20.8 (2016). DOI: 10.1142/S021902491750056X.
[39] O. Marzouk R. Ben-Abdallah M. Breton. “Wrong-Way Risk of Interest Rate Instruments”. In: *Journal of Credit Risk* 15.2 (2018), pp. 21–44. DOI: https://ssrn.com/abstract=3398187.
[40] B. Manly S. Amstrup L. MacDonald. *Handbook of capture-recapture analysis*. Princeton University Press, 2006.
[41] Marek Rutkowski Tomasz R. Bielecki Monique Jeanblanc. *Credit Risk Modeling*. Center for the study of Finance and Insurance, Osaka University, Osaka, Japan.
[42] J. Z. Huang Y. H. Eom J. Helwege. “Structural Models of Corporate Bond Pricing: An Empirical Analysis”. In: *Review of Financial Studies* 17 (2003), pp. 499–544.